An analysis of annual environmental conditions and heat gains, and theoretical assessment of approaches to improve summer thermal comfort, of the Energy Research Centre at the University of Cape Town.

Guy Edward Cunliffe

CNLGUY001

Dissertation presented in partial fulfilment of the requirements for the degree of
Master of Science in Engineering in Sustainable Energy Engineering

Energy Research Centre

Faculty of Engineering and the Built Environment

University of Cape Town

February 2017

Supervisor: Mr Andrew Hibberd

Co-supervisor: Ms Mascha Moorlach

(This page has been intentionally left blank)

Plagiarism Declaration

Name: Guy Cunliffe

Student Number: CNLGUY001

Course: MEC5061Z

Declaration

I know that plagiarism is wrong. Plagiarism is to use another's work and pretend that it is one's own.

I know the meaning of plagiarism and declare that all the work in the document, save for that which is properly acknowledged, is my own. This dissertation has been submitted to the Turnitin module and I confirm that my supervisor has seen my report and any concerns revealed by such have been resolved with my supervisor.

I have used the **Harvard UCT (2015)** convention for citation and referencing. Each contribution to, and quotation in, this essay/report/project/**dissertation** from the work(s) of other people has been attributed, and has been cited and referenced.

I have not allowed, and will not allow, anyone to copy my work with the intention of passing it off as his or her own work.

Signature Signed by candidate

Date 03 March 2017

Acknowledgements

First and foremost, I wish to thank Mr Andrew Hibberd and Ms Mascha Moorlach for their guidance, supervision, and exceeding patience throughout this project. I learned a lot through this experience, and am very grateful for my supervisors' role in that process.

Acknowledgement must also be given to Ms Liesle Van Wyk of the UCT Physical Planning Unit, for assisting with providing floor plans and section drawings of the Menzies 6th floor.

I would also like to thank my coursework lecturers for providing the groundwork of my energy knowledge, and Jesse Burton in particular for continually encouraging my learning progress.

I would further like to thank Prof Harald Winkler and my colleagues at the ERC – researchers, students and support staff – for their many and varied contributions throughout my master's study.

I would also like to express my sincere gratitude to my family – my parents, John and Beverley, and my sister, Amy – who continuously supported me throughout my educational journey.

Finally, I wish to thank my two best friends, James and Genevieve, for their encouragement and understanding throughout, which helped immeasurably during the many long hours of writing.

Abstract

The Energy Research Centre (ERC), a research centre located at the University of Cape Town (UCT), is considering retrofitting its offices with measures to improve its occupants' thermal comfort, particularly during Cape Town's summer months. While a simple solution would be to install an active cooling system, first consideration should be given to the deployment of preventative cooling measures and retrofits. By these means, the costs of an active cooling system would be reduced, as well as the building's relative increase in energy consumption and indirect greenhouse gas emissions.

This dissertation examines internal thermal conditions of the ERC under current building conditions and predicts levels of thermal discomfort likely to be experienced by occupants, with emphasis on Cape Town's summer season. Heat gain components to the ERC are quantified, and a *Base Case* cooling scenario is determined; this characterises the peak cooling load and active annual cooling energy required to alleviate summer thermal discomfort, if no other interventions are implemented. Thereafter, the impacts of a selection of preventative cooling measures on the *Base Case* cooling scenario are assessed, and a theoretical payback period for each progressive measure is evaluated, relative to projected installation and operational costs of an active system designed to meet the *Base Case*.

A model of the ERC offices is developed in *DesignBuilder*, which characterises thermal properties of the building envelope, thermal loads of lighting, electronic equipment and building occupants, and effects of prevailing weather patterns and solar radiation at the site of the building. Physical energy simulations of the model are run in *EnergyPlus*, which uses a series of algorithms based on the Heat Balance Method to quantify internal psychrometric conditions and heat gains in half-hourly iterations. An *EnergyPlus* Ideal Loads Air System component is input into the simulation to quantify the active cooling load required to maintain comfortable design conditions.

The results indicate that 7 814.5 hours of thermal discomfort are experienced annually across the ERC (divided into eight thermal zones in the *DesignBuilder* model), with 37.6% of discomfort hours occurring between December and March, and 12.8% in February alone. Notably, a greater proportion of discomfort hours, 38.9%, were predicted for winter months (June through August). However winter thermal discomfort was not addressed in detail here, as the scope of the dissertation was limited to analysing ERC cooling only. Solar gains through external windows were found to be the largest single source of annual heat gain (20.65 MWh_{th}), followed by heat gains due to lighting heat emissions (19.99 MWh_{th}). Profiles during typical summer conditions showed significant heat gain also arises from conduction through the ceiling, due to existing but sporadic and thin layers of fibreglass ceiling insulation, with gaps that allow thermal bridging between the roof space and ERC thermal zones.

The *Base Case* annual cooling requirements were determined to be 27.64 MWh_{th}, while peak cooling load was found to be 66.87 kW_{th}. Sensible cooling dominated total cooling loads in summer months. East and west facing thermal zones required the greatest cooling energy (normalised per floor area), having been shown to experience the greatest normalised solar and lighting heat gains.

Inclusion of a 75 mm polyester fibre insulation layer above the ceiling boards would result in a 13.6% decrease in annual discomfort hours, relative to the current building condition, and reduced peak cooling load by 19% relative to the *Base Case*. Increasing thickness above 75 mm resulted in increased ceiling thermal resistance and further reduced annual discomfort hours. However, the marginal

improvements in thermal comfort were found to decrease with increased insulation thickness. A 75 mm thickness of polyester fibre insulation was therefore selected as the first preventative measure to be considered for the ERC, and was included in all further assessment of additional preventative options.

Lighting retrofits were also considered, by means of two progressive measures: *Delamping* – the removal of fluorescent luminaires from overly lit thermal zones – and *Relamping* – replacement of remaining fluorescents and light fixtures with more energy efficient technology (as well as the *Delamping* and Insulation measures). *Delamping* was found, from simulation analysis, to reduce lighting heat gains by 31%, relative to the *Base Case* and annual cooling requirements by 24%, with total projected costs after 10 years reduced by 15.6% relative to the *Base Case*. *Relamping* had a less pronounced impact on cooling requirements, but resulted in 15 % lower lighting energy use compared to *Delamping* only.

The final measure considered was a *Shading* measure, whereby the replacement of the existing solar window film, currently fitted to each of the ERC's external windows, with internal adjustable shading. The *Shading* retrofit (in addition to all previous preventative measures) was found to cause a 35% reduction in annual cooling energy relative to the *Base Case*, as well as a 7% relative to the *Relamping* scenario. However, cost evaluation showed that costs of implementing the *Shading* retrofit significantly outweighed net incremental annual savings achieved under the measure, and was thus not recommended as a preventative option for the ERC. Alternative shading options, such as fixed external shading, may prove more cost effective in mitigating the ERC's solar heat gains, and should be considered in further research.

From these results, it was concluded that a combination of insulation and lighting upgrades would provide the greatest benefit, in terms of thermal comfort, to the ERC, and would result in a more cost effective active cooling system, should one be proposed. The dissertation ended with recommendations for further work, including further analysis of ERC heating requirements in winter, and investigation into additional and alternative cooling methods, such as passive or solar cooling.

Table of Contents

Note: EBE Faculty: Assessment of Ethics in Research Projects form is appended after the end of the Dissertation.

List of Figures

List of Tables

Nomenclature

Abbreviations

Acronym	Description
°C	Degrees-Celsius (unit of temperature)
ANN	Artificial Neural Networks
AR5	Fifth Assessment Report of the Intergovernmental Panel on Climate Change on Climate Change Mitigation (2014)
ASHRAE	American Society of Heating, Refrigerating and Air-Conditioning Engineers
ASHRAE-55	ANSI/ASHRAE Standard 55: Thermal Environmental Conditions for Human Occupancy
BAU	Business-as-usual
BESTEST	NREL/IEA Building Energy Simulation Tests
CFD	Computational Fluid Dynamics
CSIR	Council for Scientific and Industrial Research, South Africa
DB	Dry-bulb Temperature
EPA	United States Environmental Protection Agency
ERC	Energy Research Centre
GBCSA	Green Building Council of South Africa
GHG	Greenhouse gas
GSSA	Green Star South Africa Certification
GW_{th}	Gigawatt – thermal capacity
HVAC	Heating, ventilating and air conditioning
IEA	International Energy Agency
IEA-SHC	International Energy Agency's Solar Heating and Cooling Programme
IPCC	Intergovernmental Panel on Climate Change
J	Joules (S.I. unit of energy)
kg	Kilogram (S.I. unit of mass)
K	Kelvin (S.I. unit of temperature)
kW	Kilowatt (unit of electrical power, equal to 1 000 Watts)
kW_{th}	Kilowatt (unit of heat flow)
kWh	Kilowatt-Hour (unit of electrical energy)
kWh_{th}	Kilowatt-Hour (unit of thermal energy)
m	Metre (S.I. unit of length)
m^2	Square-metre (S.I. unit of area)
m^3	Cubic-metre (S.I. unit of volume)
NPV	Net Present Value
NREL	National Renewable Energy Laboratory, United States
PET	Polyethylene Terephthalate (plastic material)
PF	Polyester fibre insulation material
PMV	Predicted Mean Vote (thermal comfort index)
PMV	Predicted Mean Vote
PPD	Predicted Percentage of Dissatisfied
SABS	South African Bureau of Standards
SANEDI	South African National Energy Development Institute
SANS	South African National Standards
UCT	University of Cape Town
US-DOD	Department of Defence, Unites States government
US-DOE	Department of Energy, United States government
W	Watt (S.I. unit of power)
WC	Bathroom (water closet)

Symbols

Symbol	Description [unit]
$h_{c,clo}$	Convective heat transfer coefficient at clothing surface [W/m^{2}K]
h_c	Convective heat transfer coefficient [W/m^{2}K]
$h_{r,clo}$	Radiative heat transfer coefficient at clothing surface [W/m^{2}K]
h_r	Radiative heat transfer coefficient [W/m^{2}K]
C_m	Thermal capacitance [J/K]
E_{res}	Latent heat loss through respiration [W/m^2]
E_{sk}	Latent heat loss through the skin [W/m^2]
F_{object}	View factor for a specific object in radiation heat transfer
P_H	High pressure of an absorption refrigeration cycle [kPa or bar]
P_L	Low pressure of an absorption refrigeration cycle [kPa or bar]
Q_H	Heat rejected to heat sink at T_H [W]
Q_{HVAC}	Heating or cooling load provided by active (HVAC) system
Q_L	Heat removed (cooling load) from cooled space in air conditioning [W]
$Q_{LW,I}$	Internal long-wave radiation [W]
$Q_{LW,O}$	LW radiation at external building surfaces [W]
Q_{LW}	Long-wave radiation [W]
$Q_{SW,lights}$	Short-wave radiation from interior lighting [W]
$Q_{SW,sol}$	Short-wave solar radiation [W]
Q_{abs}	Heat removed from absorber by cooling loop [W]
$Q_{c,res}$	Convection heat loss through respiration [W/m^2]
$Q_{c,sk}$	Convection heat loss through the skin [W/m^2]
Q_{cond}	Heat transfer by conduction [W]
$Q_{conv,I}$	Internal surface convection [W]
$Q_{conv,O}$	External surface convection [W]
Q_{conv}	Convection heat transfer [W]
Q_e	Absorption refrigeration cooling effect (heat removed from chilled water loop through evaporator) [W]
Q_{gen}	Heat input to generator in absorption refrigeration cycle [W]
$Q_{inf+vent}$	Sensible heat transfer effects from infiltration and ventilation
Q_{out}	Heat removed from condenser by cooling loop [W]
Q_r	Heat transfer by radiation [W]
Q_{stored}	Heat stored in an object, based on its thermal mass [J]
S_{co}	Heat stored in the body core[W/m^2]
SQ_{cool}	Sensitivity of annual cooling requirement [%]
$SQ"_{peak}$	Sensitivity of peak cooling load [%]
S_{sk}	Heat stored in the skin surface [W/m^2]
T_∞	Fluid temperature [K or °C]
T_{DB}	Outdoor dry-bulb air temperature [K or °C]
T_H	Ambient temperature of heat sink in air conditioning application [K or °C]
T_L	Temperature of cooled space in air conditioning application [K or °C]
T_{SH}	Temperature of the generator heat source in absorption refrigeration [K]
T_a	Indoor air temperature [K or °C]
T_o	Operative temperature [K or °C]
T_s	Surface temperature [K or °C]
W_{in}	Work input to an air-conditioning refrigeration cycle [W]
q_i	Heat flux response at time i [W/m^2]
α_d	Thermal diffusivity [W/mK]
α_s	Solar azimuth angle [° or rad]
β_s	Solar angle of altitude [° or rad]
A	Surface area [m^2]
COP_R	Coefficient of performance of electric refrigeration

Symbol	Description [unit]
$COP_{ab,C}$	Coefficient of performance of ideal (Carnot) absorption refrigeration
COP_{ab}	Coefficient of performance of absorption refrigeration
EER	Energy efficiency ratio of a cooling system [Btu/Wh]
L	Thermal load acting upon a body [W/m^2]
M	Rate of metabolic heat production [W/m^2]
PMV	Predicted Mean Vote
PPD	Predicted Percentage of People Dissatisfied [%]
R	Thermal resistance (R-value) [m^{2}K/W]
$R_{ceiling}$	Thermal resistance of the ceiling [m^{2}K/W]
$SEER$	Seasonal energy efficiency ratio of a cooling system [Btu/Wh]
U	Thermal transmittance (U-value) [W/m^{2}K]
V	Material volume [m^3]
W	Work done by the body [W/m^2]
c	Material specific heat capacity [J/kgK]
d	Thickness of a material [mm]
di	Insulation thickness [mm]
k	Thermal conductivity [W/mK]
k	Material thermal conductivity [W/mK]
ε	Surface emissivity
ρ	Material density [kg/m^3]
σ	Stefan-Boltzmann constant [W/m^{2}K^4]
ω	Absolute humidity ratio [$g_{water\ vapour}/g_{air}$]

1. Introduction

The purpose of good commercial building design is to ensure occupants can work in conditions that are comfortable and conducive to productivity. In particular, buildings should provide indoor environmental conditions that provide thermal comfort to occupants (Huizenga et al, 2006:393), for their physiological and psychological health, and to encourage productivity (Wagner et al, 2007:758).

Building designers are also faced with the challenge of sustainability. The Fifth Assessment Report (AR5) of the Intergovernmental Panel on Climate Change (IPCC) found that buildings accounted for 32% of global final energy consumption in 2010 – of which 40% was used for space heating and cooling – and that building energy use could more than double by 2050, compared to 2010 levels (IPCC, 2014:681). There is hence a growing need for alternative, low energy space heating and cooling solutions.

Within this context, the Energy Research Centre (ERC) is considering retrofitting its offices with measures to improve regulation of internal thermal conditions, while minimising increase in its energy use. The current building design causes thermal discomfort to occupants in both summer and winter, which affects the well-being and productivity of the staff and students who work there.

This dissertation examines summer discomfort in the ERC, caused by high internal air temperatures and unregulated humidity. Thermal conditions under existing building properties are characterised, and annual cooling energy requirements are estimated. Thereafter, the impact of a selection of preventative cooling retrofits on the predicted cooling load and energy requirements are assessed. It is hypothesised that, by these means, the energy requirements of a potential active cooling system would be lowered, compared with a system designed to cool the ERC under its current condition. These preventative measures would thus provide relative savings in energy costs, and reduce the environmental impact of thermal comfort provision at the ERC.

1.1. Background to the Energy Research Centre

The Energy Research Centre is located on the sixth floor of the north wing of the Menzies building at the University of Cape Town in South Africa. Menzies houses the Mechanical Engineering Department, and comprises lecture theatres, classrooms, offices, workshops, laboratories and computer labs. Figure 1-1 shows part of the building, with the exterior of the ERC highlighted on the top level. The ERC area itself comprises several offices, a bathroom, small kitchen, lounge and two seminar rooms. The total floor area of the ERC is 695 m^2. The ERC has, on average, thirty research staff, and provides postgraduate teaching and supervision for up to twenty students.

Figure 1-1: North-west corner of Menzies; the ERC exterior, on the top floor, is highlighted within the red lines

The ERC area of Menzies has been sub-optimally designed from a thermal energy perspective. The external walls are constructed with plastered concrete, without insulation or water proofing, while the ceiling has only sporadic insulation, with large gaps negating resistance to heat transfer through the ceiling boards. Sliding windows extend around the perimeter of the ERC envelope, and are single glazed with a solar film layer on the inner surface of the glass, and partial external shading provided by overhangs extending off the building's pitched roof. The solar film reduces glares, but also limits daylight entry such that occupants typically work with the interior fluorescent lights on. These are regulated by magnetic ballasts, which emit waste heat, and provide some areas of the ERC with excessive illumination.

The ERC does not have an active thermal conditioning system. Occupants use desk fans and electric heaters for thermal comfort, and have complained of discomfort in summer and winter. This research is motivated by this problem, and seeks to examine energy efficient solutions that would improve thermal comfort.

1.2. Research objectives

The dissertation aims to respond to the following problem statements:

1. Characterise thermal conditions and heat gains on the ERC office area, and quantify cooling load requirements to minimise summer thermal discomfort for ERC occupants.
2. Assess how cooling requirements may be reduced through implementation of a selection of preventative cooling retrofits.

The objectives of the research are to:

- Characterise the ERC's typical internal environmental conditions and predicted levels of thermal discomfort, under current building conditions, particularly during summer;
- Quantify annual and periodical heat gains and losses of the ERC interior;
- Estimate '*Base Case*' cooling load and cooling energy requirements of the ERC (without intervention) to alleviate summer thermal discomfort;
- Assess the impacts of a selection of preventative cooling techniques on the *Base Case* cooling requirements; and
- Evaluate cost effectiveness of each preventative measure relative to estimated costs of an active cooling system designed to meet the *Base Case* cooling load.

1.3. Methodology

The approach of the dissertation was to characterise ERC thermal performance through a series of energy simulations, performed on a computer model of the physical and thermal properties of the ERC building envelope. The model was developed in *DesignBuilder* (v4.7) and simulated through the built-in *EnergyPlus* simulation engine (v8.3); the full simulation methodology is described in Chapter 3.

The modelling approach of the study draws on the methodology of a similar dissertation by Neethling (2011), in which the energy performance of a building at the University of Stellenbosch was compared with a notional building modelled according to provisions in the South African National Standard on National Energy Efficiency (SABS-SANS 204:2011).

Table 1-1 summarises the set of scenarios investigated in this study. Potential preventative cooling measures were identified based on the *Current* and *Base Case* results, and were analysed cumulatively, rather than individually, to show the impact of progressive implementation. Chapter 3 describes the results of the *Current* and *Base Case* simulation results, while Chapter 4 discusses the results of simulation analysis of the selected prevented measures.

Table 1-1: Description of scenarios investigated in this dissertation

Scenario	Description
ERC: Current	Characterisation of heat gains and thermal conditions of the ERC under existing conditions
ERC: Base Case	Estimate of required cooling load and energy, based on existing conditions, to alleviate summer thermal discomfort
Preventative Retrofit Impacts	Impact of progressive (cumulative) preventative measures on cooling load and energy requirements

Finally, cost effectiveness of each preventative measure is evaluated in Chapter 5, based on the following methods:

- Installation cost estimates of a theoretical active cooling system were made based on peak cooling loads determined from simulation and a derived rand-per-kW_{th} cost relationship for South African air conditioning systems (Buys & Mathews, 2005).
- Annual operational costs were forecast for the theoretical systems under the *Base Case* and successive preventative scenarios.
- A payback period was determined for each (progressive) preventative measure, representing the length of time for savings in cooling energy costs to fully offset additional installation costs of the respective measure(s).
- Finally, Net Present Values (NPV) were determined from annual savings calculated for each measure, relative to the *Base Case*.

1.4. Scope and Limitations

The following limitations apply to the research scope of the dissertation.

1. ERC cooling

The study is limited to considering cooling during Cape Town's summer, and excludes heating in winter. Cape Town's summer typically occurs from December through March, where outdoor dry-bulb (DB) temperature maximums exceed 33 °C. While it is acknowledged that comprehensive thermal comfort analysis should consider year-round building conditions, the scope is limited here to energy efficient cooling only. ERC heating is left for further work.

2. Preventative cooling limitations

The preventative techniques assessed in this research do not represent an exhaustive list of possible options for the ERC. The measures were chosen based on the most significant heat gain sources identified in the *Current* and *Base Case* analysis, and were thus limited to ceiling insulation, lighting energy efficiency and internal window shading. Additional measures, such as altering the colour of the envelope, or the use of plants or vegetation for shading, could also be effective, but are not considered here. Additionally, passive cooling (e.g. night flushing or evaporative cooling) and solar cooling, while briefly introduced in the literature review, are not investigated with respect to the ERC in this study.

3. High level active cooling analysis

Finally, the study omits detailed design or specification of an actual active cooling system. Brief discussion is provided from literature on the type of air-conditioning system the ERC might consider, but explicit identification of such a system is not undertaken here. Rather, assumptions on the cost of a hypothetical system are made, based on the cost factor findings of Buys and Mathews (2005), to facilitate theoretical cost evaluation. Further analysis of active cooling systems is left for further work.

2. Literature Review

This chapter presents a review of the literature that informed this research. The environmental context of energy efficient cooling is expanded, followed by a review and description of the rational method for thermal comfort modelling. The fundamentals of heat transfer are revised in the context of analytical characterisation of building heat flow, and building energy modelling techniques are reviewed, with background provided on *EnergyPlus* and *DesignBuilder*. The remainder of the literature review discusses space cooling, first by introducing the preventative techniques assessed in this dissertation, followed by additional discussion on passive cooling and solar cooling technology – however, these concepts are not investigated further in the context of ERC cooling here.

2.1. Environmental Impact of Space Cooling

The IPCC's Fifth Assessment Report found that in 2010 the building sector accounted for approximately 32% of global final energy consumption and 30% of global electricity use, as well as 19% of all direct and indirect greenhouse gas (GHG) emissions (IPCC, 2014:681). Cooling accounted for only 7% of building energy consumption in 2010, which is relatively low compared to shares of 33% for space heating and 16% for lighting (IPCC, 2014:681). In the European Union (EU), for example, while buildings account for 40% of total energy consumption, cooling accounts for only 10% of building energy use (ECOFYS, 2015:2).

However, cooling energy use typically exceeds heating in warmer and more tropical regions of the world. In Singapore, for example, cooling accounts for 60% of electricity end use in the building sector, which itself is responsible for 31% of total annual electricity consumption (Chua et al, 2013:87). A dissertation by Martin (2011) calculated the average energy intensity of a sample of commercial buildings in Cape Town, and found that, on average, 110 kWh/m^2 was consumed annually for cooling and ventilation, compared with only 55 kWh/m^2 for heating (Martin, 2011:12).

The International Energy Agency's (IEA) *World Energy Outlook 2015* notes that "higher incomes, a growing population, demographic changes and structural changes in many economies [could] contribute to [building] energy demand increasing by nearly one-quarter by 2040" (IEA, 2015:77). In China, for example, notable growth in cooling demand has already been observed, with around 64 million air conditioning units sold in 2013 alone (Davis & Gertler, 2015:5962). Future global cooling demand is at further risk of being exacerbated if average temperatures rise, as predicted, due to the effects of climate change (Ürge-Vorsatz et al, 2007:380).

These projections have severe implications for future building-environmental sustainability, particularly if the majority of the world's energy demand continues to be supplied by fossil fuels, as is forecast under the IEA's 'Current Policies' scenario (IEA, 2015:310). It is therefore within this context that alternative, sustainable cooling approaches must be considered, whereby thermal comfort can be provided with minimal further detriment to the surrounding environment.

2.2. Thermal Comfort

Within the context of environmental sustainability, the primary purpose of good commercial building design – to provide comfortable working spaces conducive to productivity – must still be prioritised. Inadequate thermal design can directly and indirectly affect occupants' mental and physical health, manifesting for example in complaints of 'sick-building syndrome' symptoms among building occupants (Redlich et al, 1997:1013). This section defines thermal comfort, and discusses methods for identifying and modelling design conditions that are conducive to occupant satisfaction.

2.2.1. Modelling Thermal Comfort

The American Society of Heating, Refrigerating and Air-Conditioning Engineers (ASHRAE) first developed ASHRAE Standard 55, on *Thermal Environmental Conditions for Human Occupancy*, in 1966. ASHRAE have subsequently published several updated versions of Standard 55. This study refers to the 2004 version, although a more recent edition was released in 2013 (but was not available to the author at the time of writing). ASHRAE Standard 55 defines thermal comfort "*that condition of mind which expresses satisfaction with the thermal environment*" (ASHRAE-55, 2004:4).

A person's experience of thermal sensation is governed physiologically by the rate of heat exchange between their body and their surroundings. However, as the ASHRAE definition implies, the notion of thermal comfort is highly subjective, and cannot be attributed to a universal set of psychrometric parameters. Perception of thermal comfort varies depending on activity level, personal preference, health, and ability to control or adapt to conditions. Indeed, Huizenga et al (2006) and Leaman and Bordass (1998) both found a lack of personal control to be the most common reason given when people reported thermal discomfort in buildings, suggesting a more psychological than physiological perception of comfort.

Two approaches have thus emerged to model thermal comfort:

1. The rational method
2. The adaptive method

The rational method is based on the physiological experience of thermal sensations, from which physical relationships between the body and the environment are quantified. This approach is supported, for example, by a survey study of more than 34 000 building occupants in North America and Finland, which showed high linear correlation between respondents' self-assessed productivity levels and temperature satisfaction (Huizenga et al, 2006:396).

The adaptive method meanwhile addresses a person's psychological experience of comfort, and requires analysis of data collection from field studies and surveys, as in Huizenga et al (2006). The underlying principle of the adaptive method is that a person is not a "passive recipient of thermal stimuli" (Brager & de Dear, 1998:84) but will respond to thermal scenarios by various different means.

This dissertation follows the rational method, based on the data and methodology of ASHRAE-55. While this approach may not fully account for human variability, it better fits the physical modelling and energy simulation process applied later in the study.

2.2.2. Human Thermal Balance

Povl Ole Fanger provided the foundational work on thermal comfort in buildings and developed a series of equations that modelled human physiological responses to environmental conditions (Fanger, 1982). These equations form the basis of physical thermal comfort modelling today, and are adopted in ASHRAE-55 as well as the 2013 ASHRAE *Handbook of Fundamentals*. At a high level, they are expressed as follows:

$$M - W = \left(Q_{c,sk} + Q_{r,sk} + E_{sk}\right) + \left(Q_{c,res} + E_{res}\right) + \left(S_{sk} + S_{co}\right) \text{ [W/m}^2\text{]} \quad (2\text{-}1)$$

Where:

- M is rate of metabolic heat production
- W is work done by the body
- $Q_{c,sk}$ and $Q_{c,res}$ are convection heat loss from the skin and through respiration respectively
- $Q_{r,sk}$ is radiant heat loss from the skin
- E_{sk} and E_{res} is evaporative heat loss from the skin and through respiration respectively
- S_{sk} and S_{co} are heat stored in the skin and body core, respectively.

Equation 2-1 includes sensible heat transfer, driven by temperature difference between the skin and surrounds, and latent heat transfer, due to water vapour evaporation off the skin.

Fanger (1982:25) showed that the body's heat balance is influenced by six variables:

1. Metabolic rate (the body's internal heat production)
2. Clothing insulation
3. Air temperature
4. Mean radiant temperature (average temperature of objects surrounding the body)
5. Air humidity
6. Air velocity

Air temperature and mean radiant temperature can be combined into a single parameter, *operative temperature*, as follows (ASHRAE-55, 2004:5):

$$T_o = \frac{h_{r,clo}T_{\bar{r}} + h_{c,clo}T_a}{h_{r,clo} + h_{c,clo}} \text{ [K]} \quad (2\text{-}2)$$

Where:

- $T_0, T_{\bar{r}}$ and T_a are operative, mean radiant and air temperature respectively
- $h_{r,clo}$ and $h_{c,clo}$ [W/m^{2}K] are the radiative and convective heat transfer coefficients at the body's clothing surface

2.2.3. Predicted Mean Vote

The ASHRAE thermal sensation scale was developed to quantify people's thermal sensations (ASHRAE-55, 2004:5), and is shown in Table 2-1.

Table 2-1: ASHRAE Thermal Sensation Scale (ASHRAE-55, 2004:5)

PMV Value	Thermal Sensation
+3	Hot
+2	Warm
+1	Slightly warm
0	Neutral
-1	Slightly cool
-2	Cool
-3	Cold

ASHRAE defines *Predicted Mean Vote* (PMV) as "an index that predicts the mean response of a large group of people according to the ASHRAE thermal sensation scale [shown in Table 2-1 (ASHRAE-55, 2004:3)]. PMV was conceived as a measure of the difference between heat flow required for a body to be in thermal comfort and actual heat flow the body experiences, and is expressed as follows (ASHRAE, 2013:9.18):

$$PMV = [0.303\exp(-0.036M) + 0.028]L \text{ [W/m}^2\text{]} \quad (2\text{-}3)$$

Where:

- L represents thermal load acting on the body
- M describes the body's internal heat production (as in equation 2-1)

M and L depend on combinations of the six comfort variables listed in § 2.2.2, and can be characterised by expanding Fanger's heat balance equation (2-1), as demonstrated in the ASHRAE Fundamentals Handbook (ASHRAE, 2013:9.3). Any combination of the six variables will produce a resulting PMV value.

For a given set of conditions, the *Predicted Percentage of people Dissatisfied* (PPD) can be found from the PMV value (ASHRAE, 2013:9.18):

$$PPD = 100 - 95\exp[-(0.03353PMV^4 + 0.2179PMV^2)] \text{ [\%]} \quad (2\text{-}4)$$

The PPD equation (2-4) shows that, even for thermally neutral conditions (PMV = 0), 5% of people are still expected to experience discomfort, reinforcing the human element of thermal comfort perception.

2.2.4. ASHRAE Comfort Zone

ASHRAE applies the PPD principle to define the ASHRAE thermal comfort zone, defined as "a range of operative temperatures that provide acceptable thermal environmental conditions". The definition implies an upper and lower bound of T_o in which a given combination of humidity, air velocity, metabolic rate and clothing insulation will be comfortable for a specified threshold number of occupants (typically PPD $\leq$ 20%, or PMV ϵ $[-0.5,0.5]$).

The ASHRAE comfort zone is shown visually on a psychrometric chart in. Figure 2-1. The chart shows the range of operative temperature T_0 and humidity ω predicted to be comfortable for 80% or more occupants, assuming air speeds not greater than 0.2 m/s, and human metabolic rate between 1.0 and

1.3 Mets (1 Met = 58 W/m^2). Separate comfort zones are shown for summer and winter clothing, since the latter has greater insulation as people typically dress more warmly in winter.

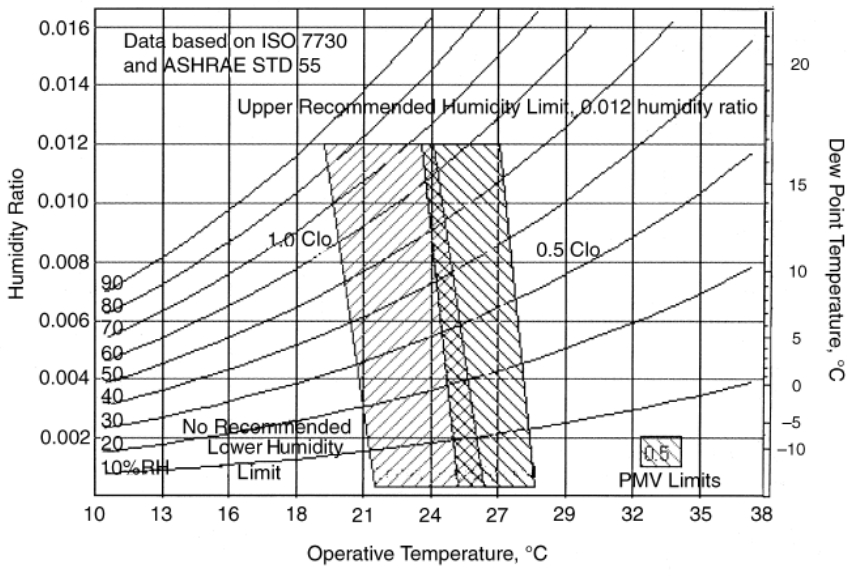

Figure 2-1: An example of the ASHRAE Comfort Zone, shown for summer and winter clothing (ASHRAE-55, 2004:5)

This dissertation predicts annual thermal comfort in the ERC based on the ASHRAE-55 comfort zone, with assumptions of typical summer and winter clothing insulation and typical office activity levels within the ERC. The following section revises how a building's internal environment is affected by heat flow, to and from the building space.

2.3. Building Heat Flows

The psychrometric conditions of a building are affected by sensible heat flows, which cause changes in temperature, and latent heat flows, which change the moisture content (i.e. humidity) of internal air. Buildings are exposed to various heat transfer components, as illustrated in Figure 2-2.

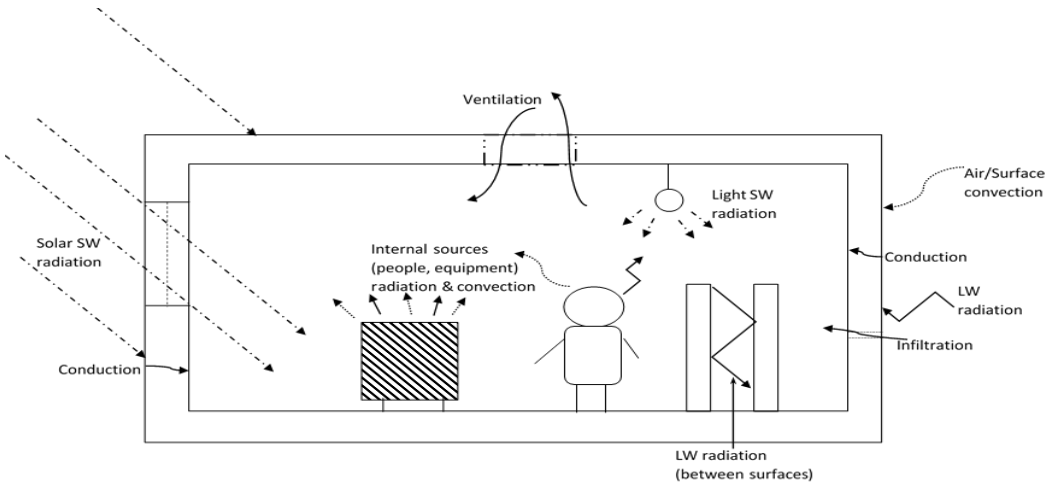

Figure 2-2: Heat gains to an internal building space based on different modes of heat transfer

Sensible heat flows are governed by the principles of heat transfer, which are discussed in the following sub-section, while latent heat flows depend on the transfer of moisture to and from the building, through infiltration and ventilation. Discussion of hygrothermal behaviour of buildings is omitted from this review, as this dissertation is mostly concerned with sensible heat gains.

2.3.1. Heat Transfer

There are three modes of heat transfer, *conduction*, *convection* and *radiation*. Each of these is described as follows.

Conduction is driven by a difference in temperature difference, either between the surfaces of a material, or between two materials in contact, in proportion to the thermal conductivity and contact surface area of the material(s). This is expressed as follows, based on *Fourier's Law*:

$$Q_{cond} = \frac{kA(T_1 - T_2)}{d} \text{ [W]} \quad (2\text{-}5)$$

Where:

- Q_{cond} is rate of conductive heat transfer
- k is thermal conductivity [W/mK]
- A is surface area [m^2]
- T_1 and T_2 are temperatures of the hotter and colder surface/material respectively
- d is the distance between the two surfaces

Heat flows via conduction through the construction layers of a building envelope when a temperature difference occurs between the inner and outer building surface, from the warmer to cooler surface. Multiple layers of material are used in construction to increase the thermal resistance (also known as the *R-value*) of the building, to reduce the rate of heat transfer. The overall *R-value* of a building surface (e.g. external wall) is determined from the thickness and thermal conductivity of each layer:

$$R = \sum_i \frac{d_i}{k_i} = \frac{d_1}{k_1} + \frac{d_2}{k_2} + \cdots \text{ [m}^2\text{K/W]} \quad (2\text{-}6)$$

Thermal transmittance (or *U-value*) is defined as the inverse of thermal resistance:

$$U = \frac{1}{R} = \frac{1}{\frac{d_1}{k_1} + \frac{d_2}{k_2} + \cdots} = \sum_i \frac{k_i}{d_i} \text{ [W/m}^2\text{K]} \quad (2\text{-}7)$$

Equation 2-5 can thus be simplified for a building element as follows:

$$Q_{cond} = UA(T_1 - T_2) \text{ [W/m}^2\text{K]} \quad (2\text{-}8)$$

In reality, a material heated on one surface will not transfer all the heat to the other surface, but will store some of the heat, depending on its thermal capacity. This is determined by the material's thermal mass, which depends on its density, size and heat capacity (Van Straaten, 1967:7):

$$C_m = \rho c V \text{ [J/K]} \quad (2\text{-}9)$$

Where:

- C_m is thermal mass (or capacitance) of the body, indicating the amount of heat [J] required to raise its temperature by 1 Kelvin
- ρ is material density [kg/m^3]
- c is specific heat capacity [J/kgK]
- V is the material volume [m^3]

Heat energy stored by material would thus be found as:

$$Q_{stored} = C_m \Delta T \text{ [J]} \quad (2\text{-}10)$$

Where ΔT is the temperature difference across the material.

Convection

Heat transfer between a surface and a flowing fluid occurs by convection, the rate of which depends on the convective heat transfer coefficient as well as the temperature difference:

$$Q_{conv} = h_c A (T_s - T_\infty) \text{ [W]} \quad (2\text{-}11)$$

Where:

- Q_{conv} is rate of convection
- T_s and T_∞ are the surface and fluid temperature respectively
- h_c is convective heat transfer coefficient
- A is the area of the surface

Distinction is made between natural convection, which is driven by buoyancy forces due to variations in density and temperature, and forced convection, whereby external energy (e.g. from a pump, a fan, or wind flow) drives fluid flow.

The heat transfer coefficient h_c is not a constant fluid property, but varies depending on the type of fluid flow, the density and viscosity of the fluid, and the smoothness and temperature of the surface. The dynamic interaction of these variables makes the task of analytically modelling convection highly complex. Several algorithms have been presented in literature to model h_c for various geometries, orientations (i.e. vertical or horizontal surfaces), flow regimes (laminar or turbulent), and for natural and forced convection (e.g. Alamdari & Hammond, 1983; Awbi, 1998, Beausoleil-Morrison, 2000 and Fohanno & Polidori, 2006).

Radiation

Finally, heat transfer by radiation occurs with the exchange of electromagnetic waves between two or more objects at different temperatures, based on the following equation:

$$Q_r = \varepsilon\sigma A_s(T_s^4 - T_{sur}^4) \text{ [W]} \quad (2\text{-}12)$$

Where:

- Q_r is rate of radiant heat transfer
- ε is the surface emissivity of the body (indicating its ability to emit infrared energy)
- σ = 5.67 x 10^{-8} W/m^{2}K^4 is the *Stefan-Boltzmann constant* (Çengel & Boles, 2008:94)
- T_s and T_{sur} are the surface and surrounding temperatures respectively
- A_s is the object's surface area

Under typical commercial building conditions, at moderate temperatures, it may be reasonable to assume a constant radiation heat transfer coefficient h_r determined as follows (Neethling, 2011:20):

$$h_r = \varepsilon\sigma(T_s + T_{sur})(T_s^2 + T_{sur}^2) \text{ [W/m}^2\text{K]} \quad (2\text{-}13)$$

Buildings typically experience two forms of thermal radiation:

1. Longwave radiation (LW)
2. Shortwave radiation (SW)

LW radiation occurs between objects at different temperatures which emit and absorb thermal energy based on their view factors of each other. Internal building surfaces and objects at different temperatures will exchange radiant heat transfer until thermal equilibrium is reached, while electronic equipment and occupants continually release radiant heat into the room. For example, an external building surface may undergo heat exchange with the ground, dust particles in the sky, and other objects in its surroundings. This is represented in the following equation:

$$Q_r = \varepsilon\sigma A_s\left[F_{ground}\left(T_{ground}^4 - T_s^4\right) + F_{sky}\left(T_{sky}^4 - T_s^4\right) + F_{surr}(T_{surr}^4 - T_s^4)\right] \quad (2\text{-}14)$$

Where F_{ground}, F_{sky} and F_{surr} are view factors between the surface and the ground, sky and surroundings respectively, such that $F_{ground} + F_{sky} + F_{surr} = 1$ (Hall & Allinson, 2010: 20).

Typical SW heat gains are caused through absorption of direct and diffuse solar radiation, transmitted through external windows to the building interior. Solar radiation is transferred at shorter wavelengths, in the form of ultra-violet and infrared rays directly from the sun, and contains greater energy than LW radiation (Clarke, 2001:232). Incident solar radiation on external surfaces will be partly absorbed and partly reflected (depending on the surface's absorptivity and reflectivity). Thereafter, it will emit LW radiation back into the surrounding environment, based on the surface's emissivity. The

degree to which an opaque surface absorbs or reflects solar radiant energy depends partly on its colour, with lighter surfaces and reflective coatings having greater reflectivity than darker surfaces.

The rate of direct incident solar radiation on a building surface depends on its orientation and the position of the sun, expressed in terms of its angle of altitude and azimuth angle (the sun's perpendicular projection onto the ground relative to true north). The sun's daily path, relative to a location on earth, depends on the latitudinal position and time of year. In Cape Town the sun reaches greatest altitude in summer (December). Fixed shading devices can be designed which utilise this difference to regulate the amount of sunlight entering the building in summer and winter.

2.3.2. Heat Balance Method

Pedersen et al (1997) developed the Heat Balance Method, derived from the *First Law of Thermodynamics*, to quantify the various heat transfer processes that occur in buildings. This method is included in the ASHRAE Fundamentals Handbook (ASHRAE, 2013) and forms the basis of the iterative solving algorithms of the *EnergyPlus* simulation software.

The Heat Balance Method applies several simplifying assumptions to calculate the heat exchanges, the most notable of which are as follows (Pedersen et al, 1997:461):

- All air in a thermal zone is well stirred, with continuous uniform temperature distribution throughout the space
- Conduction through the building envelope occurs in one direction only.

Heat balances acting on a building are calculated for four separate but connected processes, listed below (ASHRAE, 2013:18.15):

1. Convection and radiation at outside building surfaces
2. Conduction through the fabric (walls and roof)
3. Convection and radiation off internal surfaces
4. Heat exchange with the internal air

These balances are summarised in equation form as follows (ASHRAE, 2013:18.15):

External surface heat balances: $Q_{SW,sol} + Q_{LW,O} + Q_{conv,O} - Q_{cond} = 0$ (2-15)

Where:

- $Q_{conv,O}$ is convection exchange between the external surface and surrounding air
- $Q_{LW,O}$ is LW radiation exchange between the external surface and surrounding objects
- $Q_{SW,sol}$ is SW solar radiation
- Q_{cond} is heat flux through the building envelope from the outer to inner surface

Transient conduction through the fabric

Building heat flow through building elements depends on the surface temperatures, which fluctuate depending on solar radiation, wind flow and outdoor and indoor temperature variation, rather than remaining constant as assumed under steady-state conditions. Transient conduction depends on thermal mass of an element in addition to its conductivity, and is defined below according to Fourier's Heat Equation:

$$\nabla^2 T = \frac{\rho c}{k}\frac{\partial T}{\partial t} = \frac{1}{\alpha_d}\frac{\partial T}{\partial t} \quad (2\text{-}16)$$

Where:

- α_d is thermal diffusivity, the rate at which materials reach thermal equilibrium based on unsteady temperature change (Hall & Allinson, 2010: 8)
- ρ is density, c is specific heat capacity and k thermal conductivity
- $\frac{\partial T}{\partial t}$ indicates variation of surface temperature with time
- $\nabla^2 T$ represents spatial temperature gradient across the material

For unidirectional heat flux, as is assumed in building thermal modelling, $\nabla^2 T$ can be simplified to $\frac{\partial^2 T}{\partial x^2}$. Methods for solving equation 2-16 are discussed in § 2.4.1 to follow.

Internal surfaces: $Q_{cond} + Q_{LW,I} + Q_{SW,lights} + Q_{SW,sol} + Q_{conv,I} = 0$ (2-17)

Where:

- Q_{cond} is conduction through the envelope from the outer to inner surface
- $Q_{LW,I}$ is LW radiation exchange between the internal surfaces and internal objects
- $Q_{SW,lights}$ is SW radiant heat gains from internal lighting
- $Q_{SW,sol}$ is internal solar heat gain through external windows
- $Q_{conv,I}$ is convection exchange between the internal surfaces and surrounding air

Finally, a heat balance equation is solved for the air within the thermal zone itself:

Air heat balance: $Q_{conv,I} + Q_{inf+vent} + Q_L = 0$ (2-18)

Where:

- $Q_{conv,I}$ is convection exchange between the internal surfaces and surrounding air
- $Q_{inf+vent}$ is the heat transfer effect from ventilation and/or infiltration
- Q_L is the cooling (or heating) load supplied to the thermal zone

The following section discusses energy modelling and simulation techniques that have emerged in order to characterise and solve heat balance equations for buildings and other large complex systems.

2.4. Building Energy Modelling

It is impractical to analytically solve all heat exchanges of a building over a long period of time with acceptable accuracy for cooling load calculations. Variations arise from dynamic external weather conditions, as well as randomness in occupancy schedules and activity levels, making analytic solutions complex and computationally expensive (Neto & Fiorelli, 2008:2169).

Energy simulation methodologies have therefore emerged that are capable of predicting thermal behaviour and energy performance of buildings based on models of the building construction, occupancy, prevailing weather conditions at the site, in addition to other influencing factors (Foucquier et al, 2013:274). Computer software has been developed that can perform whole-building simulations, of varying size and complexity, and produce results in short time periods with good precision (Crawley et al, 2008). This allows 'bottom-up' modelling of building energy scenarios, with the accuracy of predictions dependent on the quality of input data.

Building energy modelling techniques fall into three categories (Foucquier et al 2013:274; Zhao & Magoulès, 2012:3586):

1. *Physical methods*: energy modelling based on physical properties and principles, using the heat balance method or similar rational disaggregation
2. *Statistical methods:* statistical regression applied to correlate building energy flows with influencing variables, using historical data sets
3. *Artificial intelligence methods*: mathematical models of varying complexity that attempts to predict the outputs a physical system will produce from specified inputs, based on observations and learning from previous scenarios of the same system.

Statistical models use regression analysis to evaluate the correlation between two variables, such as energy consumption with a particular influencing variable, based on historical data. Regression methods have been used in literature for predicting building energy consumption based on driving climatic variables. Bauer and Scartezzini (1998), for example, developed a simplified correlation method to account for solar and internal heat gains on a building, and the effects on annual energy performance, for both heating and cooling seasons.

Artificial Neural Networks (ANN) are the most common form of artificial intelligence method used in building modelling, and are similar to non-linear regression models. These typically comprise a series of mathematical models, of varying complexity, which attempt to simulate the functioning of a biological neural network (Neto & Fiorelli, 2008:2172). An ANN model of a system does not require detailed information about that system, but instead "learns" the relationship between input parameters and output variables from historical data (Kalogirou & Bojic, 2000:482). Disadvantages of ANN, according to Neethling (2011:15), are the "black box" nature of the mathematical models used. The direct cause of a particular output is difficult to attribute to specific inputs, while computational time of ANN modelling may greatly exceed physical model simulation.

This dissertation applies physical modelling and simulation methods to characterise ERC heat gains and cooling loads, similar to the approach of Neethling (2011). These techniques are discussed further in the following sub-section.

2.4.1. Physical Energy Simulation

Physical building energy models are developed based on quantified physical properties of the building and its environment (internal and external), to predict energy flows and thermal responses. Input data required for physical energy modelling includes physical properties of the building envelope, weather data, and building operation and occupancy schedules (Zhao & Magoulès, 2012:3587). The data is input into a simulation programme, which iteratively solves a system of equations, based on the heat balance method, to determine building heat transfer, energy balances and environmental conditions, at specified intervals over a defined period of time.

Two categories of physical simulation techniques have emerged, namely (Clarke, 2001:19; Luo et al, 2010:19):

1. Numerical/Computational Fluid Dynamics (CFD) methods
2. Response Function Methods

CFD approaches use the finite volume method or finite difference method to characterise building energy balances. The building space, surface or system is discretised into a global mesh of control volumes, over which a heat balance equation is formulated and solved (Foucquier et al, 2013:274).

Response function methods, by contrast, are formulated based on the thermal response of a building element to a unit pulse of some thermal excitation, such as heat flux through a wall (Gouda et al, 2002:1255). Response function methods were first developed in the 1960s and 1970s, when the large computational effort required for detailed finite volume methods was not always available or feasible (Gouda et al, 2002:155).

Clarke (2001:19) argues that numerical methods are preferable to response functions for building simulation, since finite volume spatial discretisation more accurately models heat flow through the building envelope material, and can solve more complex flow-path interactions (in multiple directions). However, Luo et al (2010) found that both response function and finite volume methods were able to simulate surface heat flux through single and two-layered walls and provide results with good correlation to experimental data.

This dissertation therefore focuses on response function methods, and in particular conduction transfer functions. These methods are used by the *EnergyPlus* simulation engine, which was used to simulate a computer model of the ERC in this dissertation, as discussed further on.

2.4.2. Response Function Methods

The premise of response function methods is that the response of a physical system to a certain excitation can be predicted and quantified, and that the net response of the system to two or more

excitations is equivalent to the sum of the responses caused by each individual excitation (i.e. the principle of superposition applies).

This theory was first applied to building energy modelling by Stephenson and Mitalas (1967), who determined that the thermal response of a building to multiple heat stimuli could be found from the summation of individual responses to each stimulus. Unit response functions were developed to model the response of a building system or thermal load to a unit time series excitation function, e.g. solar radiation incident upon a surface for 1 time interval Δt then reduced to 0 for subsequent time intervals $2\Delta t, 3\Delta t, \ldots$ (i.e. solar radiation profile of $1, 0, 0, \ldots$ for time series $\Delta t, 2\Delta t, 3\Delta t, \ldots$).

The time series response of the system to the unit excitation is defined as the *response factor* of the system (Stephenson & Mitalas, 1967). For example, the heat flux response q_i at time i to a surface temperature pulse T, of time series $(1,0,0, \ldots)$, can be determined from the response factor series r_i (Duska et al, 2006:8):

$$q_i = r_i \cdot T \text{ [W/m}^2\text{]} \tag{2-19}$$

The overall response of a system to a series of multiple excitations (e.g. multiple heat gains to the surface of a building) is determined from the summation of the response factors for each stimulus (Mitalas & Stephenson, 1967). The heat balance of a thermal zone can thus be modelled based on the combination of a series of response factors for each mode of heat transfer acting upon the zone, as demonstrated in Mitalas and Stephenson (1967).

2.4.3. Conduction Transfer Functions

Stephenson and Mitalas expanded on the response factor method in several publications through the 1970s. Through these developments, the conduction transfer function methodology emerged as a means of iteratively solving one-dimensional conduction through a wall, based on a series of expressions combining heat flux response factors at each surface for influencing heat transfer components (convection and radiation).

These expressions can be resolved with the use of *Laplace transforms*, as was demonstrated in Mitalas (1978), whereby the output response of a system to some input can be expressed through z-transforms, and related by a z transfer function (Mitalas, 1978):

$$O(z) = I(z) \cdot G(z) \tag{2-20}$$

Where $O(z)$ is the output response, $I(z)$ the inpur function and $G(z)$ the transfer function. Equation 2-20 can be rearranged to express $G(z)$ in terms of the input and output functions $I(z)$ and $O(z)$, and expanded using z-transforms, representing time intervals of j length ($j = \Delta t$):

$$G(z) = \frac{O(z)}{I(z)} = \frac{O_t + O_{t-j}z^{-1} + O_{t-2j}z^{-2} + \cdots + O_{t-n}z^{-n}}{I_t + I_{(t-j)}z^{-1} + \cdots + I_{t-m}z^{-m}} \tag{2-21}$$

$G(z)$ itself can be expanded in terms of a series of coefficients of the system transfer function:

$$G(z) = \frac{a_0 + a_1z^{-1} + a_2z^{-2} + \cdots + a_mz^{-m}}{1 + b_1z^{-1} + \cdots + b_nz^{-n}} \tag{2-22}$$

By combining the equation 2-21 and 2-22, the output of the system at time t can be determined from the time series of inputs over time-steps $(t-j, t-2j, \dots, t-m)$, and the time series of previous outputs at $(t-j, t-2j, \dots t-n)$ as follows (Duska et al, 2006:9):

$$O_t = (I_t a_0 + I_{t-j} a_1 + I_{t-2j} a_2 + \cdots + I_{t-m} a_m) - (O_{(t-j)} b_1 + O_{t-2j} b_2 + \cdots + O_{t-n} b_n) \quad (2\text{-}23)$$

Duska et al (2006:9) showed that this expression can be rewritten in terms of conductive flux through a wall's inner (2-24a) and outer (2-24b) surfaces, A and B, at time t as follows:

$$\dot{q}_{A,t} = \sum_{j=0}^{m}(T_{A,m-j} \cdot a_{A,j}) - \sum_{j=0}^{m}(T_{B,m-j} \cdot a_{B,j}) - \sum_{j=1}^{n}(\dot{q}_{A,t-j} \cdot b_j) \quad (2\text{-}24a)$$

$$\dot{q}_{B,t} = \sum_{j=0}^{m}(T_{B,m-j} \cdot a_{B,j}) - \sum_{j=0}^{m}(T_{A,m-j} \cdot a_{A,j}) - \sum_{j=1}^{n}(\dot{q}_{B,t-j} \cdot b_j) \quad (2\text{-}24b)$$

Key to the implementation of the conduction transfer function method is accurately determining the z-transform coefficients $a_{0\to m}$ and $b_{1\to n}$. Examples of approaches include finite difference methods, as well as frequency domain and time domain methods. These are reviewed in detail in the literature, e.g. Clarke (2001) and Luo et al (2010), and are not discussed further here.

The full derivations of conduction transfer functions, as well as algorithms for modelling surface convection and LW and SW radiation, are also not shown here, but can be found, for example, in the Engineering Reference manual of the *EnergyPlus* simulation package (EnergyPlus, 2015). The software is discussed further in the following sub-section.

2.4.4. EnergyPlus Simulation Software

Several software packages are available that can perform whole-building energy simulations, including *BLAST*, *DOE-2.1E*, *ECOTECT*, *Energy Express*, *EnergyPlus*, *eQUEST*, *ESP-r*, *HEED*, *IDA indoor climate and energy*, *Power Domus*, *Trace 700*, and *TRNSYS* (Transient System Simulation Program). A detailed comparison of the performance capabilities, calculation methodologies and level of building detail accommodated by each of these packages was performed by Crawley et al (2008).

The U.S. Department of Energy's (US-DOE) *EnergyPlus* software was used in this study. The software was chosen due to its availability, as it is open source and available through the *GitHub* online repository, whereas other software packages with similar capabilities require the purchase of a paid license. Furthermore, *EnergyPlus* was commonly used in many studies found in literature, and has been rigorously validated and tested, as described further on.

EnergyPlus is a whole building energy simulation program, funded by the United States Department of Energy (US DOE), and developed in collaboration with the US National Renewable Energy Laboratory (NREL). The US DOE had previously supported a simulation program called *DOE-2*, while the US Department of Defence (US-DOD) sponsored *BLAST*. The two programs were merged in 1996 to form *EnergyPlus*, which thus draws legacy components from both predecessor programs (Crawley et al, 2001:320).

EnergyPlus is an "energy analysis and thermal load simulation tool" (EnergyPlus, 2016:5) capable of detailed calculation of heat gains and thermal conditions of building models, as well as performance analysis of heating, ventilating and air-conditioning (HVAC) systems. It functions purely as a simulation engine, with a basic user interface (pictured in Figure 2-3), and is best used with an additional program that provides a more user-friendly graphical user interface.

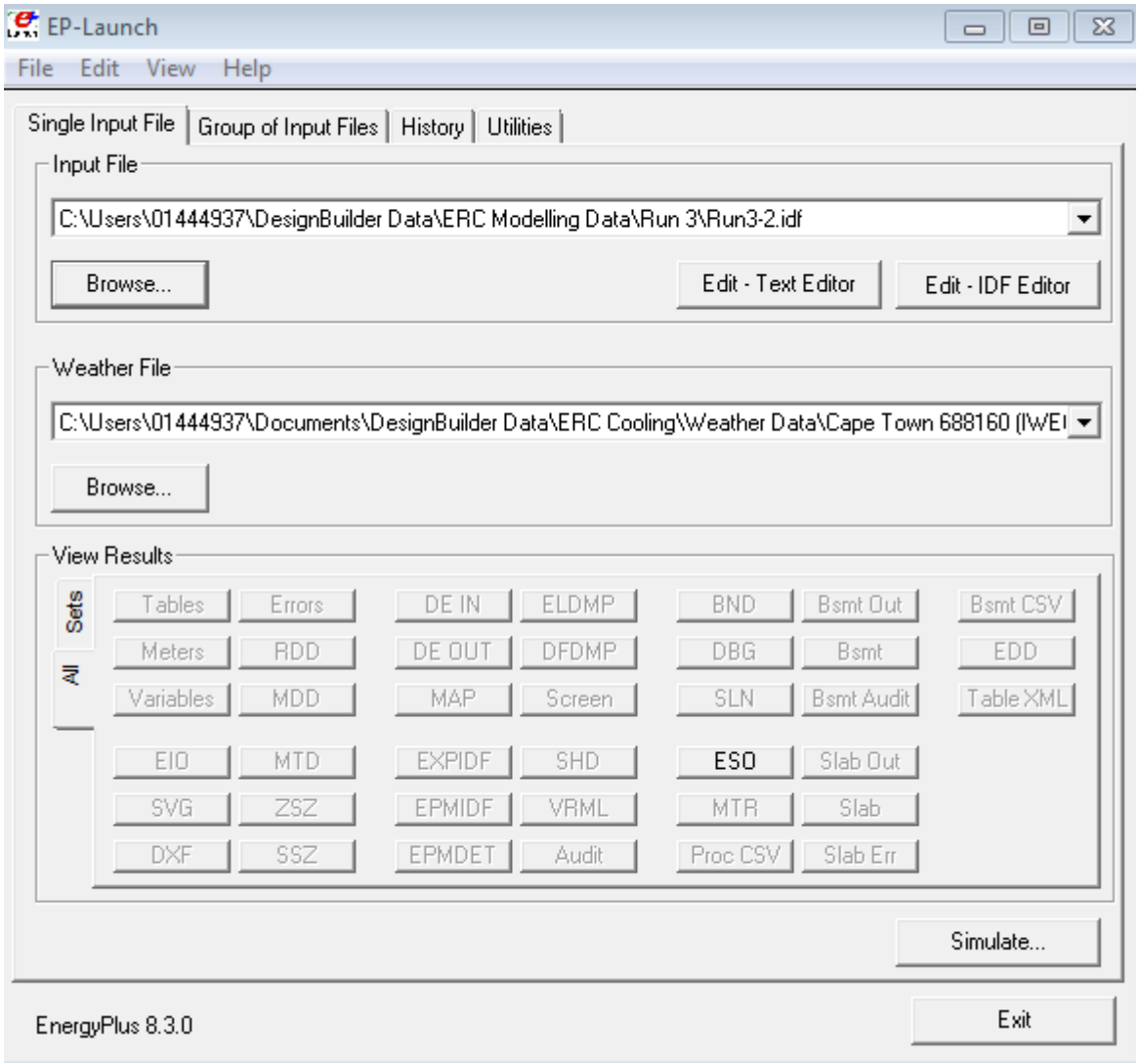

Figure 2-3: Screenshot of the EnergyPlus *simulation engine user interface*

EnergyPlus has been developed with a series of modules that model different components of building energy systems; for example, there are separate modules for simulating shading or daylighting, as well as different components, coils and loops of air conditioning equipment (Neethling, 2011:16). The software was originally written in *FORTRAN 90* (Crawley et al, 2001:321), but was later converted into C++, with the release of version 8.2 in 2014 (EnergyPlus, 2016:9). The modular nature of the code allows it to be developed concurrently by different developers, who can modify specific elements of one module without altering other modules or the overall program structure; this allows new features to be added with relative ease (Crawley et al, 2001:321). The code is open source and available on *GitHub* (EnergyPlus, 2016:9).

The *EnergyPlus* simulation engine performs a series of heat balance calculations at each time step, which calculate thermal loads and responses of the building thermal zones, as well as and the response of heating and cooling plant servicing the zone. The program is structured with three primary components (Crawley et al, 2004:295; Neethling, 2011:17):

1. Heat and mass balance simulation module, which simulates loads on the building
2. Building systems simulation module, which calculates the response of the building, as well as HVAC systems, components and loops to the loads
3. An overall simulation manager, which integrates the other components via a feedback loop, and controls the overall simulation process.

In this study, the UK-based commercial package *DesignBuilder v4.7* (released in 2016), was used as the graphical user interface (GUI) for *EnergyPlus*. A model of quantified physical properties of the ERC was developed in *DesignBuilder*, and simulated through the built-in *EnergyPlus* simulation engine (DesignBuilder, 2016). *DesignBuilder* was selected for its relative, intuitive ease of use, as well as its capabilities to present and report on simulation output data in a clear, elegant manner. A model of the Menzies building, created in *DesignBuilder*, is depicted in Figure 2-4.

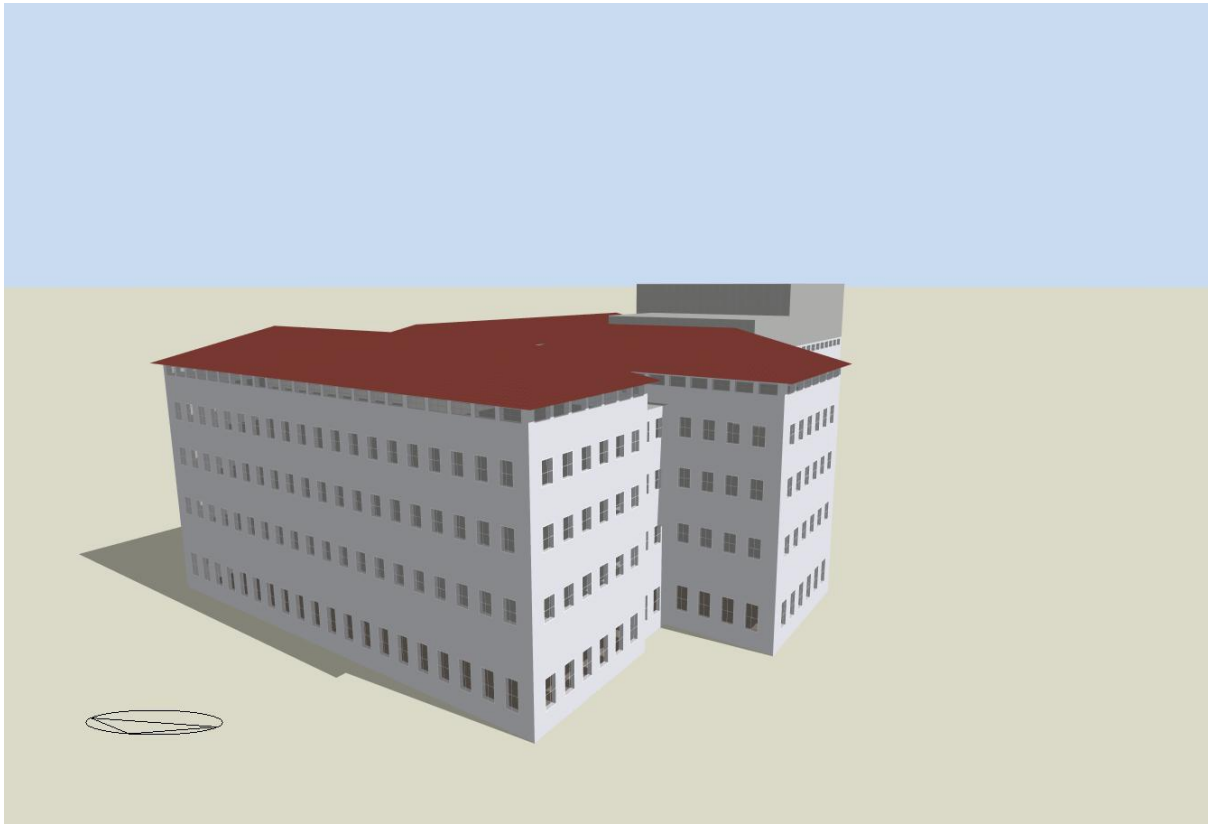

Figure 2-4: Menzies building model, as visualised in DesignBuilder

Initial modelling attempts were made using the *EnergyPlus OpenStudio* plug-in, also developed by NREL, which is compatible with *Google SketchUp Pro* (OpenStudio, 2016). However, *OpenStudio* was found to be more difficult to use without an extensive learning process, and geometry creation was more onerous than in *DesignBuilder*. The latter also included a more appropriate selection of construction, lighting, glazing and building activity templates in its data library, which reduced time spent on model characterisation.

2.4.5. Energy Modelling Validation

Models should always be validated, to the extent that it is possible, with actual measurement, in order to assess accuracy and improve reliability (Clarke, 2001:282). Models of physical systems have to be validated either through evaluation using empirical data measured from the actual system, or by comparison against results from other models with demonstrated accuracy and validation.

Comparison techniques are frequently applied in literature to validate energy models, whereby a model is calibrated based on results from another validated building energy model (Ryan & Sanquist, 2012:376). The advantage of comparison validation is that 'real' building data is not required, so long as the comparative model has itself been validated (Judkoff & Neymark, 2008:23), and allows validation of individual modelling parameters that have significant influence over the results.

NREL, in conjunction with the IEA, developed a series of building energy simulation test suites (BESTEST) to evaluate and benchmark energy modelling software packages (Judkoff & Neymark, 2013:1). *EnergyPlus* has been validated through various BESTEST suites, through which simulation results were shown to match analytical solutions or were within the bounds of other programs, as in Henninger and Witte (2014) for example. Older versions of *EnergyPlus* were tested over a range of cases by simulating different building specifications, according to ANSI/ASHRAE Standard 140-2007, and comparing the simulation results with results from 8 other programs (Henninger & Witte, 2010:17). In most cases, *EnergyPlus* results fell within the range of results of the other programs, and did not fall more than 15.6% out of the bounds of other programs at any stage (Henninger & Witte, 2010:23).

Loutzenhiser et al (2009) demonstrate comparative validation of *EnergyPlus* simulation by measuring energy flows through a window (glazing and frame) of a test cell in Switzerland, and comparing it with predictions from building energy simulation programs, including *EnergyPlus*, *DOE-2.1E* and *IDA-ICE*. The results showed a 5.8% magnitude difference in sample average between empirical and *EnergyPlus* data, compared with 6.0% for *IDA-ICE* and 9.9% for *DOE-2.1E* (Loutzenhiser et al, 2009:93).

Finally, another comparison technique is to contrast an existing building with a notional building of the same geometry and location, but with input data otherwise defined according to a given, validated test standard. This approach forms part of the GBCSA's *Green Star South Africa* (GSSA) Energy Calculator and Modelling Protocol for benchmarking new and existing energy efficient buildings, with notional buildings defined according to provisions in SANS 204:2011 (GBCSA, 2010:2). The application of this method was demonstrated in Neethling's assessment of the energy performance of a building at the University of Stellenbosch (Neethling, 2011).

2.5. Energy Efficient Cooling

The remaining sections of the literature review discuss cooling systems in building. This section describes a selection of preventative techniques for reducing building heat gains, namely:

1. Thermal insulation (§ 2.5.1.)
2. Energy efficient lighting (§ 2.5.2)
3. Window shading (§ 2.5.3)

§ 2.5.4 briefly introduces passive cooling techniques, which utilise natural energy flows to remove heat. These methods could potential be applied to the ERC, but are not analysed further in this dissertation.

2.5.1. Thermal Insulation

Thermal insulation layers increase the thermal resistance of a building envelope. This reduces conductive heat gain during summer, and mitigates heat loss through the envelope in winter. Reflective insulation can also be applied, in which a reflective surface is used to create a radiant barrier for a surface exposed to an open space. Reflective insulation is not included here, but is reviewed for example in Lee and Lim (2016).

A simple case study by the GBCSA showed that the installation of 30mm polystyrene ceiling boards in low cost housing in South Africa reduced peak summer air temperatures by 4 – 6 °C, compared with houses without ceilings (GBCSA, 2012:4); the ceiling board acts as an insulation layer between the roof and the house interior.

A more detailed simulation study of buildings in Turkey showed that retrofitting extruded polystyrene insulation in walls, roofs and floors of buildings reduced peak cooling loads by up to 33%, relative to uninsulated buildings (Aktacir et al, 2010:602). Total insulation volume assessed in the study ranged from 61.50 m^3 to 128.93 m^3, with thicknesses ranging from 30 to 80 mm for each tested surface.

The results showed design cooling loads ranged by only 5.1% across the range of insulation volumes tested, compared to a 33% increase in cooling load when insulation was removed (Aktacir et al, 2010:602). This shows that sensitivity of thermal loads to fabric thermal resistance is reduced with increasing thermal resistance, and that significant improvements to cooling energy efficiency can be made with relatively small insulation thickness. Van Straaten (1967:67) noted that insulation, while greatly improving building heat regulation, is subject to “the laws of diminishing returns”.

Aktacir et al (2010) further showed that design capacity and installation costs of an active heating, cooling and ventilating (HVAC) system could be reduced by up to 22% with installation of insulation, while seasonal operating and maintenance costs of the system would be reduced by between 17% and 27%, depending on the type and thickness of insulation material installed (Aktacir et al, 2010:605).

Mathews et al (1999) conducted a general study on the potential energy saving impact of retrofit ceiling insulation installed across all South African households. Impacts were assessed via simulation of models representing typical South African households, with assumptions of typical floor area, plot

size and resident behaviour (Matthews et al, 1999:506). The study was very broad, and could not be verified from actual data of a representative sample, but nevertheless estimated that around 2 000 MW could potentially be saved in winter-peak electricity demand with ceiling insulation retrofits, through reduced heater usage (Matthews et al, 1999:512). Ceiling insulation was found to be more viable as a preventative retrofit measure than altering window sizes, building layout or building colour (Mathews et al, 1999:507).

Thermal conductivity properties of a selection of common insulation materials are shown in Table 2-2, from a range of literature sources. While thermal resistance is inversely proportional to thermal conductivity, it should be noted that actual heat gain through a building material is also dependent on other properties, such as density, heat capacity and moisture affinity (van Straaten, 1967:54).

Table 2-2: Thermal conductivity of common insulation materials from literature

Material	SANS 204:2011 (pp. 20)	Al-Homoud (2005:357)	Jelle (2011:2551)	Papadopoulos (2005:81)
Cellulose fibre	0.040		0.040 – 0.050	
Expanded polystyrene	0.035	0.035 – 0.040	0.030 – 0.040	0.029 – 0.041
Extruded polystyrene	0.028		0.030 – 0.040	0.025 – 0.035
Flexible glass fibre	0.040	0.040 – 0.045	0.030 – 0.040	0.030 – 0.045
Mineral wool	0.033		0.030 – 0.040	0.033 – 0.045
Polyester fibre blanket	0.046	0.040 – 0.042		0.041
Polyurethane foam	0.025	0.020 – 0.025	0.020 – 0.030	0.020 – 0.027

Health and safety should also be considered when selecting insulation materials. For example, an important property of any building material is its fire-resistance. Certain materials such as cellulose fibre, which is manufactured from recycled newspaper pulp, are more fire hazardous than fibreglass or rock wool (Papadopoulos, 2005:82). Additionally, while fibreglass is the most common form of ceiling insulation material in South Africa, exposure to the skin can cause mild to severe irritation (Al-Homoud, 2005:362), and there is some concern that it may be carcinogenic (Papadopoulos, 2005:82), although the US Environmental Protection Agency (EPA) recently concluded that the carcinogenetic risk of fibreglass is not reflected in most studies (EPA, 2016).

Notwithstanding health and safety factors, the findings of Aktacir et al (2010) and Mathews et al (1999) show that insulation should be one of the first considerations for improving thermal comfort, owing to the relative ease of installation and the ability to reduce cooling and heating energy requirements.

2.5.2. Energy Efficient Lighting

The IPCC's Fifth Assessment Report found that lighting accounted for 16% of global final energy consumption in commercial buildings in 2010 (IPCC, 2014:681). Lighting systems generate waste heat

in addition to light, and can cause large internal heat gains in buildings (Energy Star, 2006:4). However, lighting heat gains also reduce heating load requirements in winter (Sezgen & Huang, 1994), and there is thus some uncertainty as to whether improving lighting energy efficiency would produce a net saving in annual building energy consumption. This depends on the extent to which the reduction in cooling and lighting energy is offset by an increase in heating energy, with contrasting evidence in Sezgen and Koomey (2000) and Zmeureanu and Peragine (1999).

The net energy impact of a lighting upgrade project will depend on the type and location of the building, as well as existing lighting and HVAC systems in place, and other factors that make each case unique. However, for the purposes of this study, which only considers ERC cooling, it is clear that inefficient lighting will cause excessive heat gains to buildings during summer.

Lighting energy efficiency projects should follow a systematic approach that considers potential interactive effects of the lighting system on other building activities and energy systems. The best approach is one which optimises energy savings at facility level while minimising initial and maintenance costs (Neethling, 2011:59), and does not compromise the provision of quality lighting for occupants to perform their designated tasks.

The types of measures implemented in lighting efficiency upgrade projects fall into three categories (Magwaca, 2011):

1. *'Delamping'*: Luminaires are removed in areas where current lighting provides excessive levels of illumination, above what is necessary for designated tasks of those areas.
2. *'Reducing'*: Controlling and regulating lighting load according to daylight levels, through dimming and automatic switching of lights linked to occupancy sensors.
3. *'Relamping'*: Replacing existing luminaires and fixtures with technology that has greater lighting efficacy, to reduce lighting energy intensity.

Delamping is an option where existing lighting provides more illumination than is required for designated tasks to be performed. Illumination of an object, area or work surface is measured in lux, where 1 lux is equivalent to 1 lumen per m^2. The Energy Star Building Manual for lighting upgrades states that "lighting level targets should be considered average maintained levels for the task" and should further be "customized through the use of supplemental task lighting in areas requiring higher localised levels" (Energy Star, 2006:9). General offices and classrooms require 400 lux (CSIR, 2009), while corridors, canteens and other circulation areas require 100 – 200 lux. Removing lamps from light fixtures is the simplest way to reduce lighting energy consumption.

Low pressure fluorescent lamps, regulated by magnetic or electronic ballasts, are the most common form of luminaire fixtures found in commercial buildings (Magwaca, 2011). Ballasts regulate line current supply to the luminaires. When switched on, the ballast provides high initial voltage to the lamps, then rapidly reduces the current to safely maintain light discharge without damaging the lamp circuit. Ballasts increase the energy consumption of the light fixture, as they consume energy even while no lamp is connected (Edison Tech Center, 2013).

The ERC is currently fitted with T12 2 x 60 W linear fluorescent lights, most of which are connected to magnetic ballasts. Electronic ballasts have been found to have, on average, 12% better luminous efficacy [Lumens per Watt] than magnetic ballasts, and lack the 'hum and flicker' that occurs with

magnetic ballasts (Energy Star, 2006:17). Additionally, while dimmable ballasts are available in both magnetic and electronic form, magnetic ballasts require additional control gear to condition input power, which makes the dimming technology more expensive (Lutron, 2014:4).

Chung et al (2007:3146) note that magnetic ballasts do have some advantages over electronic ballasts, including longer operating life (> 30 years), lower cost, and better recyclability. However, the energy saving and heat reduction potential of electronic ballasts has made them a popular option in light upgrading projects, as reflected in case studies reported by Energy Star (2006:16). It is expected that replacing the ERC's magnetic ballasts with electronic ballasts, as well as the T12 fluorescent luminaires with smaller T8 luminaires, would provide lighting energy savings and reduce lighting heat gains, without reducing illumination below acceptable and comfortable levels (Energy Star, 2006:17; Magwaca, 2011).

Further energy savings could be realised through the increased use of natural light to provide indoor illumination (Energy Star, 2006:13), which may be an option for areas with adequate daylight exposure and ability to reduce glare. However, an effective control system would be required to dim interior lighting power to effectively balance incoming natural illumination. Automatic daylighting controls require photo sensors that can measure local illumination, as well as complex wiring and installation. This is particularly the case for fluorescent ballasts, and can result in adding significant costs for the upgrade process (Energy Star, 2006:8).

This dissertation therefore confines the scope of its analysis on ERC lighting to, first, partially removing fluorescent luminaires from thermal zones that are presently over-lit (i.e. '*Delamping*'), and then replacing existing luminaires and ballasts as described above, under a '*Relamping*' scenario. The potential impacts of these measures are discussed in § 4.2.

2.5.3. Shading

Solar heat gains through windows are another significant component of building heat gain (Givoni, 1994:28; Lam & Li, 2001:253). The external windows around the ERC offices are currently fitted with a solar film, which reduces infrared and ultra-violet rays from the sun transmitting through the glass. However, while the solar film is effective in reducing direct SW solar radiation entering the building, it also reduces visible light, causing an increase in the use of interior fluorescent lighting. Furthermore, the windows have a single glazing layer of 4 mm thickness, with low thermal resistance. Thus partial heat that is absorbed by the film is easily transferred to the building interior, where it heats the zones through LW radiation.

Shading devices are an alternative to solar film that may be more effective at mitigating solar heat gains, and regulating daylight entry into buildings. Simulation studies (Aldawoud, 2013; Datta, 2001; Loutzenhiser et al, 2007) and practical experiences (McGee & Reardon, 2013) have demonstrated shading devices to be effective at shielding internal and external building surfaces from direct and scattered solar radiation.

Shading devices are either fixed or adjustable. Fixed shading devices are typically fitted to the exterior of buildings, and form part of the architectural design (Givoni, 1994:28). External shading has the advantage of shielding the external building façade from direct sunlight, minimising heat transmission

through windows and other glazed surfaces that are covered. Examples include eaves, fixed louvres and screens.

Good design of external shading minimises direct solar radiation during summer, but also increases exposure in winter, where solar heat gain is desirable. Choice of shading device, and determination of optimum design angles, depends on window orientation, as well as the latitudinal position of the building and azimuth angles of the sun (McGee & Reardon, 2013). This concept is illustrated for residential buildings in Figure 2-5. It is notably more difficult to shade east and west facing windows, as these receive incident solar insolation during mornings and late afternoons respectively, when the sun is at lower altitude (Givoni, 1994:29).

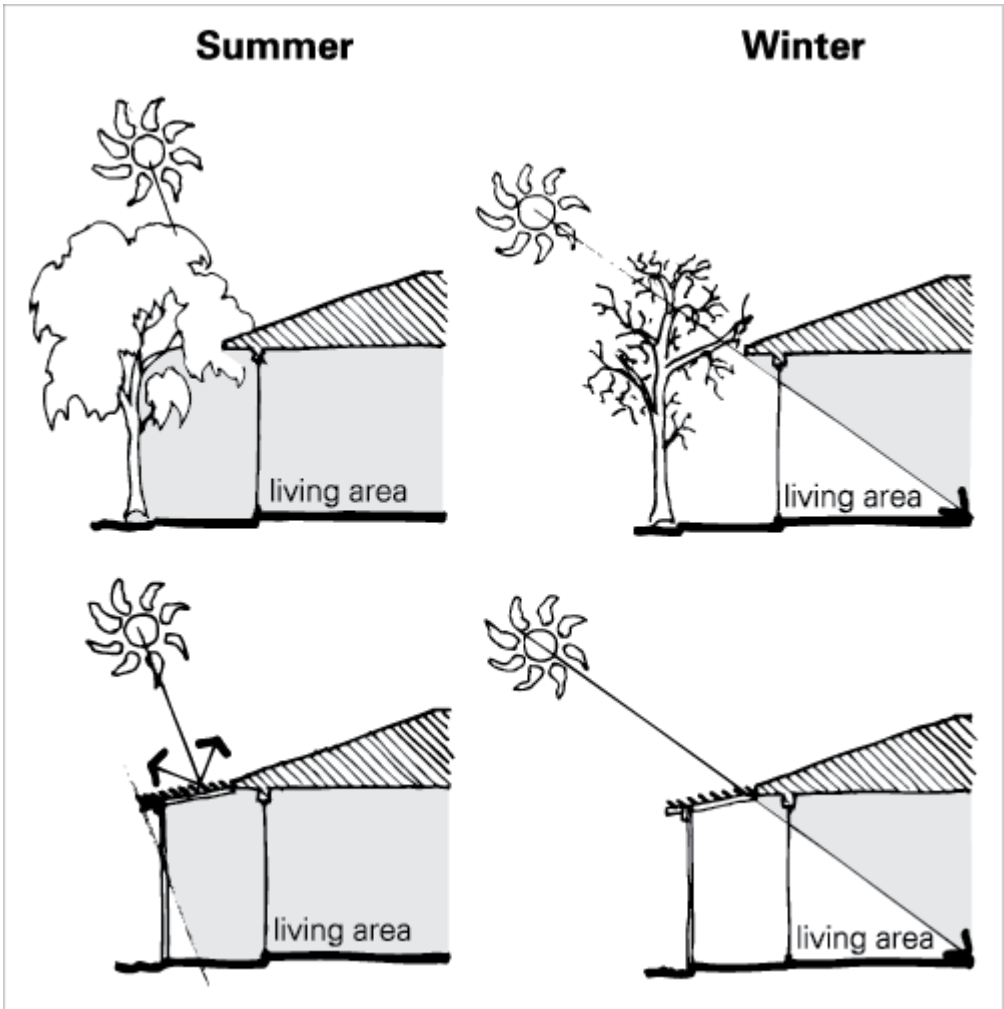

Figure 2-5: Concept of shading designed to regulate solar gains in summer and winter, from McGee and Reardon (2013)

Adjustable shading devices provide greater control over solar gains, and can be installed internally or externally. Adjustable external shades, such as shutters, adjustable louvres, awnings or retractable Venetian blinds, have the added advantage of allowing occupant control over the degree of radiation admitted, which may be desirable in winter (Givoni, 1994:29). Adjustable shading devices provide occupants with some control over solar heat gains in summer, although a study monitoring occupants' use of Venetian blinds on three office buildings in London showed frequent "inappropriate" use, with

minimal variance in occlusion levels regardless of varying seasons and external weather conditions (Foster & Oreszczyn, 2001:152).

Internal adjustable shading devices, such as Venetian blinds, roller blinds or curtains, do not prevent solar radiation passing through the glazing. Internal shading is therefore less effective at reducing heat gain in summer, unless the shading device is highly reflective (Datta, 2001:498; Foster & Oreszczyn, 2001:150), since solar radiation enters through the glass, and is then partially scattered around surfaces adjacent to the shading device. These surfaces are heated from absorbing the solar radiation, and hence emit heat into the room via LW radiation and convection.

Internal shading is, however, effective in controlling daylight entering the building, as well as reducing glare on work surfaces (Lam & Li, 1999:254). Internal shading devices are also expected to be easier to retrofit for an existing building, compared with external shading – particularly on the top floor of a multi-story building - and are thus expected to be more cost effective. Furthermore, proposed external shading devices at UCT may be in conflict with the existing architectural aesthetic of the campus.

This dissertation therefore limits its preventative analysis to the thermal effects of internal slatted blinds on ERC thermal conditions and *Base Case* cooling requirements.

2.5.4. Passive Cooling

Although passive cooling is not investigated in this dissertation, literature on the subject is briefly introduced here, as a starting point for possible further work. The review in this sub-section is based predominantly on the work of Givoni (1994).

Passive cooling refers to a series of techniques in which natural energy flows are introduced into buildings to remove heat. Such cooling strategies are distinguished from preventative cooling techniques, since they do not prevent heat entering a building, but rather expel heat that has entered or been generated within. Passive cooling is further distinguished from active cooling, as the latter is defined here to represent mechanical refrigeration, in which relatively large energy input is required to extract heat from a cooled space. Passive cooling, by contrast, utilises natural and mechanical ventilation, thermal mass manipulation, evaporative cooling, and other techniques that allow the transfer of heat from the cooled space to natural heat sinks, with relatively low energy input.

The following is a list of passive cooling techniques, identified from Givoni (1994), Florides et al (2002a) and the 2016 edition of the ASHRAE Handbook of Heating, Ventilating and Air-Conditioning Systems and Equipment (ASHRAE, 2016) :

- *Comfort ventilation*: simply opening doors and windows to allow outside air to flow into the building, cooling indoor air if the outdoor dry-bulb (DB) air temperature T_{DB} is lower than indoor air temperature T_a (Givoni, 1994:37).

- *Nocturnal ventilation* ('night flushing'): the thermal mass of the building interior is cooled by ventilation at night, when outdoor temperature is low and the building is not being used; the

cooled thermal mass then provides an internal heat sink during the following day (Givoni, 1994:52).

- *Indirect radiant cooling*: an indoor building surface (wall, floor or ceiling) is maintained at low temperature, using an air or chilled water circulatory loop, and thus absorbs and removes heat from the room via radiant heat transfer (ASHRAE, 2016:6.2).

- *Direct radiant cooling*: roof ponds (water contained on the roof in plastic bags or open ponds) covered by movable insulation act as a heat sink for the building during the day. At night the insulation is moved, and the pond is exposed to the cool sky whereupon it radiates the heat into the atmosphere. These systems were pioneered by Harold Hay's *Skytherm* system in the 1970s (Givoni, 1994:83).

- *Direct evaporative cooling*: an incoming air stream is passed through a fine water spray or evaporative pad, with water at ambient temperature, causing the water to evaporate, absorbing latent heat from, and increasing the humidity of, the air stream as it enters the building (Florides et al, 2002a:568).

- *Indirect evaporative cooling*: a secondary air stream and a heat exchanger are introduced into the direct evaporative cooling process. The secondary air stream is cooled and humidified by the same direct evaporative cooling process, and then absorbs sensible (but not latent) heat from the primary, incoming air stream (Florides et al, 2002a:568).

- *Earth coupling*: use of the soil adjacent to the building foundations to act as a heat sink, providing conduction cooling to the building structure (Givoni, 1994:191)

The applicability of these measures for an existing building depends on the building's geometry and orientation, as well as the interior design and layout of the building, occupant behaviour, and local climate. For example, Givoni (1994:40) notes that comfort ventilation would not be appropriate in hot climates, where daytime maximum temperatures exceed 32 °C. Night flushing meanwhile is better suited to climates with low (< 20 °C) minimum ambient air temperature and relatively high outdoor temperature range (Givoni, 1994:53).

While there is evident value in adopting passive cooling strategies in the early design phase of a new building, as demonstrated e.g. in Ahmed et al (2014) and Lechner (2001), greater challenges occur with passive cooling retrofits in existing buildings (Ma et al, 2012:890). Uncertainties arise from the impacts that altering a targeted system may have on other building systems, as well as longer payback periods and disruption to ongoing building operations (Ma et al, 2012:890).

For the purposes of limiting the scope of this work, retrofits considered for the ERC are therefore confined to the three preventative techniques described previously. More detailed analysis of passive cooling strategies is left for further work.

2.6. Active Cooling

While preventative and passive cooling reduce or even eliminate cooling loads in buildings (Etheridge, 2010:86), full control over the internal conditions requires additional, mechanical systems (Florides et al, 2002a:559).

A brief introduction of active cooling systems is provided here. § 2.6.1 describes 'conventional' air conditioning, defined here as the use of an electric chiller (or multiple chillers) to produce cooling, which is then distributed to required thermal zones (ASHRAE, 2016:5.1). § 2.6.2 thereafter introduces solar absorption cooling, which has emerged as an alternative to conventional air conditioning, and has undergone considerable commercial development over the last decade. The technology is not yet as mature as conventional cooling, with higher costs for the systems' chiller and solar components (Eicker et al, 2014:221; Hang et al, 2011:654). However, with rising energy prices and increased demand for renewable energy, solar cooling may become increasingly viable, particularly for large buildings with high cooling loads (Hwang et al, 2008:525).

2.6.1. Conventional Air Conditioning

The term air conditioning refers to "the control of temperature, moisture content, cleanliness, air quality and air circulation" (McQuiston et al, 2005:12). Air conditioning processes include a combination of sensible heating and cooling, to raise and lower air temperature, and humidification and dehumidification, to add and remove moisture from the air respectively.

An air conditioner acts a refrigerator for a thermal zone, by transferring heat from a low temperature (T_L) cooled space to a heat sink (typically the outdoor environment) at higher temperature (T_H). This process cannot happen naturally, since it would violate the Second Law of Thermodynamics, and thus requires work input to drive the process, and has to operate in a cycle (Çengel & Boles, 2008:328). Electric chillers provide cooling using the vapour compression cycle, the fundamental components of which are shown in Figure 2-6.

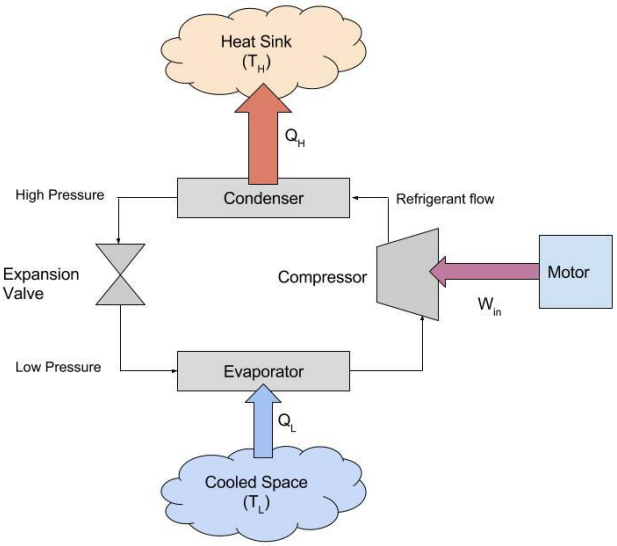

Figure 2-6: Vapour compression refrigeration cycle, adapted from Çengel and Boles (2008:610)

One method of measuring the effectiveness of a refrigeration cycle is through its coefficient of performance (COP) value, which is determined as a ratio of cooling effect to work input:

$$COP_R = \frac{Q_L}{W_{in}} \tag{2-25}$$

Where:

- Q_L is heat removed from the cooled space
- W_{in} is work input through the compressor.

The efficiency of air conditioning systems is typically measured using the energy efficiency ratio (EER) in units of Btu/Wh, which can be determined from the COP value as follows:

$$EER = 3.412\ COP \text{ [Btu/Wh]} \tag{2-26}$$

The Seasonal Energy Efficiency Ratio (SEER) is a further measure of the efficiency of the air conditioning system over an entire cooling season, and is determined by following certain testing standards (Çengel & Boles, 2008:284).

Heat is transferred through the cycle via a refrigerant – a working fluid with capability of changing phase from solid to liquid within the operating temperatures of the cycle, and relatively high heat capacity in liquid and vapour form. Chlorofluorocarbons (CFCs) were previously the most common refrigerant substances (Çengel & Boles, 2008:620) but have now been largely phased out due to their environmental impact on the ozone layer (ASHRAE, 2014:6.1). Natural refrigerants such as CO_2 and alternative hydrocarbons are used increasingly, owing to their low global warming potential (GWP; a measure of the greenhouse gas effect caused by a particular gas or substance).

Air conditioning units often form part of HVAC (heating, ventilating and air conditioning) systems, which also comprise heating and air handling and distribution components (ASHRAE, 2016:1.5). HVAC systems are either *centralised* or *decentralised*. Centralised systems comprise a central refrigeration

plant from which chilled water is distributed throughout the building to air-handling units or fan units (Henning & Albers, 2004:3). Decentralised systems are comprised of one or more individual units with their own refrigeration cycle, air-handling units and outdoor air systems, located near the target thermal zone (Murray et al, 2015:2). Examples of decentralised systems, as described in the ASHRAE HVAC Handbook (2016), include:

- Window and 'through-the-wall' air conditioner units
- Air-cooled and water cooled heat pump systems
- Multiple-unit and split unit systems
- Floor-by-floor systems
- Outdoor package systems

A multiple or split system would work best for the ERC. Multiple systems are available as standard components packaged in units that are relatively easy to install, and are designed for small (< 70 kW_{th}) cooling load (ASHRAE, 2016:2.5). Split systems consist of an indoor unit with air distribution and temperature control, with the condenser located further away from the unit (ASHRAE, 2016:2.6). Both systems are likely to have lower initial costs and require less dedicated space for plant installation, relative to a centralised system. They would be capable of serving the ERC office area on the top floor of Menzies, without disruption to other parts of the building.

Further analysis on selection and performance assessment of an air conditioning system for the ERC is beyond the scope of this dissertation. The approach taken in this study, as discussed in Chapter 5, is to evaluate a high-level cost estimate for a theoretical active cooling system, based on cost factors relating installation cost to cooling capacity determined in Buys and Mathews (2005).

2.6.2. Solar Absorption Cooling

While beyond the scope of this dissertation, the use of renewable energy to cool the ERC should be given fair consideration, owing to the reduced environmental impact relative to a cooling system using fossil-fuel-generated electricity (Otanicar et al, 2012:1294). To this end, this section briefly introduces solar absorption cooling.

Active use of solar energy for cooling has great potential to replace non-renewable energy in meeting this growing demand. The IEA *Solar Heating and Cooling Roadmap 2012* predicting global solar thermal cooling technology to reach 1 000 GW_{th} capacity by 2050, producing 1.5 EJ of cooling energy per year (IEA, 2012:5). The IEA *Solar Heating & Cooling Programme* (IEA-SHC) reported an estimate 1 175 solar cooling systems had been installed globally, as of the end of 2014 (IEA-SHC, 2015:41).

Whereas conventional air conditioning uses a vapour compression cycle, most solar cooling systems use thermal refrigeration, with absorption chillers most commonly used (Ullah et al, 2013:502; Infante-Ferreira& Kim, 2014:30). Key components of the absorption refrigeration cycle are shown in Figure 2-7, and include conventional components (evaporator, condenser and expansion valve) as well as a 'thermal compressor', which consists of a generator, absorber and liquid pump.

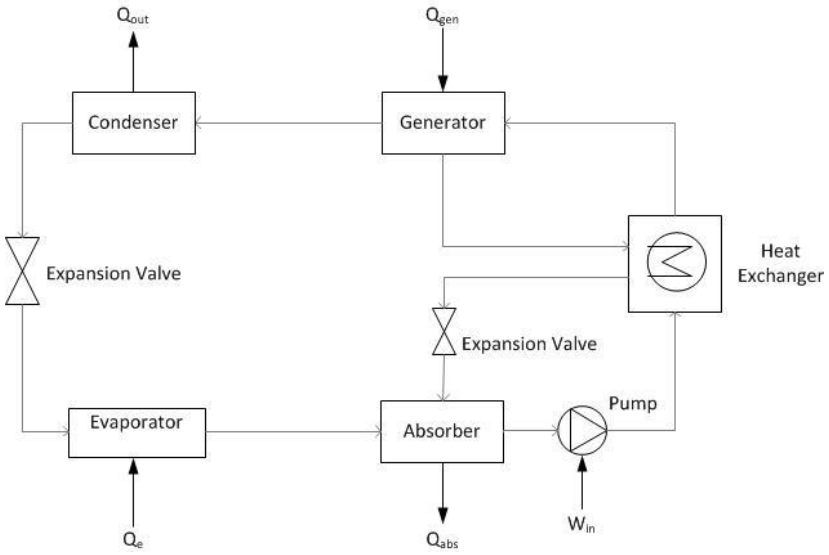

Figure 2-7: Simplified schematic of an absorption refrigeration cycle, adapted from Kreider and Kreith (1975:161)

The refrigeration effect is driven by two working fluids which interact with each other, namely a refrigerant and an absorbent. The most common working pairs (refrigerant/absorbent) are water and lithium-bromide (H_2O/LiBr) and ammonia and water (NH_3/H_2O) (Ullah et al, 2013:503). The suitability of working pairs depend on the thermophysical properties of the fluids, including their affinity, vapour pressure differences, volubility and chemical stability (Florides et al, 2003:2485; Vicatos, 1995:13). H_2O/LiBr systems are more common than NH_3/H_2O for air conditioning, as they have greater coefficient of performance (COP_{ab}) and require lower generator temperatures to provide heat input to the cycle, typically in the range of 70 – 95 °C (Florides et al, 2003:2485).

Absorption refrigeration cycles operate as follows. During operation, the refrigerant (H_2O) enters the absorber in Figure 2-7 at low pressure, where is it absorbed by the absorbent (LiBr) at low temperature, forming a 'weak' solution (i.e. high concentration of refrigerant in mixture with absorbent). The weak solution is pumped to high pressure, and passed through a heat exchanger before entering the generator. Heat (Q_{gen}) is supplied to the generator, causing the refrigerant to evaporate out of solution in accordance with *Dalton's Law* of partial pressures. In solar absorption cooling, Q_{gen} is supplied from a solar thermal system, in which solar radiation is collected and stored in a hot water storage tank at high temperature (Li & Sumathy, 2000:270).

Once the refrigerant is evaporated out of solution, it is drawn into the condenser, whereupon heat (Q_{out}) is released to the cooling cycle, which can be water or air cooled (Grossman, 2002:54). Note that the cooling loop is passed through the absorber first, to remove heat Q_{abs} and lower absorber temperature, before being passed through the condenser (Li & Sumathy, 2000:271), as the absorbent's affinity for the refrigerant increases at lower temperature.

After leaving the condenser, the liquid refrigerant is passed through an expansion valve before entering the evaporator coils at low pressure. Warm air from the cooled space is passed over the evaporator coils, allowing the refrigerant to absorb heat from the air (Q_e). The refrigerant then returns to the absorber (Henning & Albers, 2004:3).

Meanwhile, the 'strong' absorbent solution remaining in the generator, after the refrigerant has evaporated, is passed back through the heat exchanger, where it preheats the weak solution before

the latter enters the generator. The strong solution then passes through an expansion valve before re-entering the absorber at low pressure and temperature (Florides et al, 2003:2487).

Coefficient of performance of the absorption refrigeration cycle is determined as follows:

$$COP_{ab} = \frac{Q_e}{Q_{gen}+W_{in}} \quad (2\text{-}27)$$

Single-effect absorption chillers have COP_{ab} typically ranging 0.50 to 0.80, which depends largely on the inlet temperature at the generator as well as the temperature of the chilled water circuit leaving the evaporator (as with vapour compression refrigeration). COP_{ab} can be increased with the use of multi-stage generation, such as double-effect systems (Li & Sumathy, 2000:280), where a second generator is introduced at higher pressure to provide additional preheating to the weak solution. However this increases the required generator temperature (Grossman, 2002:57).

Absorption refrigeration remains the most common in solar cooling systems. As of 2009, more than 70% of large solar cooling systems (>20 kW_{th} capacity) 90% of small systems (<20 kW_{th}) used absorption chillers (IEA-SHC, 2009:8); furthermore, more than 60% of solar cooling capacity (around 10 MW) was installed in Spain, Germany and Italy (IEA-SHC, 2009:7). Other cooling technologies applied with solar thermal energy include adsorption refrigeration and desiccant cooling; these are reviewed, e.g., in Kim and Infante-Ferreira (2008) and Ullah et al (2013).

Solar cooling is beginning to emerge in South Africa (EScience, 2016), which is considered a favourable location due to its high levels of solar radiation and warm climate. Solar thermal technology is relatively mature in South Africa, *viz* increasing rollout of solar water heaters in the residential sector (Wlokas & Ellis, 2013:2) and recent commissioning of utility scale concentrated solar power (CSP) plants (e.g. Abengoa Solar, 2014). A growing list of South African HVAC vendors offer solar cooling products as part of their business, although in most cases this remains a marginal offering rather than the primary focus of the company (EScience, 2016: 34).

Bvumbe (2012) conducted case studies on the performance of two solar 35 kW_{th} H_2O/LiBr absorption chillers, installed at a private hospital and mobile phone company centre respectively in Gauteng. Simulation models of the systems were developed and used to evaluate their technical performance and estimate their economic effectiveness Bvumbe (2012:76).

The hospital's system was found to have a payback period of 13 months, relative to the costs of a conventional electric chiller (Bvumbe, 2012:88). The cost per kW_{th} of the phone company's system was found to be 28.88 ZAR, which is considerably higher than prevailing electricity rates (Bvumbe, 2012:107). However, this particular system was reportedly designed to provide all cooling from solar energy, causing the solar thermal system to be designed to provide peak cooling loads and operate during periods of low solar radiation. Literature shows that systems operate more efficiently and economically when they are coupled with back up heat generation, from electricity or an alternative source of energy (e.g. natural gas in European markets), to accommodate extreme conditions (Eicker et al, 2014:217; Fong et al, 2010:239).

Nevertheless, these experiences show the potential for growth of solar cooling in South Africa. Although the costs of solar cooling remain significantly higher than conventional cooling, there remains the possibility that the ERC, or UCT at large, could invest in this technology, as a pilot initiative

to demonstrate its effectiveness and feasibility. Relative cost savings would be realised through avoided electricity use if the ERC installed a solar cooling system over a conventional system, while UCT could achieve actual energy cost savings if it replaced existing HVAC equipment with solar cooling.

3. ERC Base Case Modelling

This chapter describes *Current* and *Base Case* thermal energy modelling of the Energy Research Centre offices. The purpose is to estimate, with acceptable accuracy, existing environmental conditions, particularly during the cooling season, and to predict annual heat gains to the offices from internal gains and the surrounding environment. As part of the *Base Case*, an initial estimate for peak cooling load and annual cooling energy requirement is also determined.

A model of the ERC was developed in *DesignBuilder*, based on the physical properties of the building envelope, as well as information and assumptions on building occupancy and lighting and equipment use and prevailing weather data for the Menzies building's location. Building geometry and materials were determined primarily from as-built section and elevation architectural buildings provided by UCT's Physical Planning Unit. Simulation analysis of the model was performed in *EnergyPlus v8.3*, through the *DesignBuilder* interface.

A schedule of simulations performed on the ERC model is shown in Table 9-1 of Appendix A. The first set of simulations (Run 1-1 through 1-3 in Table 9-1) were performed to characterise *Current* thermal conditions, external heat gains through the building surfaces and internal heat gains from occupants, computers and equipment, lighting and solar gains through exterior windows. The simulation determined annual discomfort hours based on the predicted conditions, using the ASHRAE-55 PMV/PPD methodology. Results were validated against air temperature measurements collected over three days in the ERC

Subsequent simulations were performed on the same model of the building, but with additional inputs to regulate the temperature and humidity in the ERC offices. These simulations included an EnergyPlus 'ideal thermostat' in each ERC thermal zone, programmed to deliver the theoretical maximum cooling power required to balance the heat gains. Further simulations estimated annual cooling requirements with different preventative interventions selected to reduce heat gains to the ERC, lowering design cooling loads; these are discussed in Chapter 4.

In compiling the model of the ERC offices, several assumptions and approximations were made, as complete data sets and information on many of the parameters were not available. These are described in greater detail in § 3.1 that follows, with accompanying Appendices. The simulation methodology and results are discussed in the sub-sections that follow thereafter.

3.1. ERC Model Input Data

3.1.1. Weather Data

EnergyPlus incorporates weather data from the *International Weather for Energy Calculation* (IWEC) library, which contains whole year datasets compiled at weather stations around the world and archived at the US National Climatic Data Centre (ASHRAE, 2009). The weather station nearest to the University of Cape Town (UCT) is located at Cape Town International Airport, at a straight line distance of 12.5 km from Menzies. Although UCT's microclimate is influenced by its proximity to Table Mountain, the distance from the airport weather station to the building is small enough that data recorded is considered representative of UCT's typical annual weather patterns. It should be noted

that the same weather database was used in Neethling's study of the new academic building at the University of Stellenbosch (Neethling, 2011:24).

The IWEC dataset comprises weather data recorded in hourly intervals from 01 January to 31 December 2002. Figure 3-1 shows the monthly quartile distribution of Cape Town air temperatures, as recorded in the IWEC dataset. The highest temperatures, ≥ 33 °C, were recorded between December and February, Cape Town's warmest summer months. Average monthly temperature peaked in February, at 20.9 °C, and was lowest in July (12.3 °C).

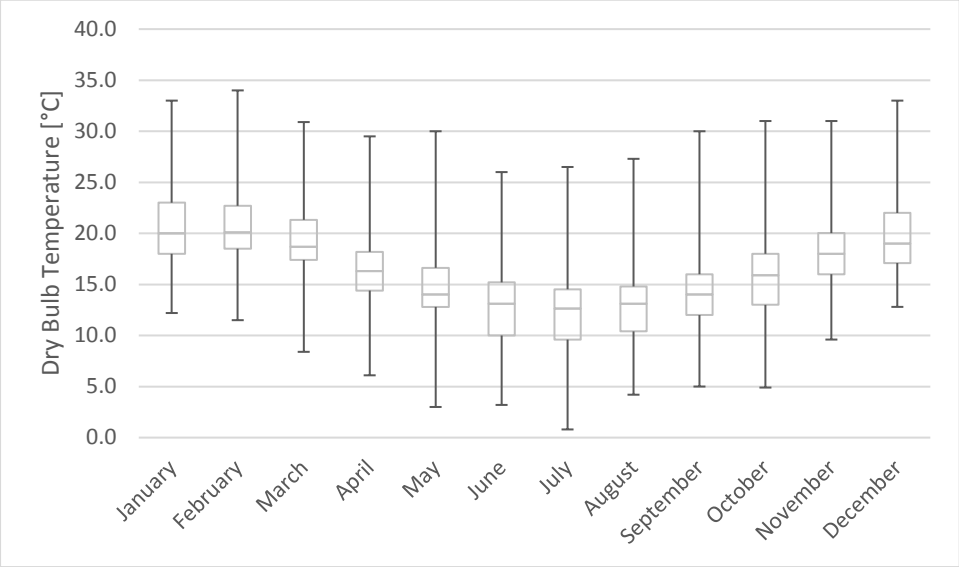

Figure 3-1: Monthly temperature quartile ranges recorded in Cape Town (IWEC dataset)

Cape Town experiences a Mediterranean climate, and typically receives the majority of its rainfall during the winter months (South African Weather Service, 2016). Humidity is therefore generally higher in winter than in summer, as reflected in average daily relative humidity profiles for selected months shown in Figure 3-2.

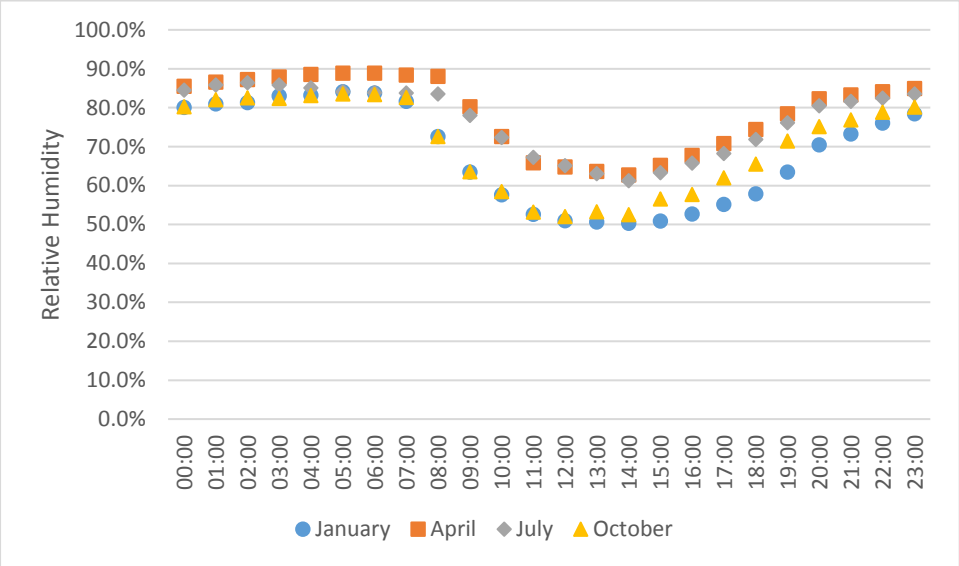

Figure 3-2: Cape Town average daily humidity profiles for selected months

Hourly outdoor dry-bulb (DB) temperature frequency distribution from the IWEC dataset is shown in Figure 3-3. The data shows that temperatures exceed 18 °C in Cape Town for less than 35% of the year, and exceed 30 °C for less than 1% of the year. Applying the Cooling Degree Day methodology of Conradie et al (2015:5), using 18 °C as a base temperature, it can be shown that Cape Town experienced 511 cooling degree-days for 2002 (as shown in Table 9-4 of Appendix B).

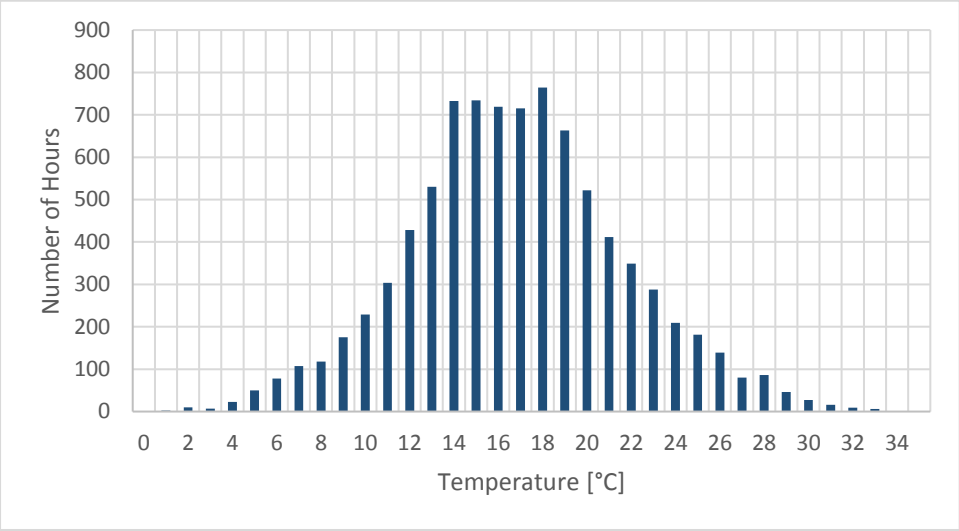

Figure 3-3: Cape Town annual dry-bulb temperature hourly distribution

3.1.2. ERC Thermal Zones

The Menzies building is an engineering academic building housing five levels, labelled 2 to 6 the Energy Research Centre on its top floor (Level 6; there is no 'Level 1' of Menzies, as the effective first floor of the building is located in the Electro-Mechanical engineering building, which is connected to Menzies but not included in the thermal model).

Menzies' geometry and layout was characterised in *DesignBuilder*, based on basic sizing for each floor from as-built architectural drawings. Each level is considered a separate thermal zone, with the offices in the ERC area of Level 6 subdivided into additional thermal zones in the model. In order to simplify the analysis and reduce computational effort, building characteristics on the lower floors of Menzies (levels 2 to 5), and the 'non-ERC' part of level 6, were characterised generically, according to standardised Activity Templates available in the *DesignBuilder* library, as described in Table 3-1.

Table 3-1: DesignBuilder activity templates applied for each level of Menzies (excl. ERC office area)

Menzies Building Level	***DesignBuilder* Activity Template**	**Description of spaces on physical level**
Level 2	Workshop	One computer lab, one postgraduate study area, two mechanical engineering workshops, one materials testing lab
Level 3	Classroom	Several small-to-medium sized classrooms, three lecture halls, one cafeteria, one computer lab, several small offices
Level 4	Laboratory	Electrical engineering power laboratory, one small computer lab, several small offices
Level 5	Computer lab	One large computer lab, several small offices
Level 6 (non-ERC)	Generic Office Area	Office area – mostly small isolated or open plan offices

The ERC offices comprise the Office Areas, Seminar Rooms, Kitchen, Bathroom and Corridor. ERC thermal zones are defined according to the eight shaded areas shown in Figure 3-4 and described in Table 3-2. The 'non-ERC' thermal zone of Level 6 is described as shown in Table 3-1 above.

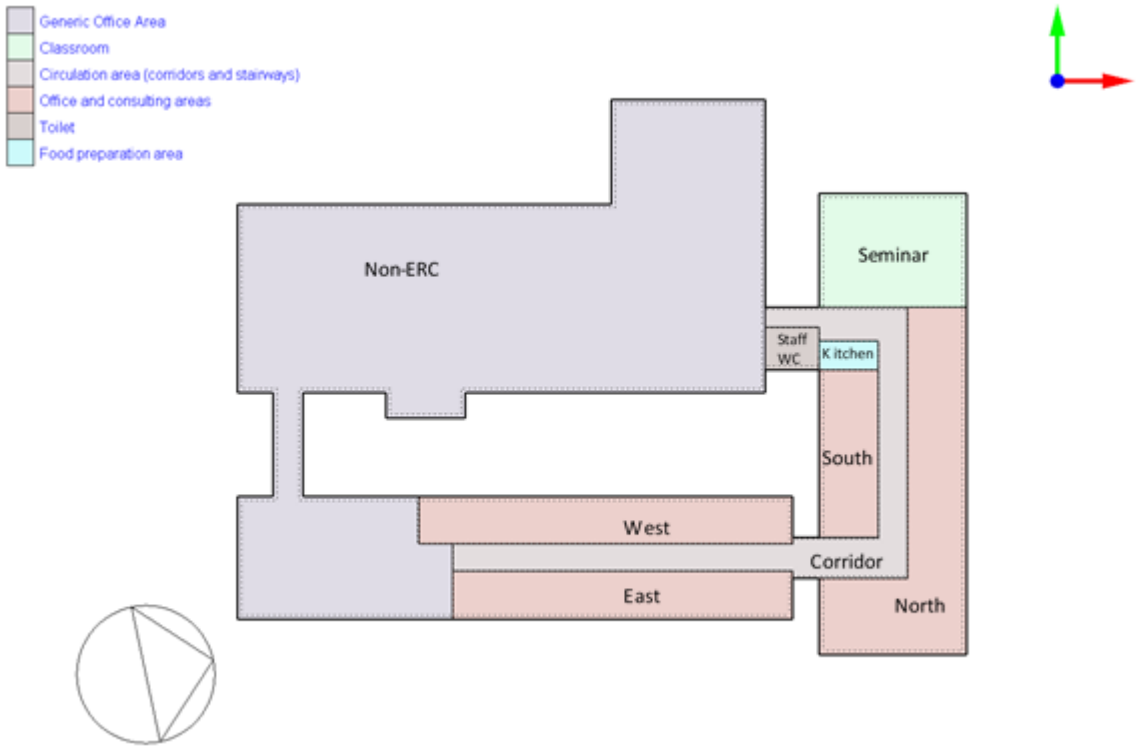

Figure 3-4: Simplified floor plan of Level 6, showing ERC and 'Non-ERC' generic thermal zones

Table 3-2: ERC thermal zones defined by space type

Thermal Zone	Space Type	Floor area [m^2]	Zone volume [m^3]
North	Office	173.05	346.09
East	Office	95.24	190.48
South	Office	65.45	130.90
West	Office	104.83	209.66
Seminar	Teaching area	100.23	200.47
Corridor	Circulation area	129.57	259.15
Kitchen	Food preparation	12.10	24.21
Staff WC	Toilet	13.51	27.01
	Total	**693.98**	**1 387.97**

3.1.3. Construction Data

Building construction materials were identified from the section and elevation drawings of the building. The thermal properties of these materials were then assumed from values found in literature. The uncertainty of this approach should be noted, since the actual thermal properties of the physical building could vary widely from the assumed as a result of fluctuating dynamic environmental conditions the building façade is exposed to, as well as the impact of wear and deterioration over the building's life.

Key construction elements influencing a building's thermal energy performance are those with a large surface area and direct exposure to the outdoor climate. These include external walls, doors, roofs and window glazing (Neethling, 2011:29). Input data for these surfaces is discussed in the following sub-sections, with additional information provided in Appendix A.

3.1.3.1. External Walls

The ERC's external walls are constructed from standard concrete masonry units. The two masonry block types which were used have empty circular and rectangular cores respectively. The external walls are plastered on both sides with a cement plaster.

Thermal properties of the concrete wall constructions were assumed to be consistent with medium weight hollow blocks as found in the CIBSE Guide A (CIBSE, 2006:3-37). The external wall properties were thus input into the Menzies building model as shown in Table 3-3, with more detailed calculations of these properties shown in Appendix C.

Table 3-3: Input thermal properties of external walls

Wall Construction Property		Value
Concrete Block Properties	Thermal Conductivity λ [W / mK]	0.62
	Density ρ [kg / m^3]	1 040
	Heat capacity c_p [J / kgK]	840
Combined External Wall Properties	R-Value [m^2K / W]	0.586
	Solar Absorptance α	0.50
	Thermal Absorptance (Emissivity) ε	0.91
	U-Value [W / m^2K]	1.707

In order to simplify the analysis, partitions of offices within thermal zones were not accounted for in the ERC model or simulations. The partitions are formed from plastered rhino board, and are assumed to provide adiabatic separations between each office. It was therefore determined that complexity could be reduced by omitting the partitions, and treating the offices as larger, open thermal zones, as shown in Figure 3-4.

3.1.3.2. Pitched Roof and Ceiling

The Menzies building has a clay tile pitched roof, with a pitch angle of 23°. The clay tiles are layered on roofing felt with a 10mm airgap. The thermal properties of the roof are assumed consistent with the clay roof properties included in the *DesignBuilder* library, including:

- Thermal resistance (R-value): 0.341 m^2K/W
- Solar absorptance: 0.70
- Emissivity: 0.90

The roof overhangs on all sides of the ERC offices by 670 mm, providing shading to all external windows – particularly north facing windows in summer, when the sun reaches its greatest solar altitudes and smallest angles of incidence at midday.

The ceiling is constructed with 25 mm ceiling boards, made from extruded rigid polystyrene foam, with an R-value of 0.895 m^2K/W. An inspection of the roof space above the ERC showed that the ceiling currently has sporadic layers of fibreglass insulation, up to 50 mm in thickness, of varying and sporadic distribution. Various gaps are spread out across the ceiling area of each thermal zone, creating thermal bridges which allow greater heat flow to the internal office space.

A retrofit of ceiling insulation would require the removal of the existing insulation before replacing it with a more suitable material, such as polyester fibre or cellulose fibre. Therefore, the ERC *Current* and *Base Case* simulations were modelled with the assumption of no insulation layer, and R-value of the ceiling was maintained at 0.895 m^2K/W.

3.1.3.3. Window Glazing

Glazing properties for the Menzies building, excluding Level 6, are set to the default *DesignBuilder* library template of 'Single glazing, no shading'.

However, the openings on Level 6 are defined in more detail, as the glazing on this floor is not consistent with other levels of Menzies. Level 6 of the building is fitted with sliding windows, with aluminium frames, that extend around the inner and outer perimeter of the building. The windows are single glazed, with a solar control film over the inside of the glass pane, which reduces solar and visible light transmission. Thermal properties for the window glazing, shown in Table 3-4, are assumed based on commercial data available from *Solar Film Foundation* (SFF) for grey, 35% non-reflective window film (SFF, 2014).

Table 3-4: Input window and glazing properties

Window and Glazing		**ERC opening construction**		
Window Type	Sliding Horizontal	**Size**	Window to Wall %	30%
	Single Glazing		Window Height [mm]	730
	Clear + solar film on inner surface		Sill height [m]	1.10
Glass Thickness [mm]	4	**Aluminium Frame**	Thickness [mm]	5
U-value [W / m^2K]	4.123		Conductivity [W / mK]	160
SHGC	0.68			
Direct solar transmission	0.60		Specific heat [J / kgK]	880
Light transmission	0.48		Density [kg / m^3]	2 800

While the Menzies building is in close proximity to other buildings on UCT's campus, its sixth floor – where the ERC offices are located – sits above all other nearby buildings or trees. It is therefore assumed that the shading effects on the lower floors of the building have a negligible effect on the ERC's thermal conditions, and these were excluded from the analysis.

3.1.4. Occupancy and Activity

Determining the occupancy schedule of a building is challenging due to the variability of human behaviour (Ryan & Sanquist, 2012:377), and thus simplifying assumptions had to be made. Schedule-based occupancy profiles were determined for each thermal zone, based on assumptions of typical ERC behavioural patterns throughout the year. Typical weekday occupancy profiles applied in the model are shown in detail in Table 9-7 of Appendix C.

ERC occupants comprise research staff, Professional Administrative and Support Staff and postgraduate students. The model assumes staff work in the offices on weekdays (not Saturday or Sunday) throughout the year, excepting public holidays and the end-of-year holiday period, while the schedule of students attending class in the seminar room was varied based on the curriculum timetable, assuming an average class size of 14 students per year. Maximum occupancy density for each office space was determined based on the uppermost number of working people expected to be found in the space at any given time (see Table 3-5).

Table 3-5: Model input occupancy density summarised

ERC Thermal Zone	**Area [m^2]**	**Typical Maximum Occupancy [people]**	**Maximum Occupant Density [People / m^2]**
North	173.05	12	0.0693
East	95.24	10	0.1050
South	65.45	6	0.0917
West	104.83	10	0.0954
Seminar	100.23	14	0.1397
Corridor	129.57	0.5	0.0039
Kitchen	12.10	1	0.0826
Staff WC	13.51	0.5	0.0370
Total	**693.98**	**54**	**0.0778**

General activity assumptions are shown in Table 3-6, including the metabolic rate and typical clothing insulation of occupants. Metabolic rate was assumed to be 65 W/m^2, based on activity data for typing (ASHRAE-55, 2004:15), and converted assuming the mean body surface area of the average person is 1.86 m^2 (Baker et al, 2002:1883). Summer clothing insulation was assumed consistent with data for trousers and short sleeve shirts, while winter clothing was assumed to conform to data for trousers, long sleeve shirts and a long sleeve jersey (ASHRAE-55, 2004:18). Infiltration rate was assumed constant at 0.50 ac/h, based on data in the GBCSA Green Start South Africa Office Protocol (GBCSA, 2010:7), and reduced to 0.25 ac/h for the Corridor zone.

Table 3-6: Input activity assumptions for ERC energy model

Activity Property	Value
Metabolic Rate [W / person]	121
Summer clothing insulation [clo]	0.57
Winter clothing insulation [clo]	1.01
Minimum fresh air [litres / s-person]	8
Infiltration rate [ac / h]	0.50

3.1.5. Equipment

ERC office equipment loads were determined based on the work of Menezes et al (2014), who developed and verified a model for predicting energy consumption of typical office appliances. The input data of Menezes et al (2014:203) was used to estimate equipment power density for each zone of the ERC. For each office area (North, East, South and West thermal zones), it was assumed that all occupants used a laptop (rated at 30 W) and 21 inch LCD screen (45 W), such that, for example, the total equipment rating of the North office area was determined as $12\ occupants \times (30 + 45) = 900$ W.

Seminar room equipment intensity was estimated from the assumption that all occupants use a 30 W laptop, while the photocopier (located in the reception room, enclosed in the seminar thermal zone) cycled intermittently between standby (at 30 W) and full power (220 W) (Menezes et al, 2014:203). Kitchen equipment intensity was determined from the typical power rating of a fridge (120 W) and coffee machine (350 W). A hand drier draws significant load when used in the staff WC, but is used only intermittently during office hours, thus consuming relatively small energy (and contributing low room heat gain) throughout the year.

Table 3-7: Summary of Equipment Data for ERC energy model

Thermal Zone	Area [m^2]	Total equipment rating [W]	Equipment power density [W/m^2]
North	173.05	900	5.20
East	95.24	750	7.87
South	65.45	450	6.88
West	104.83	750	7.15
Seminar	100.23	900	8.98
Corridor	129.57	0	0.00
Kitchen	12.10	470	38.84
Staff WC	13.51	800	2.96
Total	**693.98**	**5 020**	**7.23**

3.1.6. Lighting Data

The ERC office areas are predominantly lit by surface mounted T12 fluorescent luminaires, equipped with magnetic ballasts. Each light fitting includes 2 x 60 W T12 fluorescent tube luminaires, with a total of 60 light fittings counted. Power rating of each light fitting was assumed to be 140 W, including the 2x 60 W fluorescent lamps and an additional 20 W consumption assumed for the magnetic ballast. Overall lighting power density for the (*Current*) ERC was determined as 12.1041 W per m^2. Lighting power density per thermal zone is shown in Table 9-8 in Appendix C.

The thermal effect of the luminaires was modelled by assuming energy dissipated from the light fittings is shared amongst heat (radiant energy and convection) and visible light. *DesignBuilder* default proportions for surface mounted luminaires were assumed for these factors (DesignBuilder, 2016):

- Radiant fraction (F_R): 0.72
- Visible fraction (F_V): 0.18
- Convective fraction (F_C): 0.10
- Return air fraction (F_{RA}): 0 – this applies to thermal zones modelled with a return air duct system, in which lighting heat is transferred out the zone into the return air flow (DesignBuilder, 2016); the ERC is not fitted with a return air system.

Lighting profiles were assumed to conform to the occupancy schedules, as described in Appendix C, as ERC research staff are usually conscientious about switching off lights in rooms that are not being used. It should further be noted that, while some occupants use desk lamps and other task lighting, this was not accounted for in simulation runs, with the analysis limited only to heat gains from general lighting.

3.2. Simulation Methodology

The following section describes the methodology applied for each thermal simulation of the ERC. A schedule of all simulations analysed in this dissertation is included in Appendix A.

Physical heat balance simulations of the model were run through the *EnergyPlus* simulation engine, within the *DesignBuilder* software package. All simulations were calculated iteratively in half-hourly intervals, as more refined resolution would have greatly increased the computational effort of each run. The output data file resulting from each simulation was then loaded back into *DesignBuilder*, from which energy, heat gain and environmental parameter data could be exported and analysed.

Simulations were run over two lengths:

1. Whole year periods, with results aggregated into monthly and annual form, and
2. Cape Town *Summer Design Week* period. This is defined in the IWEC weather dataset as a single 7-day week during which typical extreme summer conditions are experienced (Ibarra & Reinhart, 2009). Cape Town's Summer Design Week occurred between 13 and 19 January 2002 in the IWEC dataset.

Heat balances were determined for each surface enclosing the ERC, i.e. external walls, windows, floor (interfacing with Menzies Level 5) and ceiling (interfacing with the unoccupied pitched roof space). Conduction through building surfaces was calculated at each interval using the Conduction Transfer

Function algorithm. External surface convection was calculated using the 'DOE-2' algorithm, while the 'TARP' algorithm was used for internal surface convection. All other *EnergyPlus* parameters, including convergence tolerances, warmup days and solar distribution, were left as default settings in the *DesignBuilder* simulation interface.

The simulation estimated whether conditions in thermal zones would cause thermal discomfort at each iteration by employing the PMV/PPD methodology, based on the ASHRAE-55 (2004) comfort zone. Air speed was assumed to be constant at 0.2 m/s, consistent with the upper bound of the ASHRAE comfort zone for PMV analysis (ASHRAE-55, 2004:6). Metabolic rate and clothing insulation of occupants were assumed constant (depending on the season), as defined in Table 3-6 above.

Regarding other thermal zones in Menzies (i.e. non-ERC area), *DesignBuilder* default activity templates were used as generic inputs (see Table 3-1), since these are of lesser concern to analysis of the ERC. Air temperature on level 5 was bounded between 18 and 23 °C, by including an 'ideal thermostat' for the level 5 zone in the model. This is representative of the cooling system operation on Level 5, which serves primarily to cool the computer labs located on that floor. Menzies levels 2, 3, and 4 were excluded from the thermal calculations to reduce computation time, as these were not expected to influence thermal performance on level 6.

§ 3.3 presents the results of the *Current* simulations – i.e. modelling the building in its current form, without any cooling intervention, and without simulation of cooling energy supply. § 3.4 then reports on the theoretical assessment of the *Base Case* cooling requirements, essentially quantifying the thermal energy that needs to be transferred out of the ERC annually in order to achieve design conditions and minimise thermal discomfort in the Cape Town summer months.

3.3. ERC Current Simulation Results

Results presented in this section are collated from output data generated from the *Current* simulations (Run 1-1 through 1-3 in Table 9-1 of Appendix A). Comprehensive data from these simulations is included in Appendix D.

3.3.1. Environmental Conditions

Table 3-8 shows average monthly operative temperature (T_O, calculated from air temperature and radiant according to Equation 2-2 in § 2.2.2) and relative humidity in the ERC, compared to average DB temperature (T_{DB}), for each month of the year. T_O is determined from the weighted average of the individual thermal zones, according to their respective floor areas:

$$T_O = \frac{\sum_i T_{O,i} A_i}{\sum_i A_i} \text{ [°C]} \qquad (3\text{-}1)$$

Where $T_{O,i}$ is average monthly operative temperature, and A_i is the floor area, of thermal zone i.

Table 3-8: Monthly average environmental conditions

Month	Outdoor	ERC	
	T_{DB} [°C]	T_O [°C]	RH [%]
January	20.8	24.3	54.5%
February	20.9	25.0	53.1%
March	19.1	23.6	58.2%
April	16.5	22.1	57.0%
May	14.8	20.8	56.1%
June	12.8	18.4	55.9%
July	12.3	18.5	55.3%
August	12.9	17.4	60.5%
September	14.3	20.0	55.5%
October	16.0	22.1	50.2%
November	18.3	22.7	53.9%
December	19.8	24.6	52.0%

Table 3-8 shows February is the warmest month, on average, with the highest average internal operative temperature of 25.0 °C, while August is the coolest month (see Table 9-9 and Table 9-10 of Appendix D for zone-specific data). Average relative humidity ranges between 50% and 60% throughout the year. Temperatures within the ERC are consistently greater than outdoor temperatures all year round, so that the heat flux will naturally flow through the building envelope from internal to external surfaces.

Figure 3-5 shows monthly predicted discomfort hours predicted under *Current* conditions, for each office-type thermal (i.e. North, East, South and West zones, excluding the kitchen, seminar rooms, corridor and staff bathroom). A total of 7814.5 discomfort hours were predicted annually, aggregated across all eight ERC thermal zones, as shown in Table 9-11 of Appendix D.

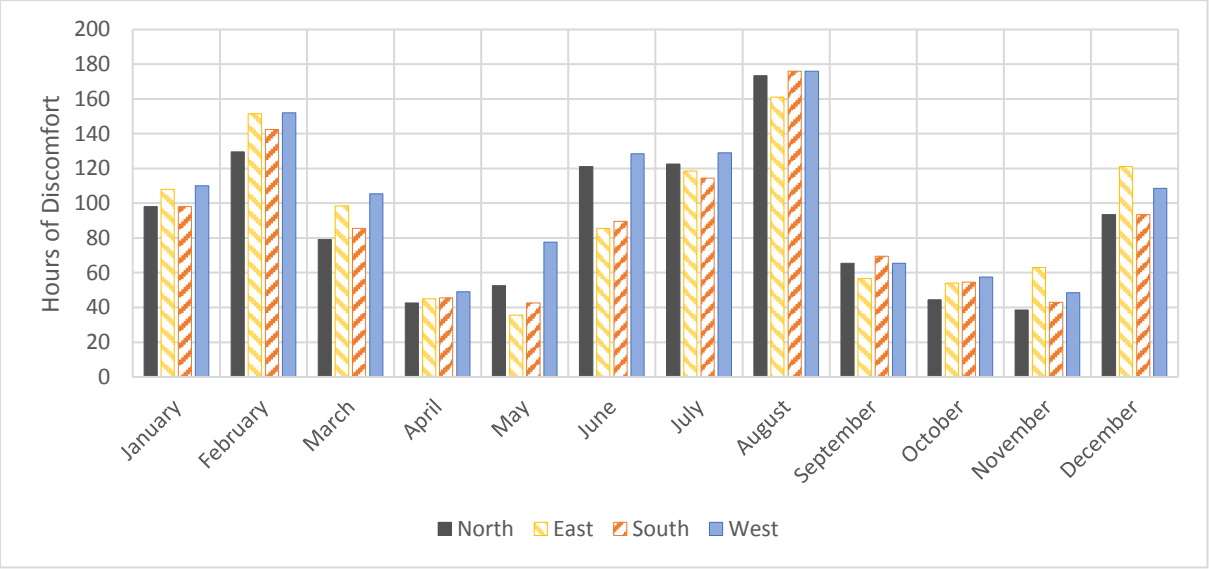

Figure 3-5: Monthly hours of thermal discomfort in office-type thermal zones (Current ERC Simulation)

The simulation predicts the greatest discomfort in Cape Town's winter months – June, July and August – where the average ERC operative temperatures are below 20 °C. Outside of these months, the greatest discomfort is experienced in February (12.8% of annual discomfort hours), which had the

highest average operative temperature in Table 3-8, followed by December (9.2% of annual discomfort hours), with the second highest average operative temperature. Detailed data for Figure 3-5 can be found in Table 9-11 of Appendix D.

Summer months (December through March) accounted for 37.6% of total annual discomfort hours, compared with 38.9% in winter (June, July and August). This suggests that the ERC requires heating in winter, in addition to summer cooling, in order to minimise year-round thermal discomfort. Occupancy hours are lower in December than in other summer months as ERC researchers typically take annual leave over the last two weeks of the month, and discomfort hours are only calculated for periods when the offices is occupied.

However, as noted earlier, ERC heating is beyond the scope of this dissertation. Winter discomfort will therefore not be directly addressed here, although the preventative measures discussed in Chapter 4 may provide some improvement to winter thermal conditions, in addition to reducing summer cooling requirements.

Of the four thermal zones shown in Figure 3-5, West offices experience the most thermal discomfort hours per year, followed in descending order by East, North and South. West facing offices were predicted to experience 476 thermal discomfort hours between December and March, including 152 discomfort hours in February. All thermal zones experienced the greatest *summer* discomfort during February (see Table 9-11), which is consistent with February being the warmest month of the year. Figure 3-6 shows combinations of operative temperature and relative humidity for each office zone in the month of February, disaggregated in terms of thermal comfort or discomfort for occupants.

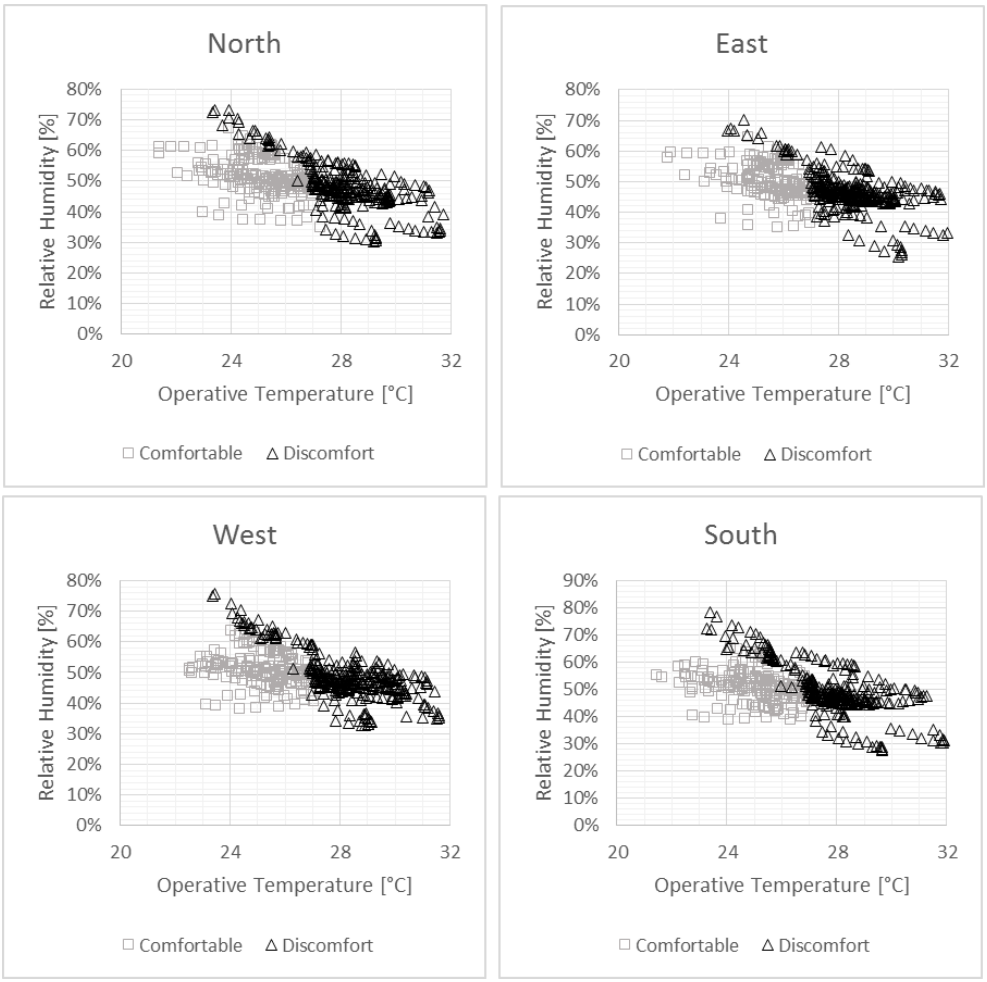

Figure 3-6: Current psychrometric conditions and thermal comfort levels of office thermal zones, as simulated during February occupancy hours

Figure 3-6 illustrates the effect of both temperature and humidity on occupants' comfort: at lower relative humidity ratios, in the range of 40% to 55%, operative temperatures up to 27 °C are mostly experienced as comfortable. Where relative humidity elevates above 55%, particularly in the range of > 60%, comfortable maximum operative temperature range is reduced to 25 °C or below. This is reflected in Table 3-9, which compares average comfortable and uncomfortable conditions predicted in February.

Table 3-9 shows a relatively small difference in relative humidity percentage points between comfort and discomfort, while temperatures under comfortable conditions were on average 3 °C lower than under discomfort conditions. From the table, one can expect the ERC to require more significant sensible cooling that regulates temperature than latent energy regulation, for humidification and dehumidification of the air.

Table 3-9: Average conditions in office thermal zones for predicted thermal comfort and discomfort in February

Office zone	Comfortable		Discomfort	
	Ave T_O [°C]	Ave RH [%]	Ave T_O [°C]	Ave RH [%]
North	25.6	51%	28.5	47%
East	25.2	52%	28.1	48%
South	25.1	51%	27.9	49%
West	25.2	51%	28.2	48%

3.3.2. Heat Gains

Figure 3-7 shows annual internal heat gains and heat transfer through the ERC envelope ('Fabric' gains/losses) for each ERC thermal zone; Figure 3-8 below shows zonal heat gains normalised by floor area. Table 9-12 and Table 9-13, in Appendix D, show detailed data for each figure. From Figure 3-7, it can be seen that solar gains (through external windows) are the largest single source of heat gain (20.65 MWh_{th} per annum), followed by lighting heat gains (19.99 MWh_{th} per annum).

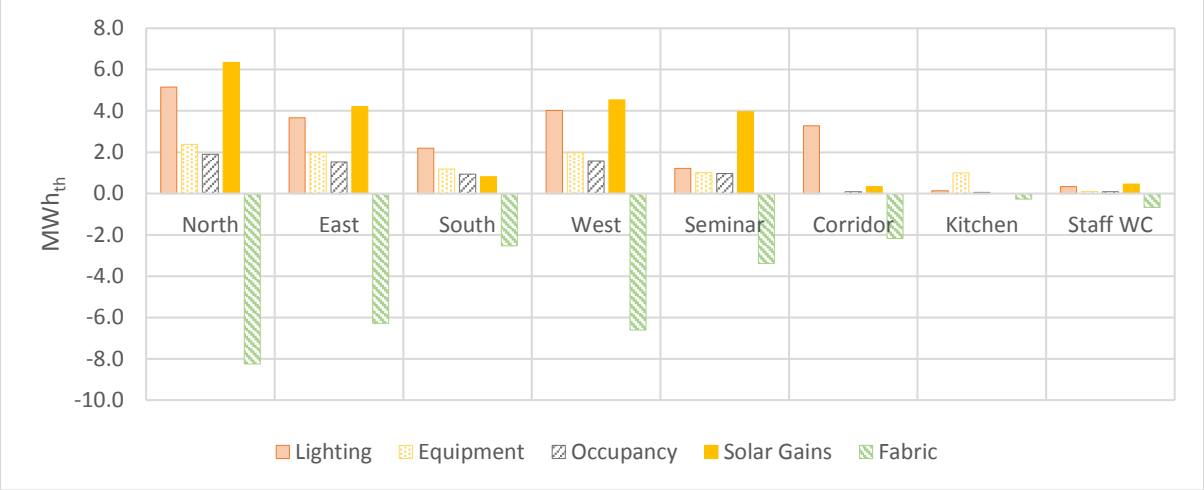

Figure 3-7: Annual net heat gains and losses attributed to internal gains and building fabric heat transfer

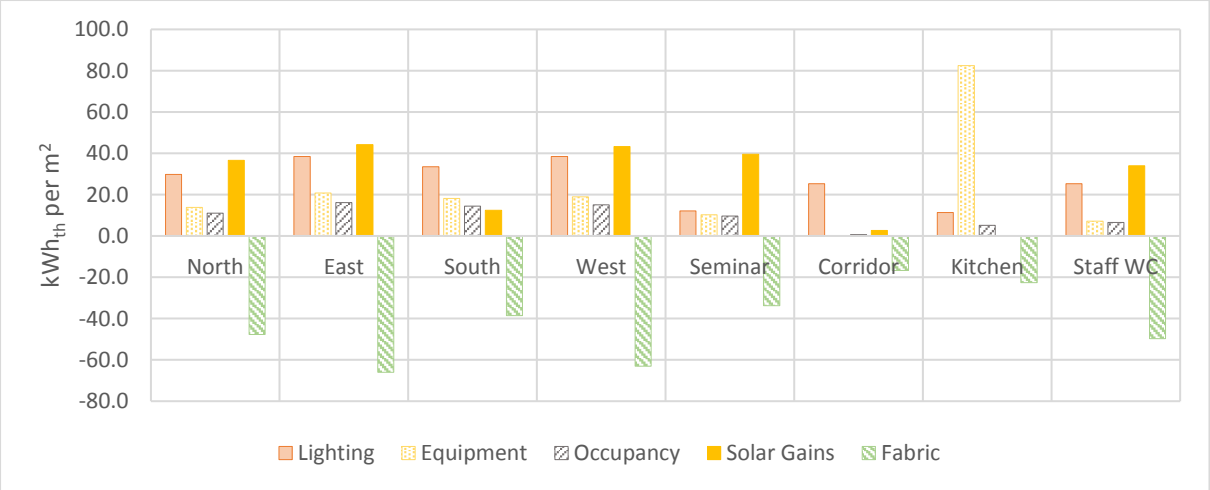

Figure 3-8: Annual net heat gains and losses normalised per thermal zone floor area

Note that *EnergyPlus* determines lighting and equipment internal heat gains by first quantifying annual lighting and equipment energy use, from the power densities and schedules input per thermal zone. Heat gain is then calculated by multiplying the energy use by a factor that accounts for heat transferred out of the thermal zone through return air flow (DesignBuilder, 2016), e.g.:

$$Q_{light} = W_{light}(1 - F_{RA})\ \text{[GJ]} \qquad (3\text{-}2)$$

Where Q_{light} is annual lighting heat gain, W_{light} is annual lighting energy use and F_{RA} is the return air fraction, as described in § 3.1.6. In the case of the ERC $F_{RA} = 0$, and therefore *EnergyPlus* calculates $Q_{light} = W_{light}$. The same approach is applied to the calculation of equipment heat gains (Q_{equip}).

The fabric heat losses shown in Figure 3-7 are calculated from the sum of conduction through ceilings, walls, floors, doors and glazing of thermal zones. In the case of glazing heat gains, these are calculated by measuring total window heat gain and subtracting transmitted solar (direct and diffuse SW radiation) gains, as these are already accounted in Solar Gains (through external windows). Net heat loss through the envelope is expected, given the average differential between indoor and outdoor DB temperatures identified in Table 3-8 previously, as well as the permanently cooled fifth floor below the ERC.

Figure 3-8 shows that solar (SW) radiation and interior lighting are the dominant sources of heat gains for each office-type zone and the Seminar Zone. The exception is the South zone, which receives little solar exposure relative to other zones. Heat gains in the kitchen are significantly dominated by equipment, which is expected due to the presence of continually operating fridges and an electric water boiler. Figure 3-9 shows overall proportions of internal heat gains across the ERC, with solar and lighting shown to account for 71% of annual internal ERC heat gain.

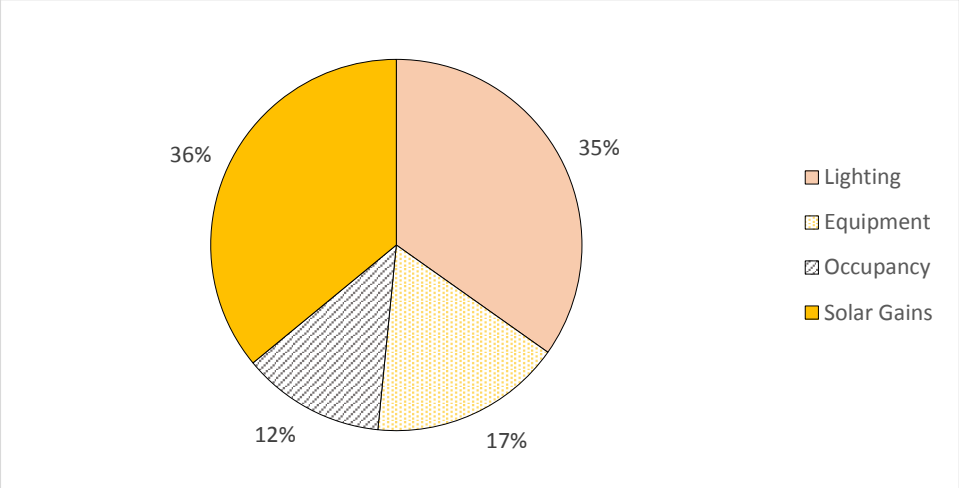

Figure 3-9: Share of internal heat gain sources

These results suggest there is potential to reduce net-ERC heat gain by means of preventative measures that can reduce lighting waste heat emissions and solar gains through the windows. These concepts are explored in greater detail in § 4.2 and § 4.3 respectively.

Figure 3-10 through Figure 3-13 summarise hourly heat gain profiles due to solar radiation, lighting, ceiling gains and a combination of other internal and fabric gains for the North, East, South and West zones, respectively, over the Cape Town Summer Design Week.

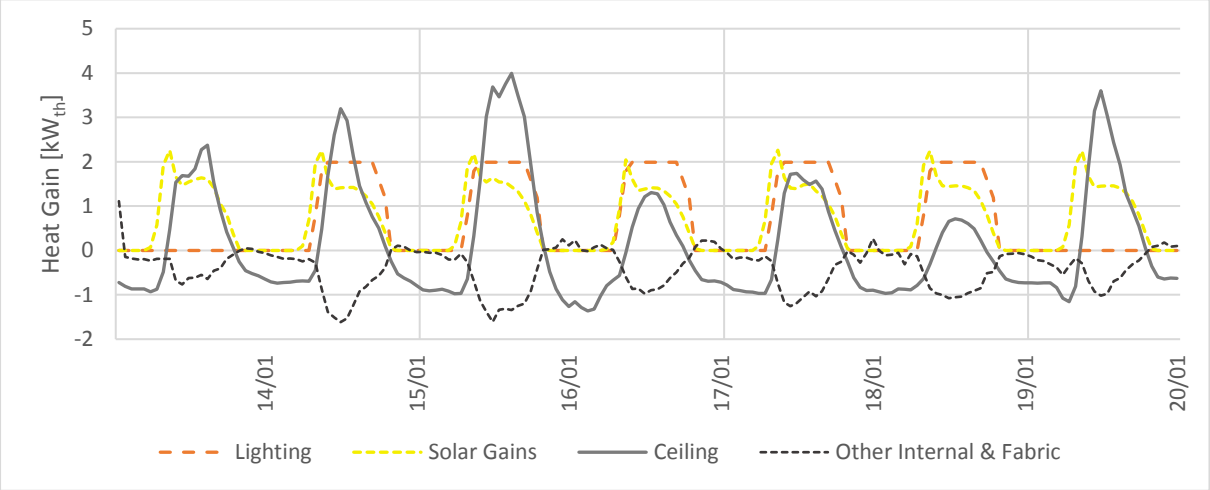

Figure 3-10: North office zone heat gains during Cape Town Summer Design Week

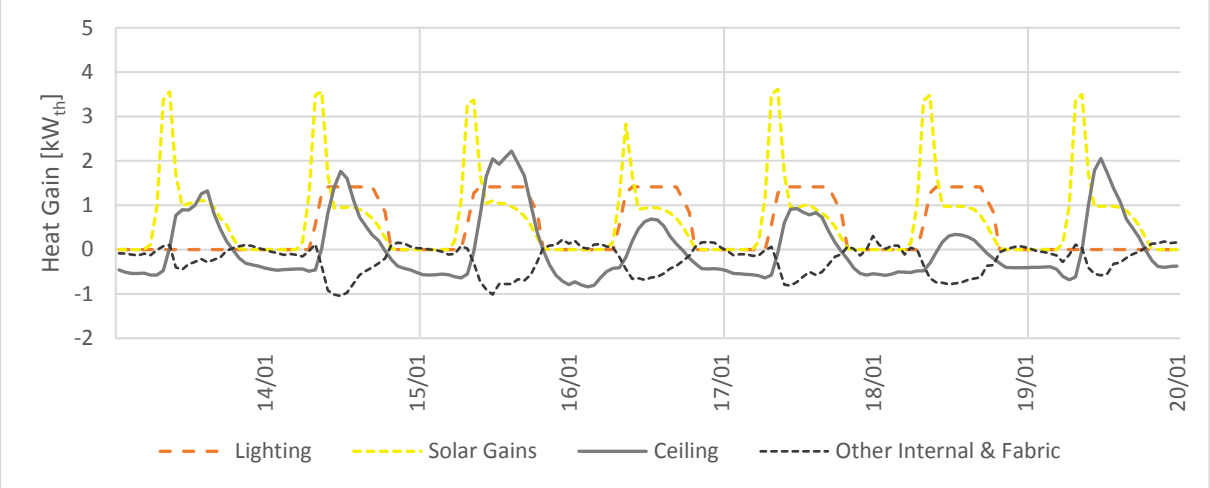

Figure 3-11: East office zone heat gains during Cape Town Summer Design Week

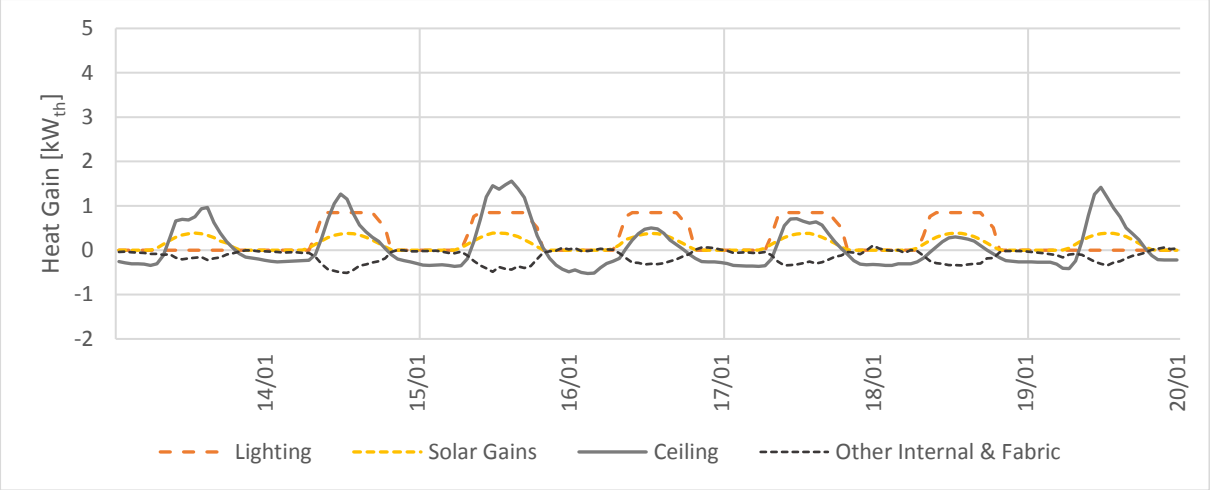

Figure 3-12: South office zone heat gains during Cape Town Summer Design Week

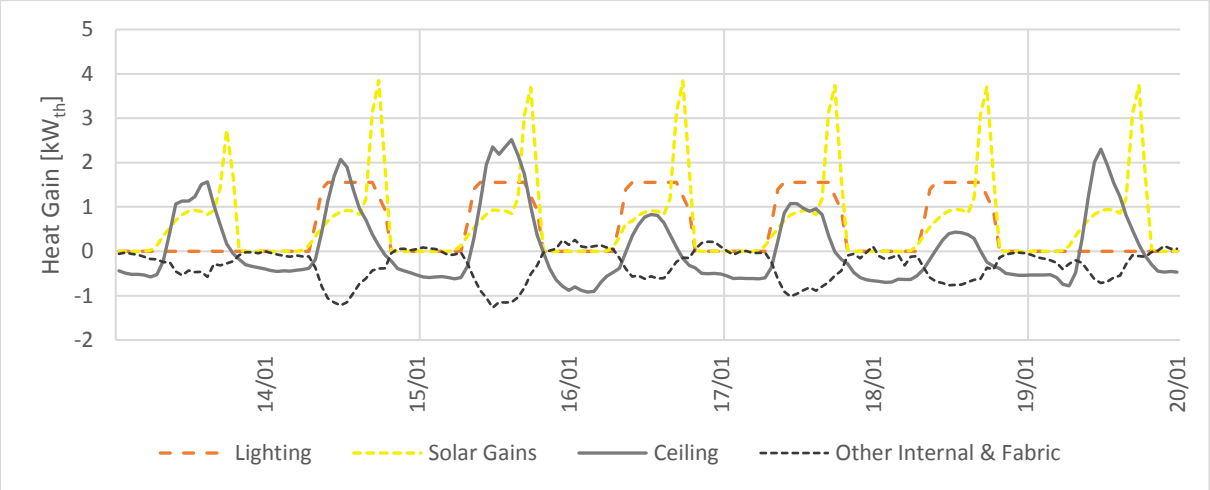

Figure 3-13: West office zone heat gains during Cape Town Summer Design Week

The figures show, firstly, the impact of orientation on solar heat gains of thermal zones. This is highlighted in the contrast between the east offices (Figure 3-11), which receive peak solar gains during the early morning around 10:00, and the west offices (Figure 3-13), where solar gains peak in the afternoon (15:00 – 17:00). The South zone receives comparatively low sunlight during the summer months, due to the angle of incidence of the sun on Cape Town in summer. The eaves of the building shade the North windows in summer, when the sun reaches its greatest altitude. At lower altitude angles, around sunrise and sunset, solar radiation is less obstructed by the shading, and can transmit more directly through east-facing and west-facing glazing respectively; hence these zones experience greater solar heat gains than North and South zones.

The second observation from Figure 3-10 through Figure 3-13 is the daily peak in heat gains through the ceiling, which occurs in each office zone around midday. This arises from the continual exposure of the Menzies roof to the sun during the day, which causes the air contained within the roof to heat above room temperature below. Owing to the lack of ceiling insulation of the *Current* model, much of that heat is transferred through the ceiling to the thermal zones below.

This suggests that a key step in cooling the ERC would be to install an insulation layer (or repair existing material). This concept is analysed in greater detail in § 4.1 further on. Note that net heat annual transfer through the ceiling is -11.74 MWh_{th} (Table 9-12), showing that the ceiling is a source of overall heat loss. Improvement to the thermal resistance of the ceiling would therefore be expected to reduce ERC heat loss during winter, providing improvement to winter thermal discomfort in addition to summer.

3.3.3. Model Validation

The results of the ERC *Current* simulations show that thermal zones consistently experience significant internal heat gains. The simplified modelling process for these gains, using assumed fixed schedules of operation, creates uncertainty and inaccuracy with the simulation results. The fixed schedules, while based on typical behaviour, do not characterise in detail the variance to these gains that would be expected from variable human behaviour and other uncontrolled, influencing factors. This uncertainty can be controlled by applying more rigorous and complex input models representing building operation, based on detailed surveys and stochastic data (Ryan & Sanquist, 2012:381), but is beyond the scope of this work.

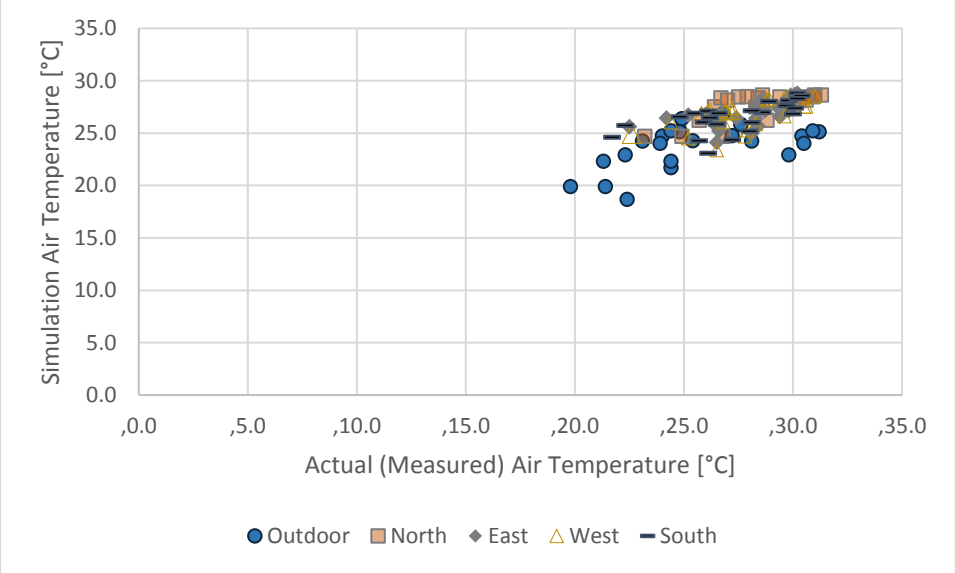

Figure 3-14: Comparison of simulated and actual air temperatures for office thermal zones

However, initial validation of the energy model for the ERC base run was performed, by comparing predicted air temperature results from the simulation with actual temperature measurements over a three-day period. Hourly temperature measurements were recorded for the North, East, West and South thermal zones and outdoor temperature, and compared with simulated air temperature predictions at the same hourly interval, as shown in Figure 3-14. Detailed data is shown in Table 9-18 of Appendix D.

Table 3-10 shows statistical correlation and coefficient of variance determined for the sample of air temperature measurements, relative to simulation results. Correlation coefficient is above 0.50 but below 0.75, indicating some correlation between the data sets, but not a direct positive relationship. However, the mean bias error (MBE) showed relatively small positive bias (below 7.5%) of the

simulated results, relative to actual data. Positive bias indicates that the simulation overestimates building temperatures, and therefore heat gains, such that cooling load estimates determined from the model are expected to be conservative. Root mean-square error (RMSE) of the simulated results showed air temperature variation around 2 °C for internal temperatures, and 3.31 °C for outdoor temperature, with the coefficient of variance (CV) ranging from 5.5 through 13%.

Table 3-10: Statistical correlation between actual and simulated sample data (per office zone)

Thermal Zone:	**Outdoor**	**North**	**East**	**South**	**West**
Correlation coefficient	0.5548	0.7360	0.6020	0.6418	0.6037
MBE	7.07%	2.78%	3.26%	3.06%	3.57%
Sample size, n	24	24	24	24	24
RMSE [°C]	3.31	1.68	1.83	2.05	1.97
Mean [°C]	25.58	28.34	27.65	27.36	27.70
CV(RMSE)	12.92%	5.92%	6.63%	7.48%	7.11%

While variance of the data is relatively low, it should be noted that temperature differences of the magnitude of 2 °C can significantly alter predictions of thermal discomfort, according to the sensitivity of the ASHRAE comfort zone.

Uncertainty is induced from modelling error, courtesy of unverified input assumptions, as well as random error of the temperature measurement process. Risk of uncertainty from the latter could be mitigated by more comprehensive temperature logging in each thermal zones, creating a larger sample size of data. Other suggestions for more methodical approaches to validation were discussed in the literature review.

3.4. ERC Base Case Simulation Results

The input energy model developed in *DesignBuilder* was simulated, as before, for a whole-year period, as well as the Summer Design Week (13 January to 19 January), in order to characterise the *Base Case* cooling requirements of the ERC.

For *Base Case* modelling, an *EnergyPlus* Zone HVAC: Ideal Loads Air System component was included in the *DesignBuilder* energy model for each ERC thermal zone. This component is available in *EnergyPlus* as a means of assessing thermal performance of a building without detailed specification of an HVAC system – i.e. modelling the air handling unit, condenser loops, chilled water loops and other HVAC components is not required. The simulation instead assumes the component has infinite cooing capacity for each thermal zone, and is regulated only by predetermined cooling schedules for the building. The component automatically adjusts supply air flow rate with every iteration of calculation, and adds or removes moisture from the air at 100% efficiency, with constant COP_R of 3.0 (EnergyPlus, 2015:913). The Ideal Loads component includes an 'ideal thermostat', which provides sensible cooling, as well as an 'ideal humidistat', which provides humidification and dehumidification to regulate latent loads.

ERC cooling load requirements were modelled throughout using the *EnergyPlus* Ideal Loads component, both for the *Base Case* and subsequent preventative cooling scenarios (Chapter 4). Air supply parameters were assumed constant for each simulation, as shown in Table 3-11. Ideal sensible

and latent cooling loads for the ERC thermal zones were thus determined for each simulation period. These load estimates do not account for system losses and inefficiencies that will occur in an actual HVAC system.

Table 3-11: Simulation input parameters applied for Ideal Loads cooling simulations

***EnergyPlus* Input Parameter**	**Property**
System Component:	*EnergyPlus* ZoneHVAC:IdealLoadsAirSystem
Fuel	Electricity from grid
Assumed Cooling System Seasonal COP	3.0
Ideal system cooling efficiency	100%
Minimum supply air temperature [°C]	12.0
Minimum supply air humidity ratio [g/g]	0.0077
Flow rate and capacity limits	Unspecified
Humidification and dehumification control type:	Humidistat
Cooling Design Set point [°C]	24.0
Relative Humidity Humidification set point	30%
Relative Humidity Dehumidification set point	60%

Cooling energy consumption can be estimated from simulated annual cooling (heat removal) requirements by means of manipulating equation 2-25 as follows:

$$W_{in} = \frac{Q_L}{COP_R} = \frac{Q_L}{3.0} \text{ [kWh]} \qquad (3\text{-}3)$$

ERC *Base Case* cooling results, based on ideal cooling simulations Run 2-1 through Run 2-3 (see Table 9-1 in Appendix A), are presented in the following sub-sections. More detailed data from these simulations are included in Appendix E.

3.4.1. Thermal Effect of Ideal Cooling

The effects of the Ideal Loads thermostat on thermal conditions within the ERC are shown in Table 3-12, while Figure 3-15 illustrates monthly discomfort hours with cooling (disaggregate data is shown in Table 9-19 through Table 9-21 in Appendix E).

Table 3-12: Comparison of average monthly thermal comfort conditions, simulated with and without cooling

Month	**Outdoor**	***Current* (No Cooling)**			***Base Case***		
	T_{DB} [°C]	T_O [°C]	RH [%]	Discomfort Hours	T_O [°C]	RH [%]	Discomfort Hours
Jan	20.8	24.3	54.5%	674.0	23.4	56.1%	0.0
Feb	20.9	25.0	53.1%	974.0	23.7	55.7%	0.0
Mar	19.1	23.6	58.2%	589.5	22.8	59.2%	0.5
Apr	16.5	22.1	57.0%	328.5	21.7	57.3%	80.0
May	14.8	20.8	56.1%	357.0	20.6	56.1%	312.0
Jun	12.8	18.4	55.9%	785.0	18.4	55.7%	789.0
Jul	12.3	18.5	55.3%	921.5	18.5	55.0%	906.0
Aug	12.9	17.4	60.5%	1335.0	17.4	60.2%	1345.0
Sep	14.3	20.0	55.5%	484.5	19.9	55.5%	483.5
Oct	16.0	22.1	50.2%	381.5	21.6	51.0%	137.0
Nov	18.3	22.7	53.9%	282.0	22.2	55.0%	29.0
Dec	19.8	24.6	52.0%	702.0	23.6	53.9%	1.0

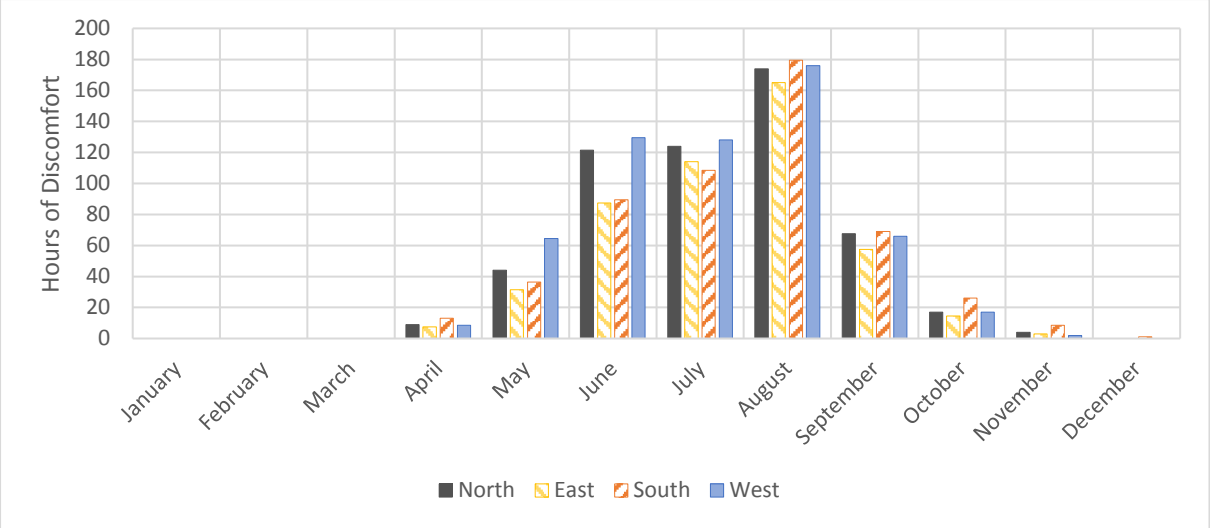

Figure 3-15: Monthly hours of discomfort in office thermal zones under Base Case simulation

Average internal operative temperature reduced by 0.5 °C (2.2%) annually and by 1 °C (4.1%) between December and March. Discomfort hours in the ERC were reduced to 0 for January and February, with only 0.5 and 1 hour of discomfort simulated in December and March respectively. Discomfort hours were further reduced by 89.7% in November, 75% in April and 64% in October (with negligible change in the cooler months, as expected). These results confirm that the peak cooling load [kW_{th}] and annual cooling requirements [MWh_{th}] computed by the *Base Case* simulation provide an adequate estimate of actual comfort cooling that would be required for the ERC.

3.4.2. Current ERC Cooling Requirements

Figure 3-16 shows annual heat gains and losses for each thermal zone, with the addition of cooling requirements to achieve comfort design conditions (described in Table 3-12 above). Total annual cooling under the *Base Case* was determined as 27.64 MWh_{th}. Figure 3-17 shows heat gains normalised by thermal zone floor area. The East and West zones require the greatest cooling (18% and 17% respectively, on a per-m^2 basis), which again illustrates the effects of building orientation on energy efficiency. The office zones collectively account for 72% of annual cooling [MWh_{th}], with another 17% required by the ERC corridor (see Table 3-13 further on in this section).

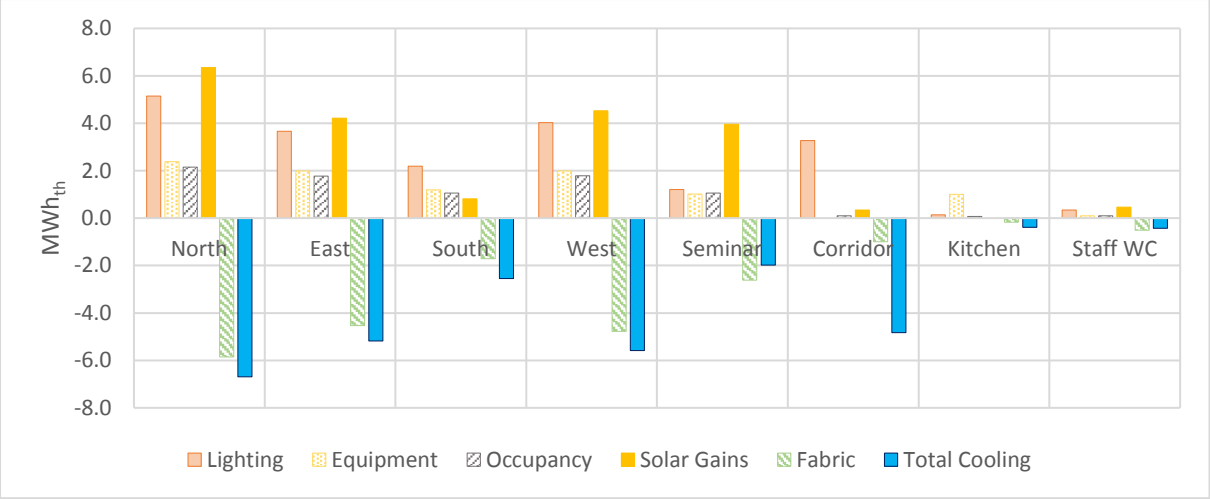

Figure 3-16: Annual Base Case heat gains and cooling energy requirements

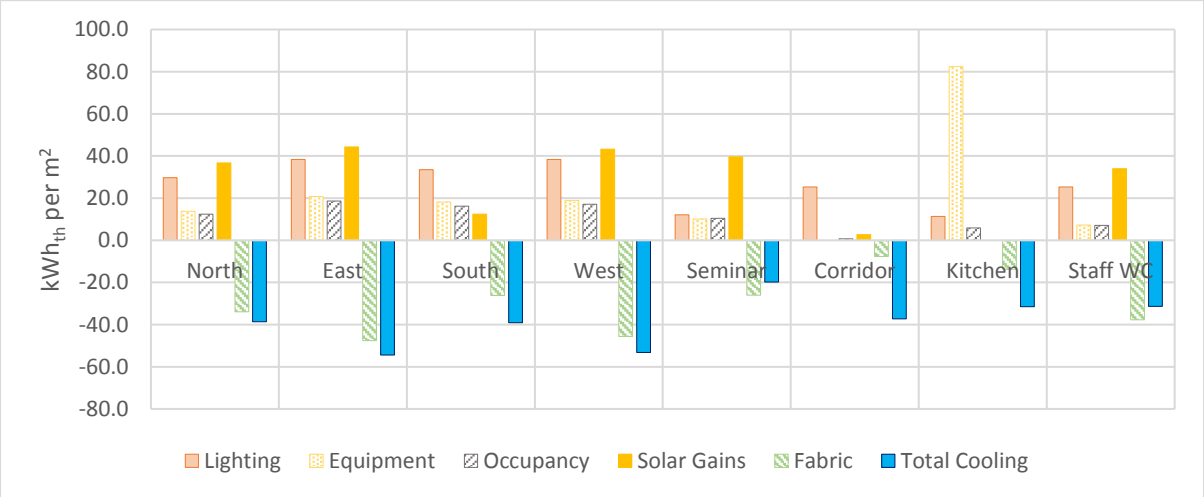

Figure 3-17: Annual Base Case heat gains and cooling energy requirements normalised by thermal zone floor area

Cooling loads simulated by *EnergyPlus* are divided into sensible cooling, from which the ideal thermostat regulates temperature, and latent cooling, whereby the ideal humidistat provides humidification and dehumidification. Figure 3-18 thus shows monthly cooling requirements for the ERC to be maintained within design conditions, disaggregated into sensible and latent cooling components. Only the office-type thermal zones are shown, as they were found to dominate ERC cooling requirements previously, with more complete data shown in Table 9-24 and Table 9-25 in Appendix E.

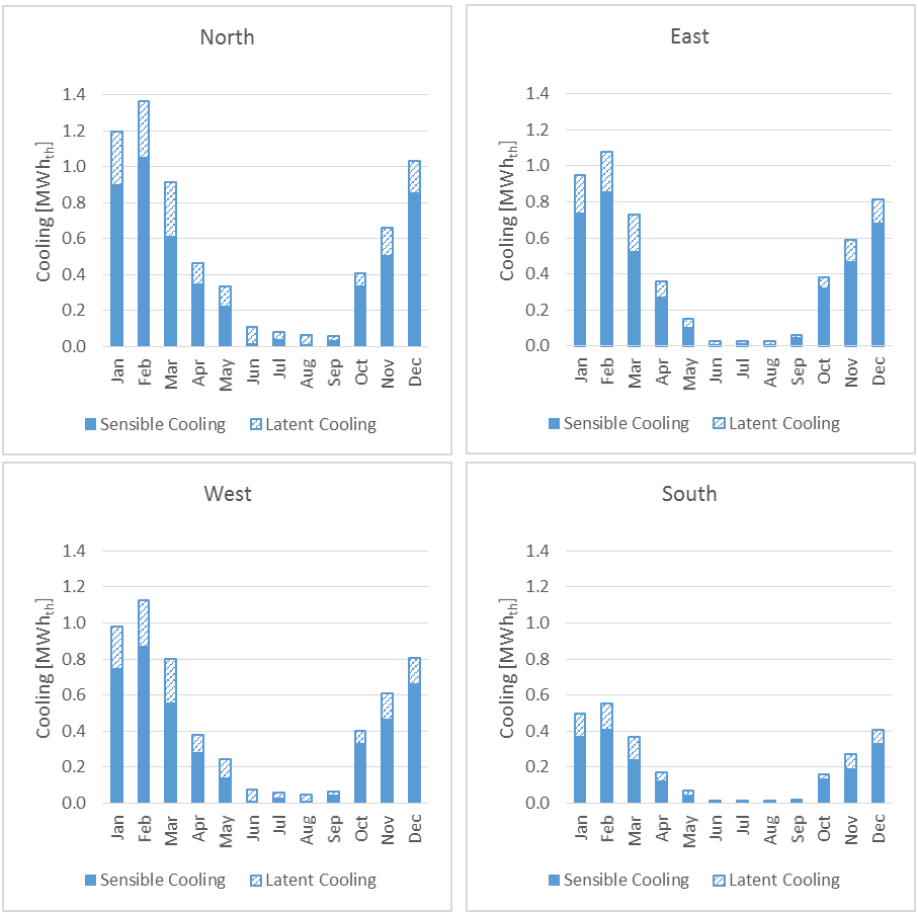

Figure 3-18: Simulated monthly Base Case sensible and latent cooling requirements for office thermal zones

The figure shows negligible sensible cooling required in the winter months, as expected, with some small latent energy regulation required to maintain humidity between design thresholds. In the warmer months (October through April), sensible cooling dominates latent cooling, with total cooling peaking in February. This was expected following the findings in § 3.3.1, which showed that February was the warmest month in the ERC, with the most hours of discomfort. Table 3-9 had also previously shown small differences in relative humidity between comfortable and uncomfortable thermal conditions, and larger differences in temperature, suggesting that sensible cooling requirements would be dominant. Cooling energy requirements are greater in magnitude for the north zone, predominantly due to its greater floor area. When normalised by floor area (as shown in Table 9-26 in Appendix E), the east thermal zone has the greatest cooling requirement (peaking at 11.34 kWh_{th}/m^2 in February), followed by the west zone (10.77 kWh_{th}/m^2).

Figure 3-19 shows the heat balance profile for the entire ERC (aggregating all thermal zones) for the Cape Town Summer Design Week (Run 2-2; data for the figure is shown in Table 9-27 in Appendix E). The figure shows cooling loads peak between midday and late afternoon in summer, coinciding with peak ceiling, solar and interior lighting heat gains as would be expected. The cooling load peaks at 16:00 on 15 January at 66.87 kW_{th}, which is considered study to be the maximum cooling load required for the ERC for the purposes of this study.

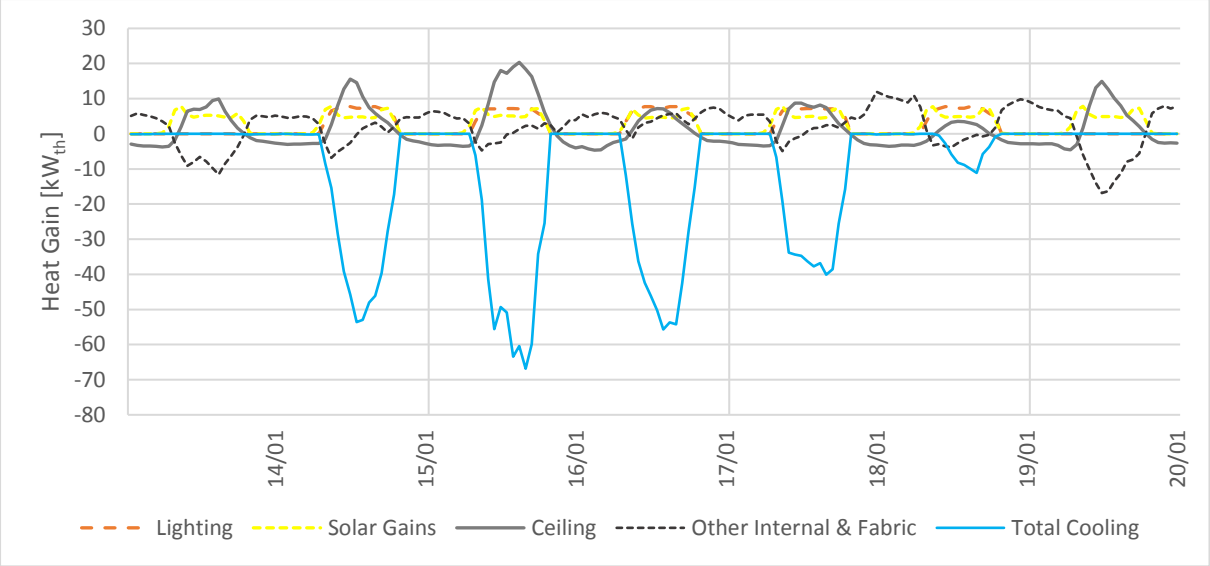

Figure 3-19: Aggregate Base Case heat balance profile for the Cape Town IWEC Summer Design Week

Table 3-13 below shows the 'contribution' of each thermal zone to the peak cooling load, and contrasts this with the annual cooling requirements for each zone. Results shown in Table 3-13 are used to define the *Base Case* annual cooling and peak cooling load requirements for the ERC, in the absence of additional preventative cooling measures.

Table 3-13: Peak cooling load and annual cooling requirements under the Base Case simulation

Thermal Zone	Peak Cooling Load [kW_{th}]	Annual Cooling [MWh_{th}]
North	16.95	6.69
East	10.99	5.19
South	8.14	2.55
West	12.85	5.59
Seminar	9.24	1.98
Corridor	18.89	4.83
Kitchen	1.27	0.38
Staff WC	1.47	0.42
Total	**66.87**	**27.64**

From results in Table 3-13, equation 3-3 can be used to determine *Base Case* annual cooling electricity consumption of 9.21 MWh per annum (as shown in Table 9-28 in Appendix E). As these are ideal assumptions (an air conditioning system operate continuously at 100% efficiency), this represents an underestimate of annual electricity use, and is not conservative. However, this ideal cooling assumption was applied consistently to all cooling simulations in this dissertation, such that all cooling energy estimates have a consistent underestimate.

This chapter has established *Base Case* cooling loads and requirements for the ERC. The chapter which follows describes further simulation analysis, which was performed to assess the impacts of a selection of preventative measures on reducing cooling loads and requirements below *Base Case* estimates.

4. Preventative Cooling Scenarios

This chapter examines a series of scenarios in which the cooling requirements identified in the *Base Case* may be offset by preventative measures that reduce heat gains to thermal zones. While there are multiple approaches by which buildings can minimise the impact of external and internal heat gains to their interior, this dissertation is limited to considering three potential retrofit options for the ERC, based on the heat gain sources identified in § 3.3 and § 3.4. These are:

1. Thermal insulation of ceilings
2. Energy efficient lighting – delamping and replacing existing lamps and ballasts
3. Internal shading of windows, to minimise internal solar heat gains

While this is not an exhaustive list of potential preventative cooling retrofits, these options are expected to be the most practical and feasible for the ERC. Other options, such as altering the interior office layout or resizing the building's windows, would likely result in further improvements to thermal comfort, but are would also be more difficult to implement on a limited budget.

Additionally, there is potential for improvements through enhanced analysis and control of occupancy behaviour, as well as more conscientious and energy efficient use of electronic equipment. For example, reductions in heat gain could be achieved by removing one of the fridges in the kitchen. However, the human element of these thermal components makes it more challenging to implement changes that would consistently reduce energy use and internal heat gains. More rigorous data, comprising surveys of occupants and actual energy metering of equipment, would allow better analysis of these factors.

Nevertheless, the findings of Chapter 3 showed that the most significant heat gains to the ERC arise from solar gains through exterior windows, interior lighting and heat flux through the ceilings particularly on warm, summer days. The three preventative measures listed above are chosen for their perceived ease of implementation, and in direct response to these principal heat gain components.

4.1. Ceiling Insulation

As discussed in § 3.1.3, the ERC currently has a thin (50 mm) layer of fibreglass insulation above its ceiling, sporadically distributed across the surface area. Large gaps occur in which no insulation covers the ceiling, which greatly reduces its overall thermal resistance. The ERC was thus modelled with an uninsulated ceiling (R = 0.895 m^2K/W) for the *Current* and *Base Case* simulation analysis.

This section analyses the potential impact of replacing the existing insulation with a different material, of varying thickness, that is consistently distributed throughout the ERC ceilings. The impacts are assessed first by examining the effects of increasing insulation thickness on annual thermal discomfort, without active cooling. Thereafter, sensitivity analysis is performed to compare predicted annual cooling and peak cooling loads for varying ceiling thermal resistance, based on increasing insulation thickness through a series of increments.

The effects of thermal insulation were analysed, as before, by means of *EnergyPlus* simulation of the ERC model, through the *DesignBuilder* user interface. The simulation methodology and basic input data (except for the ceiling constructions) was consistent with the approach defined in in § 3.2. ERC

cooling was assessed as before, in § 3.4, with the *EnergyPlus* Zone HVAC: Ideal Loads Air System. The simulations referred to in this section (Run 3-1 through Run 3-12) are summarised in Table 9-1 of Appendix A. Detailed output data from these simulations are shown in Appendix F.

4.1.1. Effect on Thermal Conditions

Polyester fibre (PF) insulation was selected over other materials listed in Table 2-2 (see § 2.5.1) because of its ease of installation, low fire and health risk, and good moisture resistance (Papadopoulos, 2005:82). Polyester fibre blankets have a lower environmental impact, compared with fibreglass, as they are manufactured from recycled plastic material, and can be more easily recycled or disposed at the end of their life. PF blankets of different thicknesses, made from recycled polyethylene terephthalate (PET) bottles, are commercially available in South Africa (Isotherm, 2015). The technical specifications of these products were used as input data for this analysis.

Table 4-1 shows the thermal properties of polyester fibre for different thicknesses, ranging from 40 to 135 mm (according to what is commercially available), as well as the effect on the overall R-value of the ERC ceilings. Thermal properties are assumed consistent with provisions in SANS 204:2011 (see Table 2-2)

Table 4-1: Thermal resistance properties of different thicknesses of polyester fibre insulation

Insulation Thickness d_i [mm]	**Insulation Density [kg/m3]**	**Thermal Conductivity [W/mK]**	**Specific Heat [J/kgK]**	**Insulation R-value [m²K/W]**	**Ceiling R-Value [m²K/W]**
0	-	-	-	-	0.895
40	11.5	0.046	1 000	0.870	1.765
75	11.5	0.046	1 000	1.630	2.525
100	11.5	0.046	1 000	2.174	3.069
135	11.5	0.046	1 000	2.935	3.830

Simulations (Run 3-1 through 3-4 in Table 9-1) of the *Current ERC* were run over the Summer Design Week period, with ceiling insulation thickness varied as shown in Table 4-1. The simulation results were used to show average daily temperature profiles with differing insulation thickness for each thermal zone during extreme summer conditions; the North zone is shown in Figure 4-1 while data for all thermal zones are shown in Table 9-29 through Table 9-33 in Appendix F.

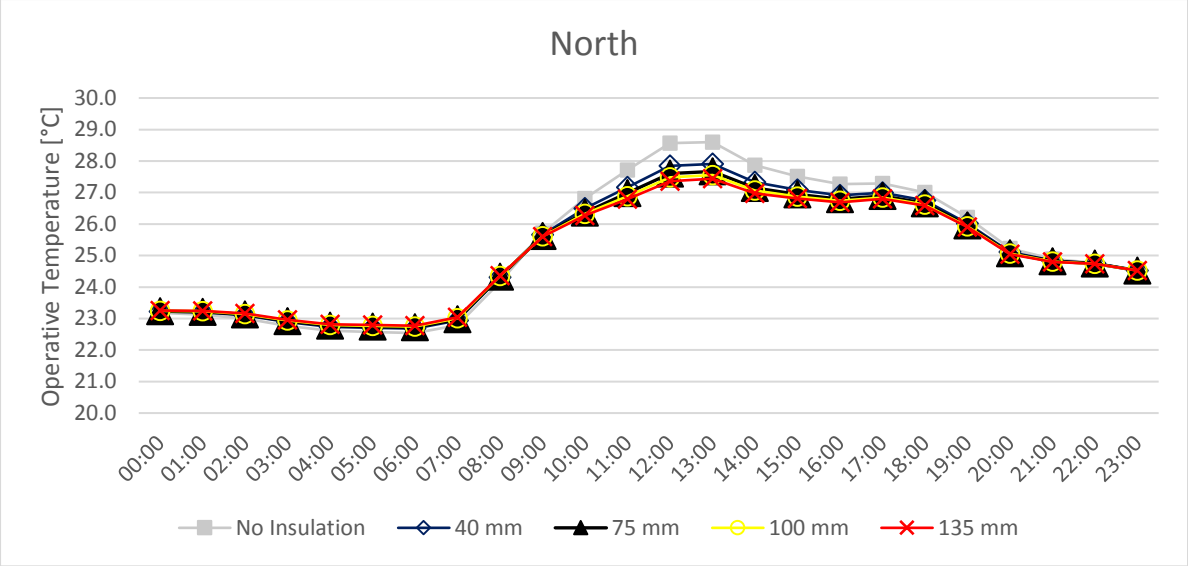

Figure 4-1: Average Summer Design Week operative temperature profile for North zone, simulated with varying insulation thickness and no active cooling component

The results show a reduction in peak operative temperature ($T_{o,max}$) of 0.8 °C – 1.0 °C in all thermal zones (e.g. North, Figure 4-1) when insulation thickness increases from 0 to 40 mm. Thereafter, subsequent increments in thickness result in lower margins of temperature reduction, as shown in Table 4-2 for the office thermal zones. Note that ΔT_o (percentage change in operative temperature) in Table 4-2 is calculated as follows:

$$\Delta T_o = \left(\frac{T_{o,max_{di}} - T_{o,max_0}}{T_{o,max_0}}\right) [\%] \quad (4\text{-}1)$$

Where:

- T_{o,max_n} is peak operative temperature with di [mm] is insulation thickness
- T_{o,max_0} is peak operative temperature with 0 mm insulation.

Table 4-2 shows that the increase from 40 mm to 75 mm thickness causes an average reduction of 1 percentage point in peak temperature, whereas the increase from 75 mm to 100 mm causes only 0.5 percentage point reduction.

Table 4-2: Peak operative temperatures at varying insulation thickness, showing percentage change from Current ERC simulation

d_i [mm]	North		East		South		West	
	$T_{o,max}$ [°C]	ΔT_o [%]	$T_{o,max}$ [°C]	ΔT_o [%]	$T_{o,max}$ [°C]	ΔT_o [%]	$T_{o,max}$ [°C]	ΔT_o [%]
0	32.0	0%	32.4	0%	31.9	0%	32.7	0%
40	31.1	-3.0%	31.6	-2.6%	30.9	-3.0%	31.9	-2.4%
75	30.7	-4.2%	31.3	-3.6%	30.6	-4.1%	31.6	-3.4%
100	30.5	-4.7%	31.1	-4.0%	30.4	-4.6%	31.4	-3.8%
135	30.4	-5.2%	31.0	-4.4%	30.3	-5.1%	31.3	-4.2%

Figure 4-2 shows discomfort hours calculated per thermal zone for varying insulation thicknesses. Discomfort decreases with increasing thickness, with smaller margins of improvement for each

increment. Total discomfort hours in the ERC decrease by 10% from 0 to 40 mm insulation, and by 4.5% from 40 mm to 75 mm (6 750.0 discomfort hours – 13.6% reduction relative to the *Current* case). From 75 mm to 100 mm, the discomfort hours reduce by only 1.9%.

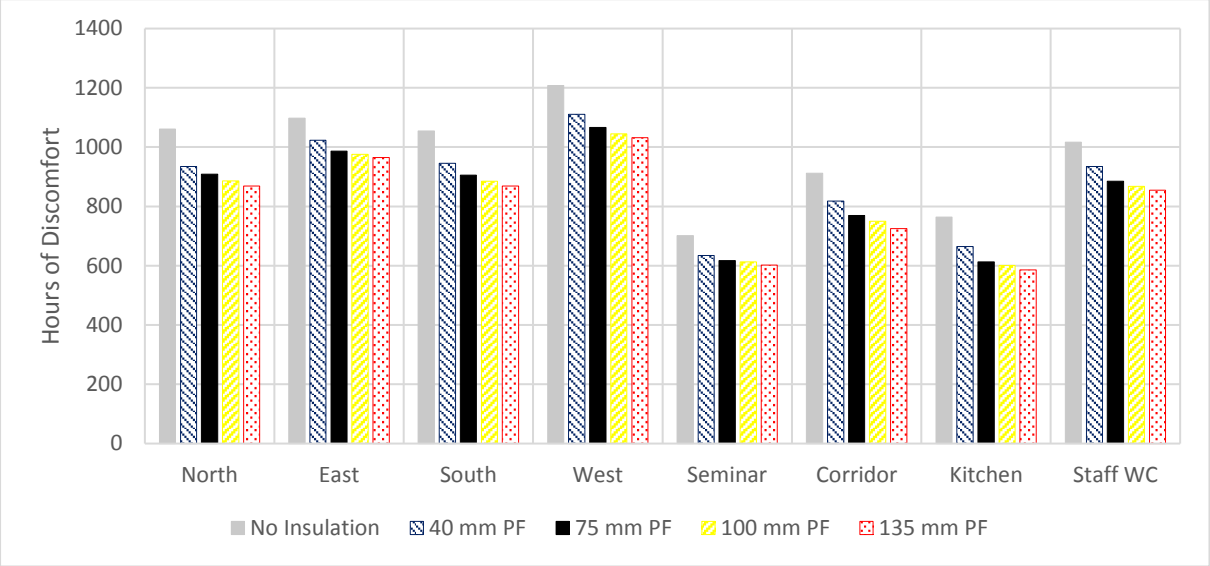

Figure 4-2: Annual simulated discomfort hours per thermal zone, with varying insulation thicknesses

The results above reflect the diminishing returns in temperature control with increasing insulation thickness, which is consistent with the findings of Aktacir et al (2010), as discussed in § 2.5.1.

The following sub-section examines the sensitivity of ERC cooling (annual cooling requirements and peak cooling loads) with different ceiling R-values, brought about by increasing insulation thickness as in Table 4-1.

4.1.2. Cooling Sensitivity to Insulation

The varying polyester fibre (PF) insulation properties defined in Table 4-1 above were applied in a series of simulations (Runs 3-5 through 3-12) to assess their impact on ERC cooling requirements, relative to the *Base Case* results. Sensitivity of annual cooling to ceiling thermal resistance was determined using the following equation, as defined in Lam and Hui (1995:28):

$$SQ_{cool} = \frac{(\Delta Q_{cool})/Q_{cool,0}}{(\Delta R_{ceiling})/R_{ceiling,0}} [\%] \qquad (4\text{-}2)$$

Where SQ_{cool} is cooling energy sensitivity, $Q_{cool,0}$ is *Base Case* annual cooling [MWh$_{th}$], and $R_{ceiling,0}$ is the R-value of the current ERC ceiling model (0.895 m^{2}K/W).

The results of the simulations are summarised in Table 4-3, showing revised annual cooling and peak cooling load for each thickness, as well as resulting sensitivity of cooling to variations in ceiling thermal resistance. Peak cooling load sensitivity ($SQ"_{peak}$) to ceiling thermal resistance is calculated using the same equation (4-2) as annual cooling sensitivity. As with the temperature profiles shown in § 4.1.1, sensitivity of cooling requirements decreases with increasing insulation.

Table 4-3: Sensitivity of simulated ERC annual cooling and peak cooling load to ceiling thermal resistance

Insulation Thickness [mm]	Ceiling R-Value [m^2K/W]	Annual Cooling [MWh_{th}]	SQ_{cool} [%]	Peak Cooling Load [kW_{th}]	$SQ"_{peak}$ [%]
0	0.895	-27.64	0%	-66.87	0%
40	1.765	-24.83	-10.4%	-57.58	-14.3%
75	2.525	-23.95	-7.3%	-54.48	-10.2%
100	3.069	-23.59	-6.0%	-53.17	-8.4%
135	3.830	-23.26	-4.8%	-51.95	-6.8%

The effect of incrementally increased insulation thickness on ceiling heat gain and cooling load profiles are shown in Figure 4-3 and Figure 4-4 respectively, with data shown for 15 January, the warmest day of the Summer Design Week (aggregated from all ERC thermal zones). Full data tables supporting these figures are shown in Table 9-35 through Table 9-38 of Appendix F.

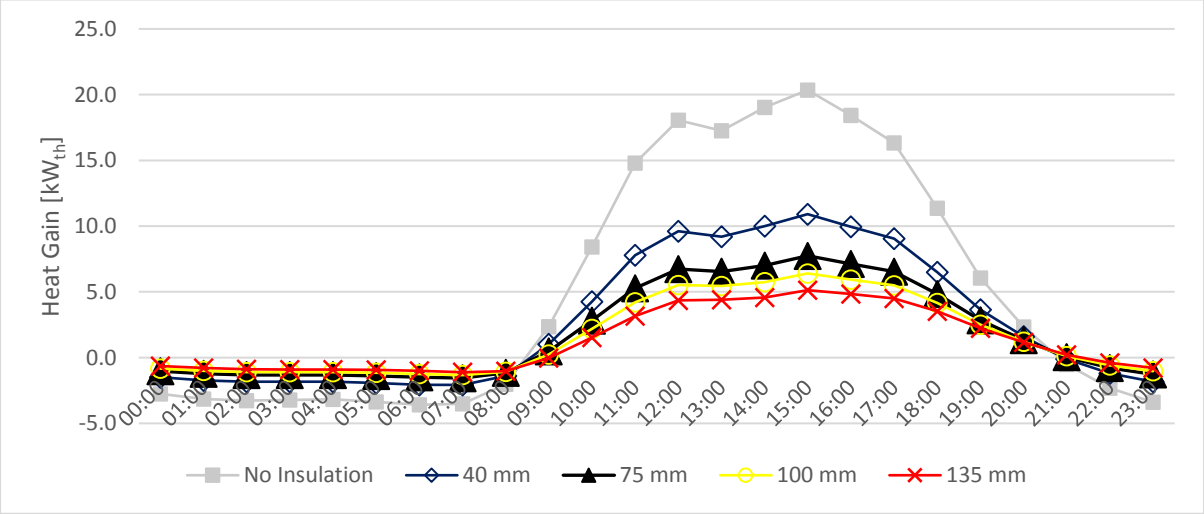

Figure 4-3: ERC aggregate ceiling heat gain simulated with varying insulation thickness during the Summer Design Week

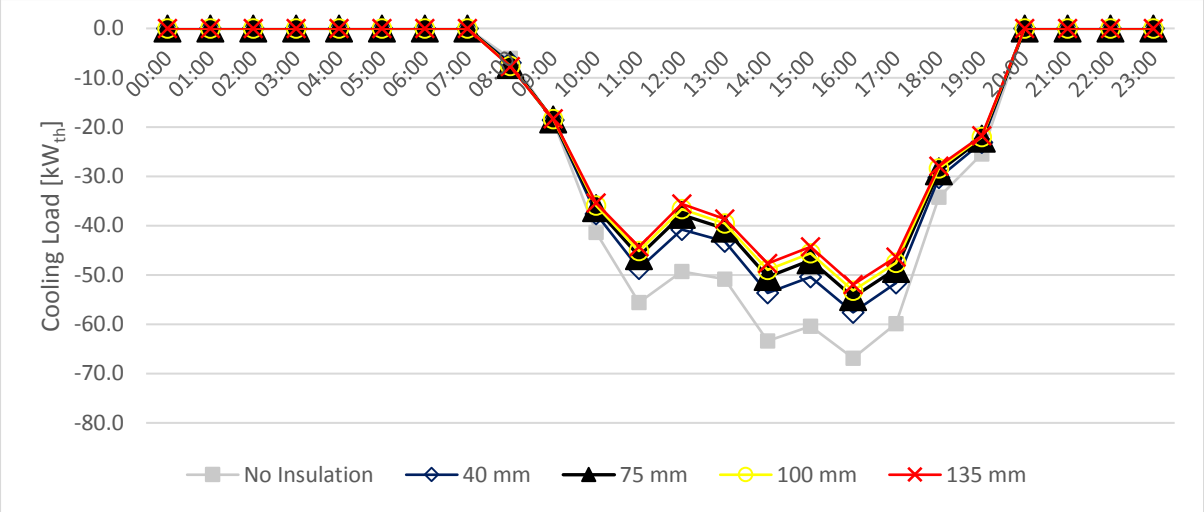

Figure 4-4: ERC aggregate cooling load simulated with varying insulation thickness during the Summer Design Week

With no insulation, ceiling heat gains peak at 20.35 kW_{th}. The introduction of 40 mm PF reduces peak ceiling gains by 46% to 10.91 kW_{th}; this has the effect of reducing peak cooling load by 14% (see Table 4-3). Increasing insulation thickness from 40 mm to 75 mm causes a further 29 percentage point reduction in peak ceiling heat gain and 5.4 percentage point reduction in peak cooling load. Figure 4-4 shows that further reduction in cooling load becomes increasingly negligible as insulation thickness increases above 75 mm.

These results show that a thickness of 75 mm polyester fibre insulation will be most optimal for reducing ceiling heat gains and cooling requirements of the ERC. This reduces peak cooling load by 18.53%, relative to the *Base Case*. The margins for improvement at greater thicknesses become smaller (less than 3 percentage points per thickness increment), suggesting these sizes would be sub-optimal from a cost-benefit perspective (particularly if the insulation material is priced per volume). While a more rigorous cost optimisation would be required to confirm this, further preventive scenarios discussed in this chapter are analysed with the assumed inclusion of 75 mm PF insulation (hereinafter referred to as the *75 mm-Insulation* Case) over and above the conditions of the *Base Case*.

4.2. Lighting Upgrade

This section considers the potential for reducing internal heat gains and cooling requirements by upgrading existing interior lighting. Two retrofit options are considered:

1. *Delamping*: lighting load is reduced by removing excess lamps for overly lit thermal zones
2. *Relamping*: replacing existing T12 linear fluorescent luminaires with T8 lamps, and magnetic ballasts with electronic ballasts.

A third option to be considered was the installation of automatic controls that reduce lighting power in response to increasing daylight illumination. However this measure is not assessed here, as it is anticipated that the cost of installing electronic ballasts capable of operating with dimmable fluorescent lights, as well as photo sensors to detect incident illumination levels, would significantly

increase the overall cost of the lighting retrofit. These measures are not expected to provide significant lighting and cooling savings beyond what the *Delamping* and *Relamping* measures would achieve.

4.2.1. Existing Lighting

An initial *Basic Lighting Control* simulation of the ERC model was run (with ideal cooling and 75 mm PF insulation, as in Run 3-6 in Table 9-1), with *EnergyPlus* simulation methodology set to automatically control lighting power input and output in each thermal zone. The simulation was used to assess whether ERC thermal zones are over-lit with the current lighting system, and the extent to which lighting savings can be achieved through *Delamping* and *Relamping*.

The simulation used pre-determined target illumination levels in each thermal zone, as defined in Table 4-4, as set points from which to regulate lighting power. At each time step, the simulation engine balanced illumination from interior lighting with incident daylight through the windows, with the assumption that interior lighting in each zone is capable of continuous (linear) dimming.

Table 4-4: Target illumination and existing maximum lighting power for the Current and Base Case scenarios

Thermal Zone	Target Illumination [lux]	Maximum Lighting Power [W]
North	400	1 960
East	400	1 400
South	400	840
West	400	1 540
Seminar	400	1 260
Corridor	200	1 120
Kitchen	500	140
Staff WC	200	140

Illumination levels were calculated at each iteration of simulation, by means of an *EnergyPlus* lighting sensor modelled in each thermal zone at an assumed working surface height of 0.80 m (DesignBuilder, 2016). Table 4-5 shows full lighting control parameters applied for the simulation. For simplicity, one photo sensor was modelled per thermal zone, accounting for 100% of lighting in that area. This was possible since individual office partitions within each zone were not included in the energy model.

Table 4-5: Lighting control inputs for Basic Lighting Control simulation (Run 4-1)

DesignBuilder Parameter	Value
Lighting Control	On
Assumed Working Plane height [m]	0.80
Control type	Linear
Minimum output fraction	0.10
Minimum power input fraction	0.10
Maximum allowable glare index	22.0
% Zone covered by lighting area 1	100%

Annual heat gains and cooling requirements resulting from the *Basic Lighting Control* simulation are shown in aggregate form in Figure 4-5, and compared to results from the *Base Case* and *75 mm-Insulation* case (without lighting control). Disaggregated data for Figure 4-5 are shown in Table

9-39 of Appendix G, while a summary report for lighting energy use, generated by *DesignBuilder,* is included in Table 9-40.

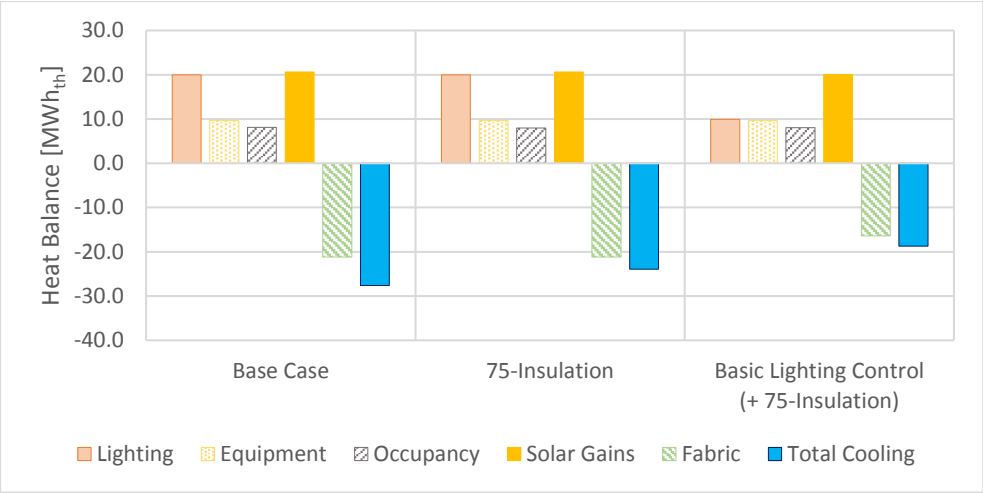

Figure 4-5: Annual heat gains and cooling for Base Case, 75 mm-Insulation and Basic Lighting Control simulations

Figure 4-5 shows that lighting heat gain decreased by 50% with the introduction of automatic lighting control, relative to the *Base Case* and *75 mm-Insulation* case. Predicted annual cooling decreased by 32% relative to the *Base Case* and 22% relative to the *75 mm-Insulation* case. The *DesignBuilder* report (Table 9-40) further shows that, relative to scheduled weekly lighting hours, full lighting load hours per week decrease significantly across the North, East, West, Seminar and Staff WC thermal zones, by 80%, 71%, 59%, 86% and 46% respectively.

These results indicate that these thermal zones receive more illumination from the existing interior lighting than is required, creating potential for significant potential energy savings (and heat gain reductions) to be achieved through *Delamping* and *Relamping*, without compromising light quality. These two measures are explored consecutively in the following sub-sections.

4.2.2. *Delamping*: Fluorescent Luminaire Removal

This sub-section assesses the impacts of the *Delamping* scenario – i.e. the removal of luminaires from each of the North, East, West, Seminar and Staff WC thermal zones (in addition to 75 mm insulation installation) – on the annual heat gains and cooling requirements of the ERC.

Simulations (Run 4-2 and Run 4-4 in Table 9-1 of Appendix A) of the ERC model were run in *EnergyPlus*, with the lighting power density input parameters lowered in each of the five selected thermal zones to reflect the reduction in lighting power servicing those zones. It was assumed that *Delamping* would be achieved by removing one T12 60 W fluorescent lamp from each light fitting within the selected thermal zones (such that one T12 60 W lamp remained in each light fitting), as this would ensure distribution of interior lighting would be unaltered. This has the effect of reducing the power rating of the fitting, and the lighting power density of the thermal zone, as shown in Table 4-6. Lighting power density is reduced by 32.89% under the *Delamping* scenario.

Table 4-6: Revised lighting power densities for Delamping simulation

Thermal Zone	Area [m²]	No. Light Fixtures	*Base Case*		*Delamping*	
			Power rating per fitting [W]	Lighting Power Density [W/m²]	Power rating per fitting [W]	Lighting Power Density [W/m²]
North	173.05	14	140	11.3262	80	6.4721
East	95.24	10	140	14.6997	80	8.3998
South	65.45	6	140	12.8342	140	12.8342
West	104.83	11	140	14.6905	80	8.3945
Seminar	100.23	9	140	12.5711	80	7.1835
Corridor	129.57	8	140	8.6440	140	8.6440
Kitchen	12.10	1	140	11.5702	140	11.5702
Staff WC	13.51	1	140	10.3627	80	5.9215
Total	**693.98**	**60**		**12.1041**		**8.2135**

Annual heat gain and cooling results from the *Delamping* simulation are shown in Figure 4-6, in comparison to the *Basic Lighting Control* and *75 mm-Insulation* case results (full data shown in Table 9-41 of Appendix G).

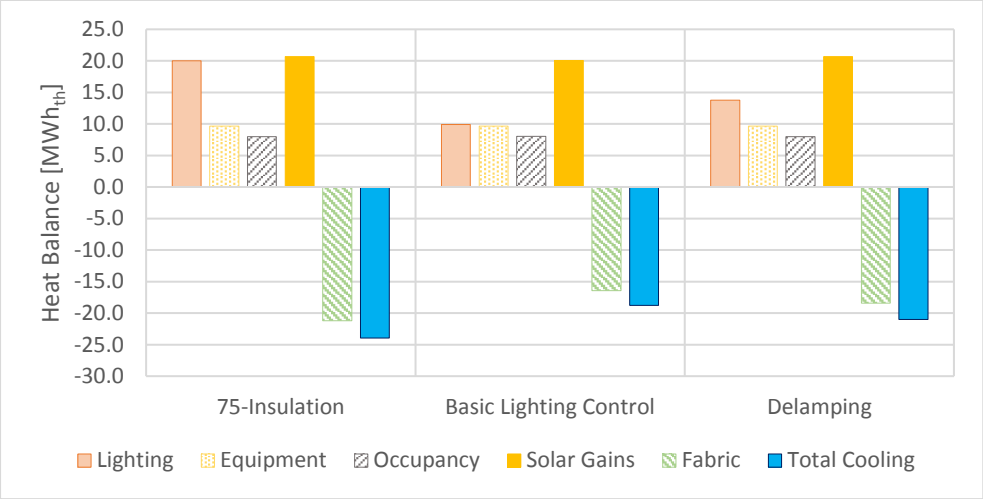

Figure 4-6: Annual heat gains and cooling for 75 mm-Insulation, Basic Lighting Control and Delamping simulations

Annual lighting heat gain under the *Delamping* scenario was found to be 13.75 MWh_{th}. This is 31% lower than under the *75 mm-Insulation* case, but 39% greater than the *Basic Lighting Control* simulation. Annual cooling requirements were reduced to 21.02 MWh_{th} for the *Delamping* scenario, compared to 23.95 MWh_{th} for *75 mm-Insulation* (and 27.64 MWh_{th} for the *Base Case*), and 18.75 MWh_{th} for *Basic Lighting Control*. These results suggest that, while delamping of selected thermal zones (amounting to the removal of 45 fluorescent lamps) significantly reduces lighting heat gains and cooling requirements, further improvements can still be realised with more aggressive retrofits. These are explored in the following sub-section, which considers the effects of replacing lamps and light fixtures.

As noted in § 3.3.2, *EnergyPlus* calculates internal heat gains from lighting and equipment by equating these to their quantified energy use, in the absence of a return air system, based on input power density and usage schedules. Lighting energy use per thermal zone is therefore assumed equal to general lighting internal heat gain. Reductions in lighting energy consumption arising from *Delamping*

are thus proportional to the changes in power rating per light fitting described in Table 4-6 (this is shown in detail in Table 9-42 of Appendix G). Additionally, cooling energy consumption reduces, in proportion with annual cooling requirements, to 7.01 MWh under the *Delamping* scenario, from 7.98 MWh for the *75 mm-Insulation* case (12% reduction), under consistent ideal cooling modelling assumptions (COP_R = 3.0 with 100% efficiency).

It should be noted that effective implementation of the *Delamping* measure would need to ensure the quality of light of targeted thermal zones was maintained to the required illumination levels. More detailed analysis would be required to determine the full effects of the *Delamping* scenario on lighting quality, uniformity and aesthetic appearance.

4.2.3. Relamping: Fluorescent Luminaire and Ballast Replacement

The ERC's annual lighting energy use was predicted to be 31% lower under the *Delamping* scenario, compared with the *Base Case* (or *75 mm-Insulation* case). However, this was still 39% greater than had been determined under the *Basic Lighting Control* simulation. Therefore, a second pair of simulations (Run 4-3 and Run 4-5) were run to assess further impacts that could be achieved through *Relamping* – i.e. replacing all existing T12 luminaires and magnetic ballasts with T8 fluorescents using electronic ballasts.

Following the *Delamping* measure, a total of 75 off T12 60 W lamps would be left in ERC interior light fittings, equipped with 60 magnetic ballasts (i.e. 45 off 1 x 60 W fixtures in North, East, West, Seminar and Staff WC zones and 15 off 2 x 60 W fixtures across the remaining South, Corridor and Kitchen zones). Under the *Relamping* simulation, all 75 lamps were assumed to be replaced with T8 59 W fluorescent luminaires, and all 60 magnetic ballasts were assumed to be replaced with electronic ballasts. The combined fixture powers of the new fluorescent fixtures were thus assumed to be 60 W for single lamp fittings and 120 W for double lamp (2 x 59 W) fittings. The revised lighting power densities for the *Relamping* scenario are summarised in Table 4-7. Net lighting power density for the ERC was thus reduced to 6.4843 W/m^2, compared with 12.1041 W/m^2 for the *Base Case* and 8.2135 W/m^2 for *Delamping* (i.e. 46% and 21% lower respectively).

Table 4-7: Revised lighting power density for Relamping simulation (Run 4-3)

Thermal Zone	Area [m^2]	No. (T8) Light Fixtures	No. Lamps per thermal zone	Fixture Power rating [W]	Total lighting power rating [W]	Lighting Power Density [W/m^2]
North	173.05	14	14	60	840	4.8541
East	95.24	10	10	60	600	6.2999
South	65.45	6	12	120	720	11.0008
West	104.83	11	11	60	660	6.2959
Seminar	100.23	9	9	60	540	5.3876
Corridor	129.57	8	16	120	960	7.4091
Kitchen	12.10	1	2	120	120	9.9174
Staff WC	13.51	1	1	60	60	4.4412
Total	**693.98**	**60**	**105**		**4 500**	**6.4843**

Annual heat gain and cooling results for the *Relamping* simulation, aggregated across all ERC thermal zones, are shown in Figure 4-7 (complete data table shown in Table 9-43 in Appendix G), along with

results from previous simulations (i.e. *Base Case*, *75 mm-Insulation* and *Delamping*). The results show that *Relamping*, as modelled according to parameters in Table 4-7, increases savings in lighting heat gain and lighting energy consumption by 21% relative to *Delamping* only; lighting energy savings predicted under the *Relamping* scenario are 46% greater compared with the *75 mm-Insulation* simulation (with no changes to *Base Case* lighting parameters).

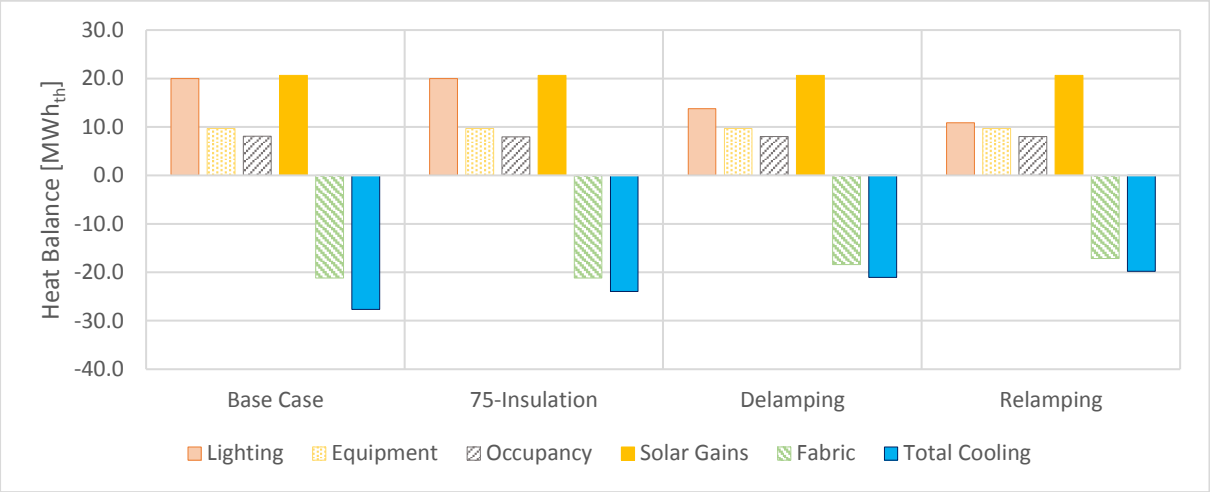

Figure 4-7: Annual heat gains and cooling resulting from Relamping, compared with previous simulation results

Furthermore, annual lighting energy consumption under the *Relamping* scenario is predicted to be 10.88 MWh, which is only 9.9% greater than what was determined under the *Basic Lighting Control* simulation (9.90 MWh per annum). Cooling energy consumption is 5.9% lower for *Relamping* relative to *Delamping*, and 17.4% lower than the *75 mm-Insulation* case. Predicted cooling energy determined by the *Basic Lighting Control* simulation was only 5.5% lower than for *Relamping*.

4.2.4. Cooling Load Impact of Delamping and Relamping

The impacts of the *Delamping* and *Relamping* scenarios on simulated peak cooling loads required for the ERC were assessed by means of two further simulations (Runs 4-4 and 4-5) for each scenario, over the Summer Design Week period. The resulting (ERC aggregate) heat balance profiles for the week are shown in Figure 4-8 (*Delamping*) and Figure 4-9 (*Relamping*) respectively, with accompanying data tables for the figures provided in Table 9-44 and Table 9-45 of Appendix G.

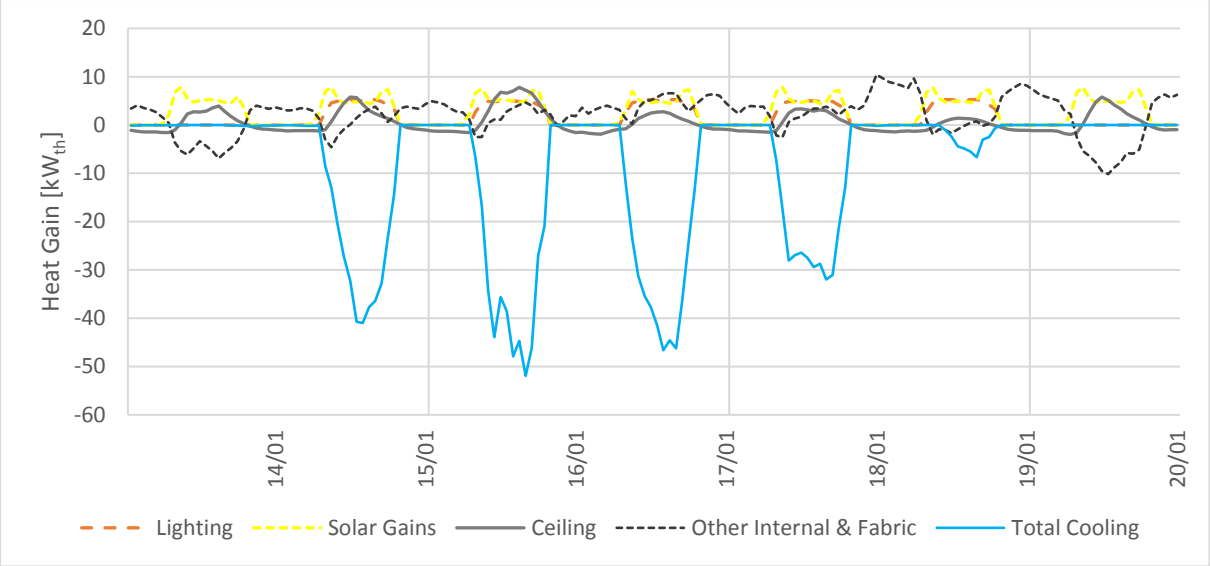

Figure 4-8: ERC heat balance profile of Delamping simulation during Summer Design Week

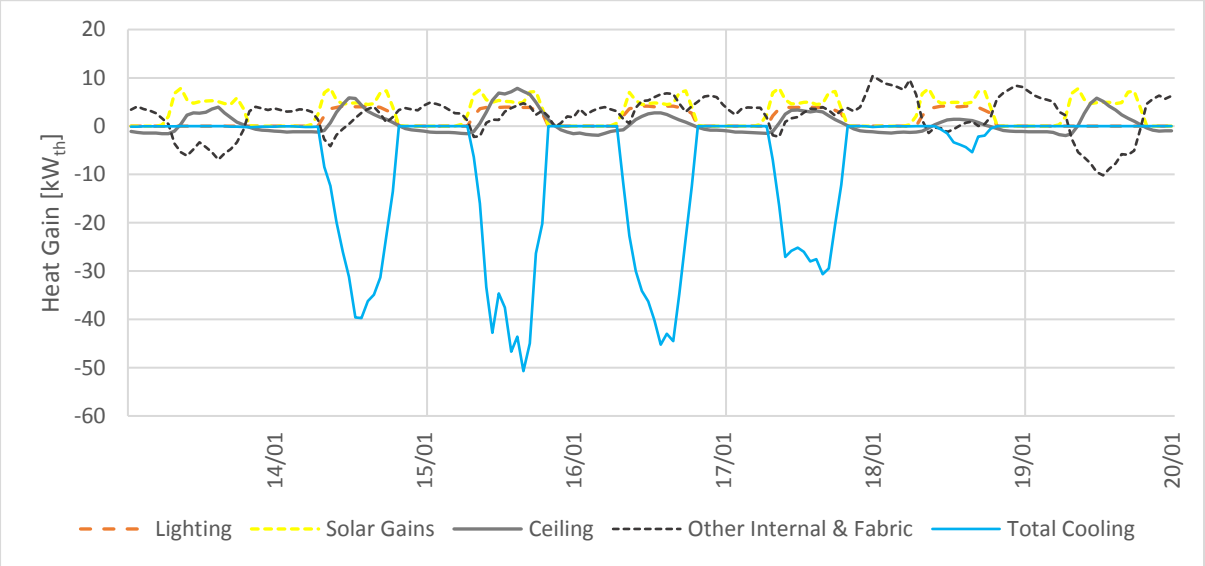

Figure 4-9: ERC heat balance profile of Relamping simulation during Summer Design Week

Figure 4-8 shows that *Delamping* reduces the peak cooling load to 51.9 kW_{th} (occurring on 15 Jan, as before), from 66.87 kW_{th} under the *Base Case* and 54.48 kW_{th} under the *75 mm-Insulation* scenario. *Relamping* further reduces the peak cooling load to 50.72 kW_{th} (see Figure 4-9). Meanwhile peak internal heat gains from lighting are reduced from 7.7 kW_{th} in the *Base Case* (see Figure 3-19 above) to 5.3 kW_{th} through *Delamping*, and further to 4.1 kW_{th} through *Relamping*.

The results of simulations of the ERC *Base Case*, as well as progressive preventative measures discussed so far, are summarised in Table 4-8. At this stage, each additional measure has progressively reduced annual cooling requirements as well as peak cooling loads for the ERC. In addition, the combined *Delamping* and *Relamping* measures result in a predicted 46% reduction in annual lighting energy use.

Table 4-8: Summarised simulation results showing effect of progressive preventative measures on lighting and cooling energy

Simulation	Annual Lighting Energy		Annual Cooling		Annual Cooling Energy		Peak Cooling Load	
	[MWh]	Rel to Base Case	[MWh_{th}]	Rel to Base Case	[MWh]	Rel to Base Case	[kW_{th}]	Rel to Base Case
Base Case	19.99	-	27.64	-	9.21	-	66.87	-
… + 75-Insul.	19.99	0%	23.95	-13%	7.98	-13%	54.48	-19%
… + Delamping	13.75	-31%	21.02	-24%	7.01	-24%	51.93	-22%
… + Relamping	10.88	-46%	19.79	-28%	6.60	-28%	50.72	-24%

The following section will describe analysis of the third preventative measure considered in this dissertation, i.e. the replacement of the solar film fitted onto the ERC windows with internal slatted blinds.

4.3. Shading Retrofit

The most significant internal heat gain, as shown in the results of the *Current* and *Base Case* Simulations (see, e.g., Figure 3-9), is attributed to solar gains through exterior windows. This suggests that the existing solar film on the windows is ineffective at regulating solar gains. This is particularly the case for the East and West thermal zones, which receive large, direct solar radiation during the mornings and evenings (respectively) in summer. The north facing offices have less exposure to solar radiation in summer, owing to the external shading provided by the overhangs of the Menzies roof. The South zone receives comparatively little sunlight, owing to the southern latitude of the Menzies building and the angles of incidence of the sun.

This section assesses the potential impacts on heat gains and cooling requirements that may be achieved through the removal of the solar film on the ERC's windows, and the installation of adjustable internal shading, using highly reflective slatted horizontal blinds. Internal shading is expected to have two advantages over the solar film:

- Highly reflective blind slats will better reflect both direct and diffuse solar radiation that enters through the windows, reducing absorption of SW radiation by internal building surfaces.
- Adjustable shading will allow occupants greater control over their environment and will allow increased daylight and solar heat to enter the building during winter.

The literature review showed that improved occupant control of the thermal environment leads to enhanced perceptions of thermal comfort (Huizenga et al, 2006), while increased solar gains and daylight could improve winter thermal comfort. A disadvantage of internal shading, compared to external shading, is that solar radiation is partially scattered around surfaces adjacent to the shading device, which then gets absorbed and emitted as LW radiation and can cause delayed heat gains to the room. However, internal shading is easier to retrofit within an existing building and is thus assumed to be more cost effective in the short term.

4.3.1. Simulation Analysis

The impacts of retrofitting the ERC with internal shading devices on annual heat gains and cooling requirements were assessed by means of two *EnergyPlus* simulations (Run 5-1 and Run 5-2 in Table 9-1). Internal shading inputs were added to the ERC model, over and above the insulation, delamping and relamping measures described previously in this Chapter.

The effect of removing the solar film from the ERC windows was modelled in *DesignBuilder* by revising the glazing input data (described in § 3.1.3.3) as shown in Table 4-9. Input properties for the glass were selected based on the 'Generic Clear 4mm Glass' template available in the *DesignBuilder* library (DesignBuilder, 2016).

Table 4-9: Revised glazing input data for Shading simulation

Glazing Parameter	Value
Thickness [mm]	4
Conductivity [W/mK]	1.00
Solar transmittance	0.816
Solar reflectance	0.075
Visible transmittance	0.892
Visible reflectance	0.081
Emissivity	0.84

Internal shading was modelled by including slatted horizontal blinds with high reflectivity, based on default data available in the *DesignBuilder* library (DesignBuilder, 2016), for the North, East, South, West, Staff WC and Seminar thermal zones (the Corridor and Kitchen do not have external windows). Complete modelling parameters for the slatted blinds are shown in Table 4-10.

Table 4-10: Shading (slatted blind) input data for Shading simulation

Shading Parameter	Value
Shading type	Internal, slatted blinds with high reflectivity
Orientation	Horizontal
Blind distance to glass [mm]	15
Slat width [mm]	25
Slat separation [mm]	1.88
Slat thickness [mm]	1
Slat angle	45° (range: 0 - 180°)
Slat conductivity [W/mK]	0.90
Solar reflectance (direct & diffuse)	0.80
Solar transmittance	0
Hemispherical emissivity	0.90
Solar set point [W/m2]	120

Shading use profiles were set to follow thermal zone occupancy profiles, as described in the ERC model input data shown in Appendix C. The *EnergyPlus* simulation controls were set to use solar radiation set points, as defined in Table 4-10, to determine when to apply the shading device; i.e. the ERC was modelled with the slatted blinds covering the entire window surface area for each iteration of simulation in which solar radiation (direct + diffuse) incident upon the window surface was calculated

to exceed the 120 W/m^2 set point. The windows were assumed to have no shading for simulation iterations where incident solar radiation fell below the set point.

4.3.2. Impact of Shading on Heat Gains and Cooling Load

Annual heat gains and cooling requirements determined from the *Shading* simulation are shown in Figure 4-10, and compared with simulation results from the *Base Case* and *Relamping* scenarios.

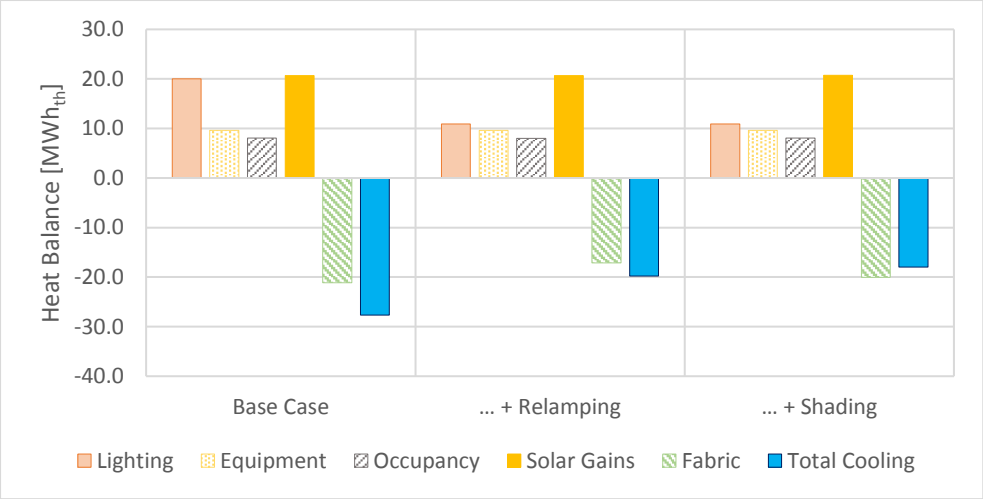

Figure 4-10: Annual heat gains and cooling from Shading simulation, compared with Relamping and Base Case results

Despite the *Shading* retrofit, Figure 4-10 shows no decrease in annual solar heat gains. Indeed, the *Shading* simulation causes aggregate annual solar heat gains to increase by a small margin to 20.74 MWh$_{th}$, from 20.65 MWh$_{th}$ under the *Base Case*. However, relative to *Relamping*, the *Shading* retrofit also appears to reduce annual cooling by 9.0%, from 19.8 MWh$_{th}$ to 18.0 MWh$_{th}$. This shows that, while altering the shading of the windows does not reduce annual solar gains, it does have a positive impact on reducing the ERC's cooling load.

Table 4-11 shows annual solar heat gains predicted for each thermal zone, comparing the *Base Case* and *Shading* simulation results. The table shows that the North, East and West zones experience a relatively small decrease in solar heat gains resulting from the *Shading* retrofit. By contrast, the South zone experiences a relatively large increase in solar heat gain of 42.9%.

Table 4-11: Comparison of annual solar heat gains [MWh$_{th}$] per thermal zone between Base Case and Shading simulations

Simulation	North	East	South	West	Seminar	Staff WC	Total
Base Case	6.34	4.21	0.81	4.53	3.96	0.46	20.65
Shading	5.81	4.10	1.16	4.27	4.57	0.50	20.74
% Change	-8.4%	-2.8%	42.9%	-5.7%	15.3%	8.2%	0.4%

Furthermore, the impact of the internal shading retrofit on daily solar heat gain profiles can be observed in Figure 4-11, which compares solar heat gains for the *Base Case* and *Shading* simulations for weekdays (Monday to Friday) of the Summer Design Week (full data shown in Table 9-47 of

Appendix G). The results show that the retrofit shading devices reduce peak morning solar heat gains by an average of 35% relative to the *Base Case*. Peak afternoon solar gains experience a small reduction of 18% on average for the *Shading* scenario, relative to the *Base Case*.

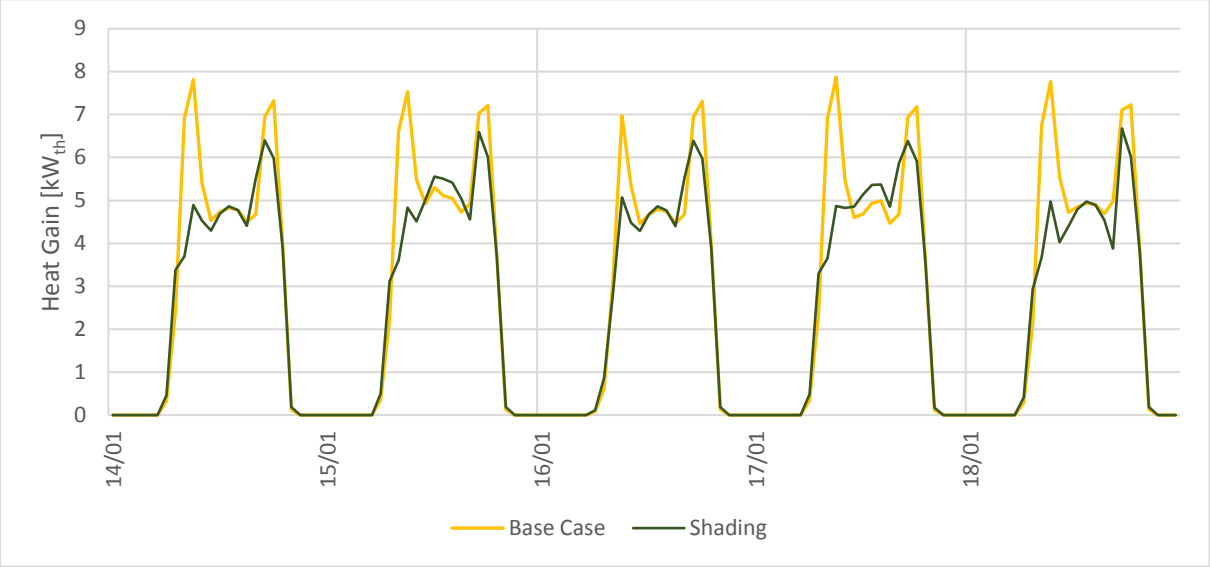

Figure 4-11: Solar Heat Gain profile during Summer Design Week, comparing Shading and Base Case simulations

The profiles in Figure 4-11 show that the morning solar gain peak, which typically occurs at 09:00 during the Summer Design Week and is dominated by radiation through east-oriented windows, is effectively mitigated by the internal shading system. However, shading has less of an effect on afternoon peak solar gains, with a notable peak still occurring between 17:00 and 18:00 of each day during the Summer Design Week. This is likely to be accounted for by the warmer temperature conditions experienced in Cape Town in the afternoons in summer, compared to the mornings, since the air has undergone a longer period of heating from solar radiation during the day. This further explains why average daily summer temperatures are warmer in the afternoon, between 13:00 and 17:00, than in the morning, as can be seen in Figure 4-1 above.

The peak cooling load of the ERC was found to be 49.3 kW_{th} under the *Shading* simulation, which is 26.3% lower than the *Base Case*. However, the improvement relative to the *Relamping* scenario is considerably smaller (2.86%). This is to be expected because the peak cooling load of the ERC has occurred consistently at 16:00 on 15 January (during the Summer Design Week) across each of the simulated scenarios (*Base Case* through *Shading*). The heat gain profiles in Figure 4-11 show that the *Shading* retrofit has less impact on solar gains at this hour of the day.

The progressive impacts of preventative measures on ERC cooling requirements and peak cooling loads are shown in Table 4-12. The reductions of annual cooling, cooling energy and peak cooling loads with each progressive measure are shown relative to the *Base Case*. The table shows that the implementation of all four measures, up to and including the *Shading* scenario, would potentially allow 35% in relative savings of cooling energy, compared with an active cooling system designed for *Base Case* conditions. The required cooling capacity of the potential active system is shown to reduce by 26% under the *Shading* scenario, relative to the *Base Case*.

Table 4-12: Impact of progressive preventative measures on ERC cooling requirements, from Base Case through Shading simulation results

Simulation	Annual Cooling		Annual Cooling Energy		Peak Cooling Load	
	[MWh_{th}]	Rel to Base Case [%]	[MWh]	Rel to Base Case [%]	[kW_{th}]	Rel to Base Case [%]
Base Case	27.64	-	9.21	-	66.87	-
… + 75 mm-Insul.	23.95	-13%	7.98	-13%	54.48	-19%
… + Delamping	21.02	-24%	7.01	-24%	51.93	-22%
… + Relamping	19.79	-28%	6.60	-28%	50.72	-24%
… + Shading	18.00	-35%	6.00	-35%	49.27	-26%

Chapter 5 which follows this sub-section describes a brief, simplified analysis of potential costs for a theoretical, active cooling system to be installed and operated in the ERC, in order to meet the *Base Case* cooling requirements shown in Table 4-12. The base cooling cost profiles are then contrasted with revised cost forecasts with each progressive preventative scenario, to determine the extent to which initial capital expenditure on these measures would be offset further on by relative savings owing to reduced size and energy consumption of the cooling system.

5. Cooling Cost Evaluation

This chapter assesses the impacts of the four preventative measures, shown in Table 4-12, on projected costs of a theoretical active cooling system, sized to meet the ERC cooling requirements. Impacts are assessed by comparing cumulative annual costs for the *Base Case* scenario with revised cost forecasts determined for each progressive preventative measure.

As noted in § 2.6.1, design, selection and technical performance analysis of an actual air conditioning or alternative mechanical cooling system is beyond the scope of this dissertation. Rather, the analysis here is simplified by employing cost factor assumptions for a packaged air conditioning system, based on empirical findings of Buys and Mathews (2005:1156), to estimate the potential installation costs of a cooling system for the ERC. Further assumptions are made regarding costs incurred through operations and maintenance (O&M), energy consumption and capital costs for the various preventative cooling measures.

This enables a simplified evaluation of the cost effectiveness of the preventative measures, relative to the *Base Case*, by means of comparing annual discounted cash flows (or expenditures, in this case) through the *Simple Payback Period* and *Net Present Value* methods. The hypothesis of this chapter is that each progressive preventative scenario has a payback period, relative to the *Base Case*, at which point the present value of cumulative monetary value of savings incurred from lower predicted energy use and smaller sized cooling system begin to exceed the increased first cost of the system, owing to the costs of the preventative measures.

The testing of this hypothesis relies on cooling load and energy consumption results determined from *EnergyPlus* simulation runs for the *Base Case* (§ 3.4), as well as progressive preventative scenarios:

- *75 mm-Insulation* (§ 4.1)
- *Delamping* (§ 4.2.2)
- *Relamping* (§ 4.2.3)
- *Shading* (§ 4.3)

5.1. Cost Assumptions

This section describes all assumptions that were made to facilitate the cost analysis. All costs are described in monetary units of 2015 South African rands, with inflation factors used to adjust values quoted in other years (see Figure 5-1).

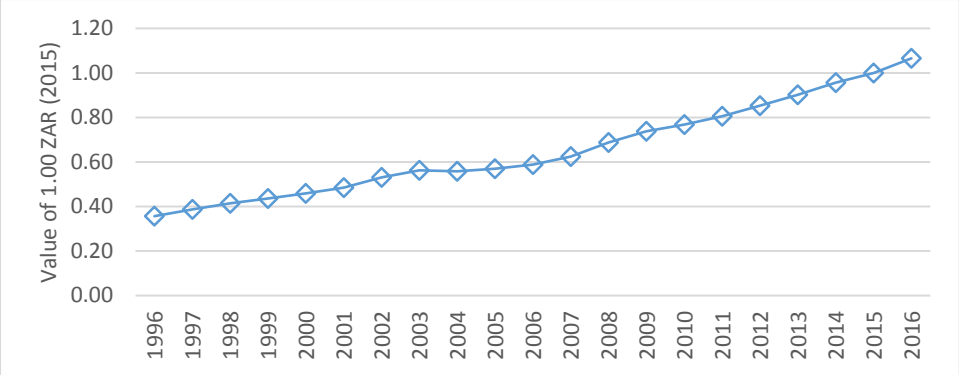

Figure 5-1: Conversion factors for 1.00 ZAR (2015) to other years, based on 12-month CPI averages (Inflation.eu, 2017)

The following cost components are relevant for forecasting annual ERC cooling and energy use expenditure:

- Active cooling system (air conditioning)
  - Installation costs
  - O&M costs
  - Energy costs (for municipal electricity consumption)
- Lighting system
  - Energy costs
  - Lamp replacement costs: it was assumed, for analysis purposes, that all fluorescent lamps (irrespective of ballast type) are replaced after four years of life
- Preventative measures
  - *75 mm-Insulation* installation (material and labour costs)
  - *Delamping* (labour cost to remove existing luminaires)
  - *Relamping* (*Delamping* + installation costs for replacement lamps and ballasts)
  - *Shading* (Labour cost to remove solar film + installation of slatted blinds)

Cost assumptions for each of these components are described in the following sub-sections.

5.1.1. Cooling System

From the literature review, it was concluded that a split, packaged air conditioning system would likely be most appropriate for serving the ERC, based on the location of the ERC within the Menzies building, the floorplan and layout of thermal zones, and the relatively small cooling capacities required (< 70 kW_{th} for the *Base Case*).

Buys and Mathews (2005:1155) determined a linear relationship based on regression on cost quotations for installation of split air conditioning units for a range of design capacities. Data was gathered from quotations obtained from 18 different suppliers, for system capacities ranging from 30 kW to 300 kW. The resulting relationship is expressed in equation 5-1 below:

$$Installation\ Cost = 2094(Design\ Capacity) + 53\ 997 \text{ [2000 ZAR]} \quad (5\text{-}1)$$

Installation costs were shown to have a linear correlation (r^2-value) of 0.7883 with design capacity (Buys &Mathews, 2005:1156), indicating evidence of a direct positive relationship.

Equation 5-1 was therefore adapted to 2015 rand units (using Figure 5-1 above) and applied to the simulation results of this dissertation. Design Capacity was assumed to be equivalent to the cooling loads (Q_L) of each respective scenario, rounded up to the nearest integer. The resulting equation was applied as follows:

$$C_{install} = 3674.\,Q_L + 238\,024 \text{ [2015 ZAR]} \quad (5\text{-}2)$$

Where $C_{install}$ is active cooling installation cost and Q_L is simulated peak cooling load [kW]. Annual cooling system O&M costs were assume to be constant, in real terms, and equivalent to 3% of the installation cost in the first year of system operation. O&M costs in future years are discounted based on assumed inflation and nominal interest rates.

Cooling installation and first-year-O&M costs thus determined for each simulation scenario are summarised in Table 5-1 below.

Table 5-1: Active cooling installation costs estimated for each simulated cooling scenario

Scenario	System Size [kW_{th}]	Installation Cost [2015 ZAR]	O&M Cost (Year 1) [2015 ZAR]
Base Case	67.0	340 894.58	10 226.84
… + 75 mm-Insulation	55.0	296 806.98	8 904.21
… + Delamping	52.0	285 785.09	8 573.55
… + Relamping	51.0	282 111.12	8 463.33
… + Shading	50.0	278 437.15	8 353.11

It should be noted that Buys and Mathews (2005:1154) observe the application of R/kW cost factors for estimating HVAC costs is limited in terms of accuracy, due to the wide variation of tender observed in their findings, and the uniqueness that each building design will present. Initial cost models can only provide estimates, and "cannot be more accurate than detailed tender prices" (Buys & Mathews, 2005:1154). However, the estimates shown in Table 5-1 are considered appropriate for the purpose of the cost evaluation discussed here.

5.1.2. Preventative Measures

Insulation

Material costs for 75 mm polyester fibre insulation were assumed to be 60 ZAR/m^2, with an additional installation labour rate of 20 ZAR/m^2. Unit costs were assumed based on actual data from commercial quotes for insulation products. The area of the ERC ceiling was measured and rounded to 700 m^2, such that the total cost of the *75 mm-Insulation* measure was found to be R 56 000.00.

Lighting

Cost assumptions for lighting retrofits are shown in Table 5-2. It is assumed that all fluorescent luminaires (T8 or T12) are replaced every four years, to account for their life cycle. The costs of new T8 and T12 lamps are shown in Table 5-2, and are discounted in future years based on assumed annual

inflation and nominal interest rates (with the assumption that lamps will decrease in value, in real terms, in future years).

Table 5-2: Lighting cost assumptions

Cost parameter	Unit cost [2015 ZAR]
New T12 Lamp Cost (Year 1)	20.00
New T8 Lamp Cost (Year 1)	30.00
Electronic ballast unit cost	250.00
Delamping labour rate [R per lamp]	30.00
Relamping labour rate [R per fixture]	65.00

The *Delamping* and *Relamping* scenarios both include the labour costs of removing 1 x T12 60W fluorescent lamps from the light fixtures in each of the North, East, West, Seminar and Staff WC zones. Additionally, the *Relamping* scenario includes the cost of new 1 x T8 59W fluorescents and electronic ballasts, as well as the cost of labour to replace the (remaining) existing lighting equipment.

Shading

A labour rate of 20 ZAR/m^2 was assumed for removal of the existing solar film from windows, consistent with the rate assumed for insulation installation. A cost estimate of 350 ZAR/m (length) was assumed for internal slatted blinds, based on commercial quotes obtained for aluminium (i.e. highly reflective) Venetian blinds of 25 mm thickness and 730 mm drop to cover the window area. *DesignBuilder* determined the total glass area of the ERC as 91.25 m^2, from which the required shading length was found to be 125 m. The total cost of the *Shading* measure was thus found to be R 45 575.00 (incl. labour).

5.1.3. Energy Costs and Assumptions

The following assumptions were made in order to forecast energy and financial costs of the various scenarios (see also Table 5-3):

1. Only actual energy charges [ZAR per kWh] were considered; other electricity tariffs, such as demand charges, network charges and administration fees were excluded.
2. The price of electricity was assumed to be 1.20 ZAR/kWh [2015 ZAR] in the first year of analysis, and to increase annually by 9.4%, based on a determination by the National Energy Regulator of South Africa for 2016/17 (NERSA, 2016).
3. Annual inflation rate was assumed to be 6%, based on the upper bound of the target set by the South African Reserve Bank (SARB,2016)
4. The nominal interest was assumed to be 7.0%, as per the prevailing repo rate at the time of writing (SARB, 2017).

Table 5-3: Energy and financial cost assumptions

Cost Parameter	Symbol	Value
Monetary units		2015 ZAR
Year 1 Elec Price [R/kWh]	EC_0	1.20
Annual electricity price rise	$i_{increase}$	9.4%
Annual inflation rate	$i_{inflation}$	6.0%
Nominal interest rate	$i_{nominal}$	7.0%
Real annual energy price rise	i_{real}	3.20%
Discount rate	$i_{discount}$	0.94%

The real annual rate of electricity price rise (i_{real}) is calculated from the annual price rise ($i_{increase}$) and inflation rate ($i_{inflation}$) as follows (equation 5-2):

$$i_{real} = \frac{i_{increase}+1}{i_{inflation}+1} - 1 \quad (5\text{-}3)$$

The annual progression of electricity prices is thus shown in real terms in Table 5-4.

Table 5-4: Annual electricity prices in present value [2015 ZAR] terms

Year	Elec Price [2015 ZAR/kWh]
1	1.20
2	1.24
3	1.28
4	1.32
5	1.36
6	1.41
7	1.45
8	1.50
9	1.54
10	1.59

Costs for annual cooling system O&M as well as fluorescent lamp replacements (every four years) were discounted according to the annual nominal interest and inflation rates, to further account for the time-value of money:

$$i_{discount} = \frac{1+i_{inflation}}{1+i_{nominal}} - 1 \quad (5\text{-}4)$$

5.2. Methodology

Two metrics were used to assess the expenditure forecasts of each preventative cooling scenario:

1. Simple Payback Period
2. Net Present Value (NPV)

The payback period of each preventative measure, relative to the *Base Case*, was determined from the length of time in years, following installation of the cooling system and additional retrofits, before cumulative costs of the *Base Case* would begin to exceed cumulative costs of the preventative scenario in present value terms. Payback periods were calculated for each preventative scenario through aggregation of annual discounted expenditures, forecast based on the assumptions described in § 5.1.

Each cost projection included initial (capital) costs of installation of the active cooling system (based on design capacity, as shown in Table 5-1) as well as installation costs of the preventative measures. Thereafter, annual O&M and energy (electricity use) costs of the lighting and cooling systems were calculated. Energy costs were calculated from simulated annual electricity consumption of the cooling and lighting systems, as determined previously, and increased annually (in real terms) as follows:

$$EC_i = EC_1(1 + i_{real})^{i-1} \text{ [2015 ZAR]} \quad (5\text{-}5)$$

Where:

- EC_i is annual energy cost (for lighting and cooling) in the i^{th} year following installation
- EC_1 is energy cost in the first year (annual energy use for cooling and lighting is assumed constant throughout the cost forecast period, as found from simulation results)
- i_{real} is determined from equation 5-3 (3.20%)

Annual O&M costs for the cooling system and fluorescent lamp costs (incurred in every fourth year) were discounted to present value terms as follows:

$$OM_i = \frac{OM_1}{(1+i_{discount})^{i-1}} \quad (5\text{-}6)$$

Where:

- OM_i is annual O&M cost for cooling system and lamp replacement (when i is a multiple of 4) in the i^{th} year following installation
- OM_1 is cooling system O&M cost in the first year, where it is assumed $OM_0 = 0.03 \times C_{install}$
- $i_{discount}$ is determined from equation 5-4 (0.94%)

Annual costs of each scenario were thus determined as the discounted sum of individual cost components for that year. For the first year, at the beginning of which the cooling system and preventative retrofits are installed, annual costs were calculated as follows:

$$Cost_1 = C_{install} + C_{retrofits} + OM_1 + EC_1 \text{ [2015 ZAR]} \quad (5\text{-}7)$$

Where:

- $Cost_1$ is total annual cost in the first year of projection
- $C_{retrofits}$ represents the combined capital cost of the retrofit measures for the respective preventative scenario
- OM_1 and EC_1 are as defined previously

Annual costs for subsequent years were calculated as follows:

$$Cost_i = OM_i + EC_i \text{ [2015 ZAR]} \quad (5\text{-}8)$$

Where:

- $i \in (1, n]$ (and n is total number of years of projection)

- EC_i and OM_i calculated as described in equations 5-5 and 5-6

Relative annual savings predicted for each preventative scenario were found by comparing the annual costs determined for each preventative scenario with those determined for the *Base Case*:

$$S_i = (Cost_{BC} - Cost_N)_i [2015\ ZAR] \quad (5\text{-}9)$$

Where:

- S_i are relative annual savings, discounted into present value terms
- $Cost_{BC_i}$ is annual *Base Case* costs in the i^{th} year
- $Cost_{N_i}$ is annual costs for preventative scenario N in the i^{th} year

The Net Present Value (NPV) of the preventative measure was thus determined as the sum of all S_i over the respective forecasting period:

$$NPV = \sum_{i=1}^{M}(S_i) = \sum_{i=1}^{M}(Cost_{BC} - Cost_N)_i \quad [2015\ ZAR] \quad (5\text{-}10)$$

Where: M is the total number of years of cost projection.

The following discussion shows the cost projection results determined from the simple payback period and NPV methodologies. NPV values were assessed for 5 and 10 year periods, to show prospective savings values of each preventative measure over medium and long terms.

5.3. Cost and Savings Forecasts

Table 5-5 below shows the *Base Case* cooling cost projections, which includes installation cost estimates of a 67 kW_{th} active cooling system, O&M costs for the HVAC system and lamp replacements, and annual electricity costs for the HVAC and lighting systems. The proportion of each cost component over the 10 year period forecast in Table 5-5 is shown in Figure 5-2.

Table 5-5: Annual cooling and lighting system cost forecasts under the Base Case scenario [2015 ZAR]

	Capital Costs	O&M Costs (OM_i)		Energy Costs (EC_i)		Total Costs	
Year	Active Cooling System $C_{install}$	Light Replacement	AC System	AC System	Lighting System	Annual $Cost_i$	Cumulative Costs
1	340 894.58	0.00	10 226.84	11 055.62	23 993.20	386 170.23	386 170.23
2	0.00	0.00	10 131.26	11 410.24	24 762.79	46 304.29	432 474.52
3	0.00	0.00	9 942.77	11 776.23	25 557.07	47 276.07	479 750.59
4	0.00	2 333.34	9 666.60	12 153.96	26 376.82	50 530.72	530 281.31
5	0.00	0.00	9 310.27	12 543.80	27 222.87	49 076.94	579 358.25
6	0.00	0.00	8 883.27	12 946.15	28 096.06	49 925.47	629 283.72
7	0.00	0.00	8 396.63	13 361.40	28 997.25	50 755.29	680 039.01
8	0.00	2 247.32	7 862.48	13 789.98	29 927.35	53 827.14	733 866.14
9	0.00	0.00	7 293.51	14 232.30	30 887.29	52 413.09	786 279.23
10	0.00	0.00	6 702.48	14 688.80	31 878.01	53 269.29	839 548.52

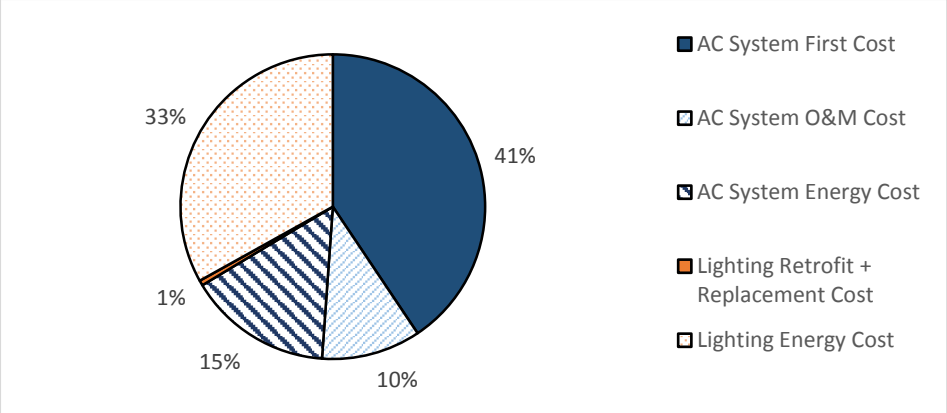

Figure 5-2: Breakdown of costs for Base Case cooling scenario over 10 years

Figure 5-2 shows that installation of the active cooling system accounts for 41% of the total cumulative costs over the 10 year period of the *Base Case*. Lighting provides the next most significant component – R 282 279.36 over 10 years, of which 98% is accounted for by energy costs.

Table 5-6 compares total cost projections for each preventative scenario, relative to the *Base Case*, based on detailed 10 year cost projections shown in Appendix H (Table 9-49 through Table 9-52). The table also shows the payback periods and NPV values, calculated 5 years and 10 years after the cooling system installation respectively, for each scenario. Each retrofit measure is shown to have a payback period, relative to the *Base Case*, extending from 4.19 years for the *75 mm-Insulation* scenario to 0.97 years for the *Delamping* scenario, thus confirming the hypothesis stated in the introduction of this chapter.

Table 5-6: Summary of cost, payback period and Net Present Value for each Preventative Scenario [2015 ZAR]

Cost Parameter	**Base Case**	**… + 75 mm-Insulation**	**… + Delamping**	**… + Relamping**	**… + Shading**
AC System First Cost	340 894.58	296 806.98	285 785.09	282 111.12	278 437.15
AC System O&M Cost	88 416.11	76 981.33	74 122.64	73 169.74	72 216.84
AC System Energy Cost	127 958.47	110 889.61	97 321.45	91 614.31	83 333.34
Lighting Upgrade + O&M	4 580.66	4 580.66	4 212.91	26 794.37	26 794.37
Lighting Energy Cost	277 698.70	277 698.70	191 030.93	151 144.94	151 144.94
Insulation Cost		56 000.00	56 000.00	56 000.00	56 000.00
Shading					45 575.00
Total	**839 548.52**	**822 957.29**	**708 473.02**	**680 834.48**	**713 501.64**
% Change	0	-2.0%	-15.6%	-18.9%	-15.0%
Payback Period [years]		4.19	0.97	1.24	3.56
NPV @ 5 years		2 322.85	60 633.38	63 960.24	26 404.65
NPV @ 10 years		16 591.23	131 075.51	158 714.04	126 046.88

Table 5-6 shows that total costs over the 10 year period are reduced with each progressive preventative measure, with the exception of the *Shading* scenario, which causes an increase in total costs relative to the previous *Relamping* scenario. The lighting upgrades present the most significant incremental impact on cost projections.

Delamping is predicted to provide a 15.6 % reduction on total costs relative to the *Base Case*, and 13.9% relative to *75 mm-Insulation* only. Payback period through this method is reduced to slightly less than 1 year. A significant saving of 31% is achieved through lighting energy costs alone. This implies immediate cooling and energy saving impacts could be achieved for the ERC by simply removing fluorescent luminaires from overly lit ERC zones (albeit more detailed assessment of *Delamping* on lighting quality, as well as winter thermal comfort, is recommended first).

Improvement to ceiling insulation requires the greatest incremental installation cost expense, and has the longest payback period in terms of relative cooling energy savings. However, peak cooling reduces by 18.53% under the *75 mm-Insulation* scenario, causing a reduction in installation cost of the active cooling system of 12.9% - the greatest singular improvement in cooling system capital cost.

The NPV of relative savings increase progressively with each additional measure, from *75 mm-Insulation* to *Relamping*, for both 5-year and 10-year horizons. However, projections of the *Shading* scenario show that, owing to an increase in total cost of R 45 57500, the NPV after 10 years reduces by R 37 555.59 after 5 years, and R 32 667.16 relative to the *Relamping* (no shading retrofit) scenario. The shading retrofit is thus not expected to be cost effective, over and above other measures, even after 10 years of forecasting. This contrasts with the difference between the *Delamping* and *Relamping* scenarios, where an increase in investment of R 22 581.46 between the scenarios results in an increase of R 26 638.53 in present value savings after 10 years.

Figure 5-3 shows a comparison of different cost components, aggregated into Capital, O&M and Energy costs, for each scenario. The figure shows that, across all scenarios, the installation costs (including cooling system and preventative retrofits). Capital costs of the *Shading* scenario are 18.08% greater than the *Base Case*, whereas the capital cost of *Delamping* is only 0.66% greater. Meanwhile energy costs vary significantly, with a 42.2 % reduction shown for the *Shading* scenario relative to the *Base Case*.

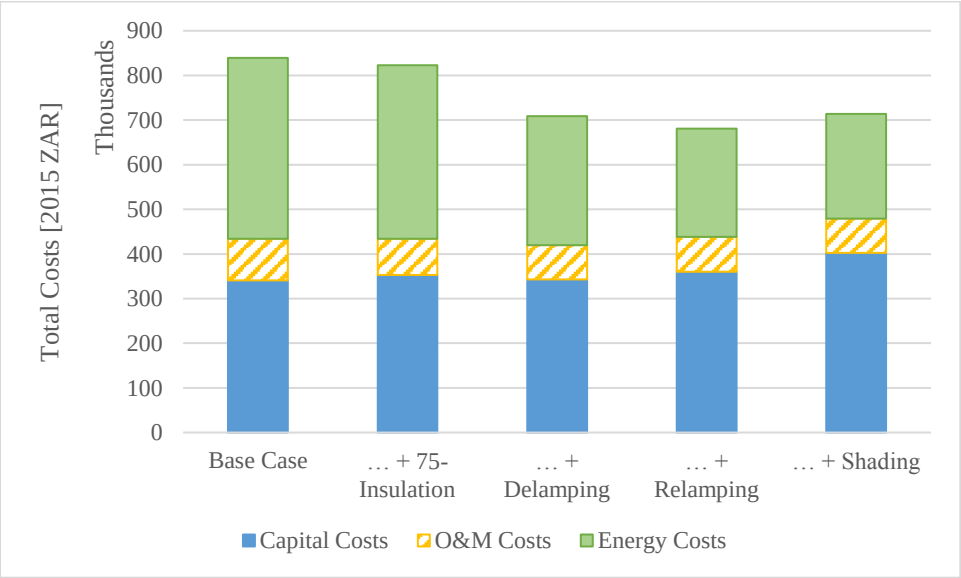

Figure 5-3: Proportion of 10-year forecast costs for capital, O&M and electricity expenditure for each preventative scenario

The *Delamping* scenario again causes the most significant change in lighting and cooling energy costs between scenarios, with a reduction of R 100 235.94 (over 10 years) relative to the *75 mm-Insulation*

scenario. Lighting energy costs for the *Delamping* scenario are reduced by 31% relative to previous scenarios, as noted previously. Implementation of *Relamping* measures would further reduce lighting energy costs by 20.88%.

6. Conclusions

This chapter presents conclusions drawn from the dissertation. The aim of the dissertation was to characterise typical summer environmental conditions within the ERC offices, under the current condition of the building, and to determine the *Base Case* annual cooling energy and peak cooling loads required to alleviate summer thermal discomfort. Thereafter the impacts of a selection of potential preventative measures were assessed, to estimate the cooling capacity and energy cost reductions they could provide.

Conclusions are presented on the *Current* conditions and *Base Case* cooling requirements of the ERC, and on the impacts and cost effectiveness of prospective preventative measures.

6.1. Current Conditions and Base Case Cooling

EnergyPlus simulation of the *Current* ERC model resulted in a predicted 7 814.5 hours of thermal discomfort experienced by occupants across all thermal zones. Winter months (June –August) accounted for the greatest share – 38.9% - of annual discomfort hours, compared with 37.6% over the summer months (December – March).

The greatest source of annual heat gain to the ERC was found to be solar gains through external windows (20.65 MWh_{th}) followed by interior (fluorescent) lighting (19.99 MWh_{th}). Other sources – electronic equipment and occupants – accounted for 29% of internal heat gains. These were considered more difficult to model and control, owing to their dependence on human behaviour. Conduction through the ceiling was found to be a significant heat gain component during occupancy hours of the Summer Design Week, based on the model assuming no ceiling insulation layer. The actual building has fibreglass insulation, but this is currently distributed sporadically with varying thickness, and large gaps across many thermal zones.

The *Base Case* results indicated annual cooling requirements of 27.64 MWh_{th} to effectively reduce thermal discomfort in summer, with peak cooling load of 66.87 kW_{th} during the Summer Design Week. The effect of this cooling was predicted to reduce annual discomfort hours by 47.8%, relative to *Current* conditions, and to eliminate all discomfort hours in January and February, with only 0.5 and 1 hours remaining in December and March respectively.

6.2. Effect of Preventative Measures on Cooling Requirements

Simulation analysis showed lower summer temperature profiles and reduced annual thermal discomfort with increasing insulation (polyester fibre) thickness, from 0 to 135 mm. However, marginal improvements in temperature and comfort diminished with each increment in thickness: discomfort hours were reduced by 10% from 0 to 40 mm, and by a further 4.5% from 40 to 75 mm (13.6% relative to 0 mm). Increments in thickness thereafter produced more negligible improvements in thermal comfort.

Cooling load and annual cooling requirement decreased, as expected, with increasing ceiling thermal resistance, but with reduced sensitivity at each insulation thickness increment. These results were consistent with the findings of Aktacir et al (2010), as described in the literature review. Increasing

thickness from 0 to 40 mm caused a 14% reduction in peak cooling load; a further 5.4% reduction resulted from increasing thickness from 40 mm to 75 mm. Further cooling reductions at greater thickness increments were lower than 5%.

Based on the results, a thickness of 75 mm polyester insulation was selected to represent the insulation retrofit (*75 mm-Insulation*), for analysis with further preventative measures. Insulation was the most expensive singular preventative measure, and resulted in a relatively small 2.0% reduction in total projected cooling costs over 10 years (relative to the *Base Case*). However, it did allow for the greatest singular reduction in peak cooling load, of 19%, to 54.48 kW_{th}.

Following insulation, *Delamping* was assessed, in which one existing fluorescent luminaire was assumed to be removed from each light fixture in the North, East, West, Seminar and Staff WC thermal zones, reducing lighting power density across the ERC by an aggregate 32.89%. This measure resulted in a simulated 31% reduction in annual lighting heat gain and 24% reduction of annual cooling energy. The *Delamping* scenario had the greatest individual impact on cooling cost projections, reducing total costs after 10 years by 15.6% relative to the *Base Case*. This measure also had the lowest relative payback period of 0.97 years, although resulted in lower cumulative savings after 5 years relative to the two more progressive measures.

Subsequently, the *Relamping* scenario reduced annual lighting heat gain to 10.88 MWh_{th}, i.e. a 46% reduction relative to the *Base Case*. *Relamping* further reduced peak cooling load by 24% to 50.72 kW_{th}. The costs incurred with replacing luminaires and ballasts increased the relative payback period of the measure to 1.24 years, but resulted in greater cumulative savings after 5 years. *Relamping* achieves lighting energy savings of 2.87 MWh relative to *Delamping* – a 20.9% reduction. This implies that energy cost savings achieved by *Relamping* would offset the additional capital expenditure, over and above *Delamping*. This would likely be a cost effective measure for the ERC, even in the absence of cooling considerations.

Finally, the replacement of solar film with internal shading had a negligible impact on annual solar heat gains, but resulted in a 7% in cooling energy savings beyond the *Relamping* scenario. These results showed that greater (idealised) control over window shading, afforded by the adjustable internal blinds, allows occupants to 'use' solar gains to their advantage. This is reflected in reduced solar heat gains in the North, East and West facing zones, and *increased* solar heat gain in the South zone, which receives lower direct sunlight exposure due to its orientation. Adjustable shading also allows greater solar radiation transmittance during winter, compared with the fixed solar film, which may reduce heating requirements.

However, cost evaluations showed the *Shading* measure to be significantly less cost effective compared with the other preventative measures. The high installation cost of the slatted blinds, to cover the entire window area of the ERC, resulted in an increase of 4.8% of total cost projections relative to the *Relamping* case, with relative payback period of the collective measures increased to 3.56 years (from 1.24 previously). Net present value of relative energy savings after 10 years is 126 047 ZAR [2015]; 32 667 ZAR lower than under the *Relamping* scenario.

Furthermore, adjustable internal shading may be suboptimal for other reasons. Firstly, an internal shading device does not prevent solar heat transmitting into the building interior, and devices that are not highly reflective may absorb and scatter incident radiation to surrounding internal surfaces.

Secondly, while the *EnergyPlus* simulation was set to assume the blinds fully cover the windows whenever incident solar radiation exceeds a pre-defined set point level, the reality of human behaviour is such that an actual shading device would not be controlled in such an ideal manner. This was reflected in the findings of Foster and Oreszczyn (2001).

It is thus concluded that the *Shading* retrofit would not be cost effective, and would not be recommended as a preventative measure for the ERC. Alternative shading options, such as fixed external shading, may prove more cost effective in mitigating the ERC's solar heat gains, and should be considered in further research. A combination of insulation and energy efficient lighting upgrades are likely to provide the greatest benefit, in terms of thermal comfort, to the ERC, and result in a more cost effective active cooling system, should one be proposed.

7. Recommendations

Findings from the research of this dissertation can be seen to form the basis from which further studies and investigations can be carried out on several areas of the subject matter. The following is a list of recommendations for potential further work relating to thermal comfort and characterisation of the ERC, and design and specification of cooling systems.

1. ERC heating

One of the main scope limitations was confining the analysis here to cooling the ERC in summer. A comprehensive assessment of thermal comfort should account for thermal conditions throughout the year, i.e. including winter as well as summer. Furthermore, simulation results of the ERC under *Current* conditions predicted a greater number of discomfort hours experienced between June and August, than December through March. Building retrofit plans should also account for the effects of heat loss in winter, in addition to preventing or removing heat gains in summer. This is notably the case for the ERC, where annual heat loss through the building envelope was found to be greater in magnitude than annual heat gains from any individual heat source.

A study, similar in approach to this but focusing on thermal conditions and heat loss in winter, would add significant value to the results found here, and would provide an overall representation of annual ERC heating and cooling requirements.

2. Improved modelling and validation

While the model developed in *DesignBuilder* in this study attempted to comprehensively characterise ERC thermal conditions, it was not without its shortcomings. Several assumptions were made in developing the model to accommodate a lack of actual data on thermal properties of the building materials, equipment use and occupancy schedules and activity levels. The uncertainty arising from these assumptions was reflected in the model validation process, which showed only moderate correlation between simulated temperature data and actual air temperature measurements.

More comprehensive validation methods should be employed to enhance the accuracy of the model, such as the comparative techniques described in Judkoff et al (2009) and Ryan and Sanquist (2012). More rigorous data collection, including surveys and statistical analysis, would improve the accuracy of simulation results of the ERC model.

3. Design and specification of active cooling

The cost evaluation of the preventative measures in Chapter 5 was limited by the high level assumptions of the active cooling system, relying on a derived linear design capacity cost factor relationship to estimate installation and O&M costs. The accuracy of cost evaluations would be greatly improved by using actual data, based on commercial quotes obtained for cooling system components.

The cooling loads calculated from the various simulation scenarios can be used to inform preliminary design analysis of an actual cooling system. HVAC simulation software, such as *EnergyPlus*, can further be used to calculate component loads and operating parameters based on assumptions of plant efficiency curves and distribution efficiency and losses. Simulation results can be used to estimate capacity and energy consumption of the system components, from which actual, accurate cost estimates can be determined.

4. Investigation into passive and renewable cooling

Finally, further investigation into passive and/or solar cooling options may be considered, as an alternative to a conventional air conditioning system for the ERC. These cooling techniques were introduced in the literature review, but could be significantly expanded on in further analysis. In particular, solar absorption cooling has shown significant growth globally in the last ten years, while commercial implementation has already been demonstrated for large buildings in South Africa. Embedded renewable energy usage could potentially emerge as a significant alternative energy market in South Africa, in which solar thermal cooling could play a significant role.

There is potential for the ERC, or indeed UCT at large, to contribute to the further commercialisation of solar cooling technology, by investing in a pilot facility designed to provide localised cooling to a building on campus. Should this be implemented in the ERC, it would contribute to reducing summer thermal discomfort with minimal increase in carbon-based energy consumption, and would provide a great opportunity for the research centre to demonstrate innovation in sustainable energy use.

8. References

Abdou, A.A. & Budaiwi, I.M. 2005. Comparison of thermal conductivity measurements of building insulation materials under various operating temperatures. *Journal of Building Physics.* 29(2):171-184.

Abengoa Solar 2014. *Our plants: South Africa.* Available: http://www.abengoasolar.com/web/en/plantas_solares/plantas_propias/sudafrica/ [12 November 2016].

Ahmed, A.F., Khan, K.M.K., Oo, A.M.T. & Rasul, R.G. 2014. Selection of suitable passive cooling strategy for a subtropical climate. *International Journal of Mechanical and Materials Engineering.* 9(1):1-11.

Aktacir, M.A., Büyükalaca, O. & Yılmaz, T. 2010. A case study for influence of building thermal insulation on cooling load and air-conditioning system in the hot and humid regions. *Applied Energy.* 87(2):599-607. DOI:http://dx.doi.org.ezproxy.uct.ac.za/10.1016/j.apenergy.2009.05.008.

Alamdari, F. & Hammond, G.P. 1983. Improved data correlations for buoyancy-driven convection in rooms [Abstract]. *Building Services Engineering Research and Technology.* 4(1):106-112. 10.1177/014362448300400304.

Aldawoud, A. 2013. Conventional fixed shading devices in comparison to an electrochromic glazing system in hot, dry climate. *Energy and Buildings.* 59:104-110.

Al-Homoud, D.M.S. 2005. Performance characteristics and practical applications of common building thermal insulation materials. *Building and Environment.* 40(3):353-366. DOI:http://dx.doi.org.ezproxy.uct.ac.za/10.1016/j.buildenv.2004.05.013.

ASHRAE 2016. *2016 ASHRAE Handbook—HVAC Systems and Equipment.* Atlanta, Georgia: American Society of Heating, Refrigerating and Air-Conditioning Engineers.

ASHRAE-55 2004. *ASHRAE Standard: Thermal Environmental Conditions for Human Occupancy.* Atlanta, Georgia, USA: American Society of Heating, Refrigerating and Air-Conditioning Engineers.

Awbi, H.B. & Hatton, A. 1999. Natural convection from heated room surfaces. *Energy and Buildings.* 30(3):233-244. DOI:http://dx.doi.org.ezproxy.uct.ac.za/10.1016/S0378-7788(99)00004-3.

Bauer, M. & Scartezzini, J.-. 1998. A simplified correlation method accounting for heating and cooling loads in energy-efficient buildings. *Energy and Buildings.* 27(2):147-154. DOI:http://dx.doi.org.ezproxy.uct.ac.za/10.1016/S0378-7788(97)00035-2.

Beausoleil-Morrison, I. 2000. The Adaptive Coupling of Heat and Air Flow Modelling within Dynamic Whole-Building Simulation. PhD. Energy Systems Research Unit, Department of Mechanical Engineering, University of Strathclyde, Glasgow UK.

Beckwith, T.G., Marangoni, R.D. & Lienhard V, J.H. 2009. *Mechanical Measurements.* Sixth ed. Upper Saddle River, New Jersey: Pearson Education.

Brager, G.S. & de Dear, R.J. 1998. Thermal adaptation in the built environment: a literature review. *Energy and Buildings.* 27(1):83-96. DOI:http://dx.doi.org.ezproxy.uct.ac.za/10.1016/S0378-7788(97)00053-4.

Burdick, A. 2011. *Strategy Guideline: Accurate Heating and Cooling Load Calculations.* Pittsburgh, Pennsylvania, US: US Department of Energy.

Buys, J. & Mathews, E. 2005. Investigation into capital costs of HVAC systems. *Building and Environment.* 40(9):1153-1163.

Çengel, Y.A. & Boles, M.A. Eds. 2008. *Thermodynamics: An Engineering Approach*. Seventh ed. New York: McGraw-Hill.

Cheng, Y. & Cheng, K.2006. General study for using LED to replace traditional lighting devices. *2006 2nd International Conference on Power Electronics Systems and Applications.* IEEE. 173.

Chua, K.J., Chou, S.K., Yang, W.M. & Yan, J. 2013. Achieving better energy-efficient air conditioning – A review of technologies and strategies. *Applied Energy.* 104(2013):87-104. DOI:http://dx.doi.org.ezproxy.uct.ac.za/10.1016/j.apenergy.2012.10.037.

Clarke, J.A. 2001. *Energy simulation in building design.* Routledge.

Crawley, D.B., Lawrie, L.K., Pedersen, C.O., Winkelmann, F.C., Witte, M.J., Strand, R.K., Liesen, R.J., Buhl, W.F. et al. 2004. EnergyPlus: New, capable, and linked. *Journal of Architectural and Planning Research.* :292-302.

Crawley, D.B., Hand, J.W., Kummert, M. & Griffith, B.T. 2008. Contrasting the capabilities of building energy performance simulation programs. *Building and Environment.* 43(4):661-673. DOI:http://dx.doi.org.ezproxy.uct.ac.za/10.1016/j.buildenv.2006.10.027.

Crawley, D.B., Lawrie, L.K., Winkelmann, F.C., Buhl, W.F., Huang, Y.J., Pedersen, C.O., Strand, R.K., Liesen, R.J. et al. 2001. EnergyPlus: creating a new-generation building energy simulation program. *Energy and Buildings.* 33(4):319-331. DOI:http://dx.doi.org.ezproxy.uct.ac.za/10.1016/S0378-7788(00)00114-6.

CSIR 2009. *Green Building Handbook for South Africa. Chapter: Lighting.* South Africa: Council for Scientific and Industrial Research.

Datta, G. 2001. Effect of fixed horizontal louver shading devices on thermal perfomance of building by TRNSYS simulation. *Renewable Energy.* 23(3–4):497-507. DOI:http://dx.doi.org.ezproxy.uct.ac.za/10.1016/S0960-1481(00)00131-2.

Davis, L.W. & Gertler, P.J. 2015. Contribution of air conditioning adoption to future energy use under global warming. *Proceedings of the National Academy of Sciences of the United States of America.* 112(19):5962-5967. DOI:10.1073/pnas.1423558112.

DesignBuilder 2016. *DesignBuilder Version 4.7.0.027.* DesignBuilder Software Ltd.

Duška, M., Barták, M., Drkal, F. & Hensen, J.2006. Analytical approach to transient heat conduction in cooling load calculations. *Proceedings of the 17th Int. Air-Conditioning and Ventilation Conference, Prague.* 7.

ECOFYS 2015. *Position Paper: A heating & cooling strategy for the European building sector until 2050.* Utrecht, Netherlands: ECOFYS.

Edison Tech Center 2013. *The Fluorescent Lamp.* Available: http://www.edisontechcenter.org/Fluorescent.html [21 November 2016].

Eicker, U., Colmenar-Santos, A., Teran, L., Cotrado, M. & Borge-Diez, D. 2014. Economic evaluation of solar thermal and photovoltaic cooling systems through simulation in different climatic conditions: An analysis in three different cities in Europe. *Energy and Buildings.* 70:207-223. DOI:http://dx.doi.org.ezproxy.uct.ac.za/10.1016/j.enbuild.2013.11.061.

Energy Star 2006. Chapter 6: Lighting. In *Energy Star Building Upgrade Manual.* Energy Star, Ed. US Environmental Protection Agency. 6.1-6.37.

8 References

EnergyPlus 2015. *EnergyPlus Version 8.3 Documentation: Engineering Reference.* U.S. Department of Energy.

EnergyPlus 2016. *EnergyPlus Version 8.6 Documentation: Getting Started.* US Department of Energy.

EPA [US Environmental Protection Agency] 2016. *Fine Mineral Fibres - Hazard Summary.* Available: https://www.epa.gov/sites/production/files/2016-10/documents/fine-mineral-fibers.pdf [15 December 2016].

EScience Associates 2016. *Solar Cooling Technologies in South Africa.* Oaklands, Johannesburg: EScience Associates (Pty) Ltd.

Etheridge, D. 2010. Ventilation, air quality and airtightness in buildings. In *Materials for energy efficiency and thermal comfort in buildings.* M.R. Hall, Ed. First ed. Cambridge, U.K.: Woodhead Publishing. 77-100.

Fanger, P.O. 1982. *Thermal comfort: analysis and applications in environmental engineering.* Malabar, Florida: R.E. Krieger Publishing.

Fayerweather, W.E., Bender, J.R., Hadley, J.G. & Eastes, W. 1997. Quantitative risk assessment for a glass fiber insulation product. *Regulatory Toxicology and Pharmacology.* 25(2):103-120.

Florides, G.A., Kalogirou, S.A., Tassou, S.A. & Wrobel, L.C. 2003. Design and construction of a LiBr–water absorption machine. *Energy Conversion and Management.* 44(15):2483-2508. DOI:http://dx.doi.org.ezproxy.uct.ac.za/10.1016/S0196-8904(03)00006-2.

Florides, G.A., Tassou, S.A., Kalogirou, S.A. & Wrobel, L.C. 2002a. Review of solar and low energy cooling technologies for buildings. *Renewable and Sustainable Energy Reviews.* 6(2002):557-572. DOI:10.1016/S1364-0321(02)00016-3.

Fohanno, S. & Polidori, G. 2006. Modelling of natural convective heat transfer at an internal surface. *Energy and Buildings.* 38(5):548-553. DOI:http://dx.doi.org.ezproxy.uct.ac.za/10.1016/j.enbuild.2005.09.003.

Fong, K.F., Chow, T.T., Lee, C.K., Lin, Z. & Chan, L.S. 2010. Comparative study of different solar cooling systems for buildings in subtropical city. *Solar Energy.* 84(2):227-244. DOI:http://dx.doi.org.ezproxy.uct.ac.za/10.1016/j.solener.2009.11.002.

Foster, M. & Oreszczyn, T. 2001. Occupant control of passive systems: the use of Venetian blinds. *Building and Environment.* 36(2):149-155. DOI:http://dx.doi.org.ezproxy.uct.ac.za/10.1016/S0360-1323(99)00074-8.

Foucquier, A., Robert, S., Suard, F., Stéphan, L. & Jay, A. 2013. State of the art in building modelling and energy performances prediction: A review. *Renewable and Sustainable Energy Reviews.* 23:272-288. DOI:http://dx.doi.org.ezproxy.uct.ac.za/10.1016/j.rser.2013.03.004.

Freewan, A.A.Y. 2014. Impact of external shading devices on thermal and daylighting performance of offices in hot climate regions. *Solar Energy.* 102:14-30. DOI:http://dx.doi.org.ezproxy.uct.ac.za/10.1016/j.solener.2014.01.009.

GBCSA 2010. *The Green Star SA - Office v1: Energy Calculator & Modelling Protocol Guide - Version 1.1.* South Africa: Green Building Council of South Africa.

GBCSA 2012. *Improving Lives By Greening Low-Cost Housing: Case study report of the Cato Manor Green Street retrofit.* Green Building Council of South Africa.

Givoni, B. 1994. *Passive and low energy cooling of buildings.* New York: Van Nostrand Reinhold.

8 References

Gouda, M., Danaher, S. & Underwood, C. 2002. Building thermal model reduction using nonlinear constrained optimization. *Building and Environment.* 37(12):1255-1265.

Grossman, G. 2002. Solar-powered Systems for Cooling, Dehumidification and Air-Conditioning. *Solar Energy.* 72(1):53-62. DOI:10.1016/S0038-092X(01)00090-1.

Hall, M.R. & Allinson, D. 2010. Heat and mass transport processes in building materials. In *Materials for energy efficiency and thermal comfort in buildings.* M.R. Hall, Ed. Cambridge, United Kingdom: Woodhead Publishing. 3-53.

Hang, Y., Qu, M. & Zhao, F. 2011. Economical and environmental assessment of an optimized solar cooling system for a medium-sized benchmark office building in Los Angeles, California. *Renewable Energy.* 36(2):648-658. DOI:http://dx.doi.org.ezproxy.uct.ac.za/10.1016/j.renene.2010.08.005.

Henning, H. & Albers, J. 2004. *Decision Scheme for the Selection of the Appropriate Technology Using Solar Thermal Air-Conditioning. Guideline Document.* IEA Solar Heating and Cooling. Task 25: Solar-Assisted Air-Conditioning of Buildings.

Henninger, R.H. & Witte, M.J. 2014. *EnergyPlus Testing with IEA BESTEST Multi-Zone Non-Airflow In-Depth Diagnostic Cases MZ320 - MZ360: EnergyPlus Version 8.2.0.* Arlington Heights, Illinois, USA: International Energy Agency.

Huizenga, C., Abbasszadeh, S., Zagreus, L. & Arens, E.A.2006. Air quality and thermal comfort in office buildings: Results of a large indoor environmental quality survey. *Healthy Buildings 2006.* June 2006. Lisbon, Portgua: UC Berkeley: Center for the Built Environment. 393.

Hwang, Y., Radermacher, R., Alili, A.A. & Kubo, I. 2008. Review of Solar Cooling Technologies. *HVAC&R Research.* 14(3):507-528. DOI:10.1080/10789669.2008.10391022.

Ibarra, D. & Reinhart, C.F.2009. Daylight factor simulations–how close do simulation beginners 'really'get? *Building Simulation.* 203.

IEA 2015. *World Energy Outlook 2015.* Paris: International Energy Agency.

IEA-SHC 2009. *Task 38: Solar Air-Conditioning and Refrigeration: State of the art on existing solar heating and cooling systems: A technical report of subtask B. Date: 2009 November 12.* Solar Heating and Cooling Programme, International Energy Agency.

IPCC 2014. *Climate Change 2014: Mitigation of Climate Change. Contribution of Working Group III to the Fifth Assessment Report of the Intergovernmental Panel on Climate Change.* Cambridge, United Kingdom; New York, NY, USA: Cambridge University Press.

Jelle, B.P. 2011. Traditional, state-of-the-art and future thermal building insulation materials and solutions–Properties, requirements and possibilities. *Energy and Buildings.* 43(10):2549-2563.

Judkoff, R. & Neymark, J. 2013. *Twenty Years On!: Updating the IEA BESTEST Building Thermal Fabric Test Cases for ASHRAE Standard 140.* Oak Ridge, Tennessee: National Renewable Energy Laboratory.

Judkoff, R. & Neymark, J. 2008. Testing and validation of building energy simulation tools. *Colorado: National Renewable Energy Laboratory.*

Kalogirou, S.A. & Bojic, M. 2000. Artificial neural networks for the prediction of the energy consumption of a passive solar building. *Energy.* 25(5):479-491. DOI:http://dx.doi.org.ezproxy.uct.ac.za/10.1016/S0360-5442(99)00086-9.

Kim, D.S. & Infante Ferreira, C.A. 2008. Solar refrigeration options – a state-of-the-art review. *International Journal of Refrigeration.* 31(1):3-15. DOI:http://dx.doi.org.ezproxy.uct.ac.za/10.1016/j.ijrefrig.2007.07.011.

Leaman, A. & Bordass, B. 1998. *Probe 15: Productivity - the killer variables.* Building Services Journal.

Lechner, N. Ed. 2001. *Heating, cooling, lighting: design methods for architects*. 2nd ed. New York: John Wiley & Sons.

Lee, S.W. & Lim, C.H. 2016. Reflective thermal insulation systems in building: A review on radiant barrier and reflective insulation. *Renewable and Sustainable Energy Reviews.* 65:643-661.

Li, Z.F. & Sumathy, K. 2000. Technology development in the solar absorption air-conditioning systems. *Renewable and Sustainable Energy Reviews.* 4(3):267-293. DOI:http://dx.doi.org.ezproxy.uct.ac.za/10.1016/S1364-0321(99)00016-7.

Loutzenhiser, P.G., Manz, H., Moosberger, S. & Maxwell, G.M. 2009. An empirical validation of window solar gain models and the associated interactions. *International Journal of Thermal Sciences.* 48(1):85-95.

Luo, C., Moghtaderi, B. & Page, A. 2010. Modelling of wall heat transfer using modified conduction transfer function, finite volume and complex Fourier analysis methods. *Energy and Buildings.* 42(5):605-617. DOI:http://dx.doi.org.ezproxy.uct.ac.za/10.1016/j.enbuild.2009.10.031.

Lutron 2011. *Fluorescent Dimming Systems: Technical Guide.* Coopersburg, Pennsylvania: Lutron Electronics.

Magwaca, M. 2011. Energy Efficient Lighting - Presentation at the Energy Research Centre. (Unpublished).

Martin, C. 2011. Establishing energy benchmarks for commercial buildings in the City of Cape Town. Masters Dissertation. University of Cape Town.

Mathews, E., Kleingeld, M. & Taylor, P. 1999. Estimating the electricity savings effect of ceiling insulation. *Building and Environment.* 34(4):505-514.

McGee, C. & Reardon, C. 2013. *YourHome.gov.au: Shading.* Available: http://www.yourhome.gov.au/passive-design/shading [2016/09/16].

McQuiston, F.C., Parker, J.D. & Spitler, J.D. 2005. *Heating, Ventilating, and Air Conditioning Analysis and Design.* Sixth ed. Hoboken, New Jersey: John Wiley & Sons.

Mitalas, G.P. 1978. *Comments on the Z-Transfer Function Method for Calculating Heat Transfer in Buildings.* Ottawa, Canada: Division of Building Research, National Research Council of Canada.

Mitalas, G.P. & Stephenson, D.G. 1967. *Room Thermal Response Factors.* Ottawa: American Society of Heating, Refrigerating, and Air-Conditioning Engineers.

Murray, P., Rysanek, A.M., Pantelic, J., Mast, M. & Schlueter, A. 2015. On Decentralized Air-conditioning for Hot and Humid Climates: Performance Characterization of a Small Capacity Dedicated Outdoor Air System with Built-in Sensible and Latent Energy Recovery Wheels. *Energy Procedia.* 78:3471-3476.

Neethling, M.M. 2011. Energy Flow Analysis of an Academic Building. MEng. Department of Mechanical and Mechatronic Engineering, University of Stellenbosch.

Neto, A.H. & Fiorelli, F.A.S. 2008. Comparison between detailed model simulation and artificial neural network for forecasting building energy consumption. *Energy and Buildings.* 40(12):2169-2176. DOI:http://dx.doi.org.ezproxy.uct.ac.za/10.1016/j.enbuild.2008.06.013.

OpenStudio 2016. *OpenStudio®.* Available: https://www.openstudio.net/.

Otanicar, T., Taylor, R.A. & Phelan, P.E. 2012. Prospects for solar cooling – An economic and environmental assessment. *Solar Energy.* 86(5):1287-1299.

Papadopoulos, A.M. 2005. State of the art in thermal insulation materials and aims for future developments. *Energy and Buildings.* 37(1):77-86.

Pedersen, C.O., Fisher, D.E. & Liesen, R.J. 1997. Development of a Heat Balance Procedure for Calculating Cooling Loads. *ASHRAE Transactions.* 103(2):459-468.

SABS - SANS 204:2011 *South African National Standard: Energy efficiency in buildings.* Pretoria: SABS Standards Division.

Sezgen, A.O. & Huang, Y.J. 1994. Lighting/HVAC interactions and their effects on annual and peak HVAC requirements in commercial buildings. *Proceedings.ACEEE Summer Study on Energy Efficiency in Buildings.Panel.* 3:229-239.

Sezgen, O. & Koomey, J.G. 2000. Interactions between lighting and space conditioning energy use in US commercial buildings. *Energy.* 25(8):793-805.

South African Weather Service 2016. *Historical Rain Maps.* Available: http://www.weathersa.co.za/climate/historical-rain-maps [30 September 2016].

Stephenson, D.G. & Mitalas, G.P. 1967. Cooling Load Calculations by Thermal Response Factor Method. *ASHRAE Transactions.* 73(1):1-7.

Ullah, K.R., Saidur, R., Ping, H.W., Akikur, R.K. & Shuvo, N.H. 2013. A review of solar thermal refrigeration and cooling methods. *Renewable and Sustainable Energy Reviews.* 24(2013):499-513. DOI:http://dx.doi.org.ezproxy.uct.ac.za/10.1016/j.rser.2013.03.024.

Ürge-Vorsatz, D., Danny Harvey, L.D., Mirasgedis, S. & Levine, M.D. 2007. Mitigating CO_2 emissions from energy use in the world's buildings. *Building Research & Information.* 35(4):379-398. DOI:10.1080/09613210701325883.

van Straaten, J.F. 1967. *Thermal Performance of Buildings.* Amsterdam: Elsevier Publishing Company.

Vicatos, G. 1995. Heat and Mass Transfer: Design and Optimisation of Absorption Refrigeration Machines. PhD Thesis. University of Cape Town.

Wagner, A., Gossauer, E., Moosmann, C., Gropp, T. & Leonhart, R. 2007. Thermal comfort and workplace occupant satisfaction - Results of field studies in German low energy office buildings. *Energy and Buildings.* 39(2007):758-769. DOI:10.1016/j.enbuild.2007.02.013.

Wlokas, H.L. & Ellis, C. 2013. *Local employment through the low pressure solar water heater roll-out in South Africa.* Cape Town: Energy Research Centre, University of Cape Town.

Zhao, H. & Magoulès, F. 2012. A review on the prediction of building energy consumption. *Renewable and Sustainable Energy Reviews.* 16(6):3586-3592. DOI:http://dx.doi.org.ezproxy.uct.ac.za/10.1016/j.rser.2012.02.049.

Zmeureanu, R. & Peragine, C. 1999. Evaluation of interactions between lighting and HVAC systems in a large commercial building. *Energy Conversion and Management.* 40(11):1229-1236.

9. Appendices

Appendix A: Schedule of ERC Simulations

Table 9-1 lists all simulations of the ERC energy model that were run and analysed in the dissertation. The following assumptions and simulation settings were kept constant throughout each run in *DesignBuilder*, as discussed in § 3.2 of the dissertation:

- Environmental conditions, heat balances and cooling loads were solved in half-hour time-steps. Results were presented in hourly intervals, and aggregated in varying time periods to highlight specific findings in the analysis
- The Menzies building was not modelled in its entirety. The *DesignBuilder* energy model included only the northern wing of Menzies, which houses the ERC offices. Thermal calculations were performed for the ERC thermal zones, as well as the fifth floor zone, the adjacent 'non-ERC' thermal zone on Level 6 and the roof space above the ERC. All other floors and thermal zones were excluded from the calculations
- Air velocity within the ERC was assumed to be 0.2 m/s, for the purpose of thermal comfort calculations.
- Simplified analysis of the effects of air infiltration and natural ventilation (from opening windows) on removing or adding heat to the zones was included in each simulation
- Thermal energy flows were resolved according to the Heat Balance Method, with heat flux through building surfaces calculated according to the Conduction Transfer Function method
- External surface convection was modelled using the *DOE-2* algorithm
- Internal surface convection was modelled using the *TARP* algorithm
- Detailed *EnergyPlus* modelling parameters, including convergence tolerances, warm-up days, solar distribution patterns and airflow network calculations were set to *DesignBuilder* default settings

Table 9-1: Schedule of ERC energy model simulations

Sim No.	Simulation	Description	Cooling	Passive Interventions	Simulation Period
Run 1-1	ERC-Current	Annual thermal conditions and heat gains for existing ERC	Off	None	Whole Year
Run 1-2	ERC-Current	Daily heat gain profiles during Cape Town IWEC Summer Design Week	Off	None	13 – 19 Jan
Run 2-1	ERC Cooling Base Case	Base case annual cooling requirements under current conditions	On	None	Whole Year
Run 2-3	ERC Cooling Base Case	Base case cooling load profile under current conditions, during Summer Design Week	On	None	13 – 19 Jan
Run 3-1	ERC + Insulation	Impact of 40 mm PF ceiling insulation on summer thermal conditions	Off	Ceiling insul. (40 mm PF)	13 – 19 Jan
Run 3-2	ERC + Insulation	Impact of 75 mm PF ceiling insulation on summer thermal conditions	Off	Ceiling insul. (75 mm PF)	13 – 19 Jan
Run 3-3	ERC + Insulation	Impact of 100 mm PF ceiling insulation on summer thermal conditions	Off	Ceiling insul. (100 mm PF)	13 – 19 Jan

Sim No.	Simulation	Description	Cooling	Passive Interventions	Simulation Period
Run 3-4	ERC + Insulation	Impact of 135 mm PF ceiling insulation on summer thermal conditions	Off	Ceiling insul. (135 mm PF)	13 – 19 Jan
Run 3-5	ERC Cooling + Insulation	Annual cooling requirement with 40 mm PF ceiling insulation	On	Ceiling insul. (40 mm PF)	Whole Year
Run 3-6	ERC Cooling + Insulation *(75 mm-Insulation)*	Annual cooling requirement with 75 mm PF ceiling insulation	On	Ceiling insul. (75 mm PF)	Whole Year
Run 3-7	ERC Cooling + Insulation	Annual cooling requirement with 100 mm PF ceiling insulation	On	Ceiling insul. (100 mm PF)	Whole Year
Run 3-8	ERC Cooling + Insulation	Annual cooling requirement with 135 mm PF ceiling insulation	On	Ceiling insul. (135 mm PF)	Whole Year
Run 3-9	ERC Cooling + Insulation	Summer Design Week cooling load profile with 40 mm PF ceiling insulation	On	Ceiling insul. (40 mm PF)	13 – 19 Jan
Run 3-10	ERC Cooling + Insulation	Summer Design Week cooling load profile with 75 mm PF ceiling insulation	On	Ceiling insul. (75 mm PF)	13 – 19 Jan
Run 3-11	ERC Cooling + Insulation	Summer Design Week cooling load profile with 100 mm PF ceiling insulation	On	Ceiling insul. (100 mm PF)	13 – 19 Jan
Run 3-12	ERC Cooling + Insulation	Summer Design Week cooling load profile with 135 mm PF ceiling insulation	On	Ceiling insul. (135 mm PF)	13 – 19 Jan
Run 4-1	ERC Cooling + Basic Lighting Control	Annual heat gain and cooling requirements with automatic lighting control (+ 75 mm PF insulation)	On	Basic daylighting control (+ 75 insulation)	Whole Year
Run 4-2	ERC Cooling + Delamping	Impact of removing 1 off T12 60 W lamp per light fixture from selected thermal zones	On	Delamping (+ 75 mm-Insulation)	Whole Year
Run 4-3	ERC Cooling + Relamping	Impact of replacing T12 60 W linear fluorescents with T8 59 W, and magnetic ballasts with electronic, (+ 75 mm PF insulation)	On	Relamping (+ Delamping & 75 mm-Insulation)	Whole Year
Run 4-4	ERC Cooling + Delamping	Impact of Delamping on heat balance profile during Summer Design Week	On	Delamping (+ 75 mm-Insulation)	13 – 19 Jan
Run 4-5	ERC Cooling + Relamping	Impact of Relamping on heat balance profile during Summer Design Week	On	Relamping (+ Delamping & 75 mm-Insulation)	13 – 19 Jan
Run 5-1	ERC Cooling + Shading	Annual heat gain and cooling requirements with shading retrofit (+ 75 mm PF insulation, Delamping and Relamping)	On	… + Slatted blind internal shading	Whole Year
Run 5-2	ERC Cooling + Shading	Summer Design Week cooling load profile with shading retrofit (+ 75 mm PF insulation, Delamping and Relamping)	On	… + slatted blind internal shading	13 – 19 Jan

Appendix B: Weather Data

Data for Figure 3-1 and Figure 3-2, in § 3.1.1, is shown in Table 9-2 and Table 9-3, respectively, below.

Table 9-2: Cape Town monthly dry-bulb temperature summary [°C]

Month	Minimum	Q1	Median	Q3	Maximum
January	12.2	18.0	20.0	23.0	33.0
February	11.5	18.5	20.1	22.7	34.0
March	8.4	17.4	18.7	21.3	30.9
April	6.1	14.4	16.3	18.2	29.5
May	3.0	12.8	14.0	16.6	30.0
June	3.2	10.0	13.1	15.2	26.0
July	0.8	9.6	12.7	14.5	26.5
August	4.2	10.4	13.1	14.8	27.3
September	5.0	12.0	14.0	16.0	30.0
October	4.9	13.0	15.9	18.0	31.0
November	9.6	16.0	18.0	20.0	31.0
December	12.8	17.1	19.0	22.0	33.0

Table 9-3: Cape Town average hourly humidity profiles per month

Hour	Jan	Feb	Mar	Apr	May	Jun	Jul	Aug	Sep	Oct	Nov	Dec
00:00	80.0%	79.2%	85.5%	85.4%	87.5%	81.0%	84.5%	88.1%	82.9%	80.2%	77.6%	82.0%
01:00	80.9%	80.4%	86.5%	86.5%	88.1%	81.9%	85.8%	88.3%	84.5%	82.0%	78.1%	83.5%
02:00	81.3%	81.6%	87.5%	87.2%	88.4%	83.3%	86.4%	88.9%	84.2%	82.5%	78.8%	84.0%
03:00	83.0%	82.3%	88.2%	87.9%	87.3%	84.5%	85.8%	89.3%	84.7%	82.4%	79.0%	84.1%
04:00	83.2%	82.8%	88.6%	88.5%	87.0%	85.6%	85.0%	89.5%	85.0%	83.1%	80.7%	84.1%
05:00	84.1%	83.0%	89.0%	88.9%	86.8%	85.9%	84.1%	89.6%	87.4%	83.5%	80.5%	85.0%
06:00	83.7%	81.1%	88.9%	88.8%	87.6%	86.2%	83.8%	89.4%	89.0%	83.3%	79.5%	82.2%
07:00	81.6%	78.9%	88.7%	88.4%	89.4%	86.3%	83.7%	89.1%	89.0%	82.6%	76.0%	76.5%
08:00	72.6%	76.3%	87.8%	88.0%	88.9%	84.6%	83.5%	88.7%	85.2%	72.5%	68.2%	71.0%
09:00	63.4%	68.4%	80.2%	80.2%	85.3%	82.6%	77.9%	80.0%	81.0%	63.5%	62.5%	63.5%
10:00	57.5%	61.5%	72.7%	72.5%	77.4%	76.4%	72.3%	72.6%	71.7%	58.4%	58.6%	58.9%
11:00	52.5%	55.6%	65.5%	65.8%	69.2%	68.0%	67.2%	65.8%	65.2%	53.1%	54.8%	55.8%
12:00	50.9%	54.5%	63.7%	64.7%	62.8%	60.4%	65.0%	63.0%	59.8%	52.0%	55.3%	54.8%
13:00	50.6%	53.3%	62.1%	63.6%	57.5%	61.0%	63.0%	60.5%	57.8%	53.2%	54.7%	53.5%
14:00	50.2%	52.2%	61.4%	62.7%	57.2%	57.3%	61.2%	58.1%	58.3%	52.5%	57.0%	52.7%
15:00	50.8%	54.1%	62.5%	65.1%	60.6%	56.9%	63.3%	61.5%	58.9%	56.5%	58.7%	53.2%
16:00	52.6%	55.9%	63.8%	67.7%	63.1%	59.1%	65.7%	65.2%	61.8%	57.6%	61.3%	55.4%
17:00	55.1%	58.0%	65.1%	70.7%	69.7%	62.6%	68.2%	69.3%	65.5%	61.9%	62.7%	56.4%
18:00	57.8%	62.9%	70.2%	74.3%	75.7%	71.2%	71.8%	74.0%	70.5%	65.5%	66.3%	61.0%
19:00	63.4%	67.9%	75.5%	78.4%	81.5%	76.1%	76.1%	79.3%	76.6%	71.4%	70.6%	66.3%
20:00	70.4%	73.6%	81.4%	82.2%	83.4%	80.1%	80.5%	85.1%	78.6%	75.1%	74.0%	73.2%
21:00	73.2%	75.0%	82.5%	83.2%	86.6%	80.7%	81.6%	86.1%	81.8%	76.8%	74.8%	76.6%
22:00	76.0%	76.3%	83.4%	84.1%	87.6%	84.4%	82.4%	86.8%	82.7%	78.8%	75.4%	79.0%
23:00	78.4%	77.5%	84.4%	84.9%	87.4%	81.5%	83.5%	87.6%	83.8%	80.1%	76.3%	81.1%

Cape Town Cooling Degree Days

Cooling degree-days are defined, in Conradie et al (2015:5), as a summation of differences between outdoor air temperature and a base temperature, for each hour where the outdoor air temperature was greater than the base temperature, normalised by number of hours in a day:

$$CDD = \frac{\left(\sum_{i=1}^{24}\left(\theta_{o,i} - \theta_b\right)_{(\theta_{o,i}-\theta_b)>0}\right)}{24}$$

Where θ_b is base temperature [°C] and $\theta_{o,i}$ is hourly outdoor temperature. Table 9-4 shows a summary of the CDD calculations based on the IWEC weather dataset for Cape Town, using 18 °C as a base temperature.

Table 9-4: Cape Town Dry-Bulb Temperature Frequency and CDD analysis

Bins [°C]	Frequency	Cumm	$T_i - T_{base}$ [°C]	n_CDD (> T_{base} °C)	n_CDD/24 [hours]
0	0	0	0	0	0
1	2	2	0	0	0
2	10	12	0	0	0
3	7	19	0	0	0
4	23	42	0	0	0
5	50	92	0	0	0
6	78	170	0	0	0
7	107	277	0	0	0
8	118	395	0	0	0
9	175	570	0	0	0
10	229	799	0	0	0
11	304	1103	0	0	0
12	428	1531	0	0	0
13	530	2061	0	0	0
14	733	2794	0	0	0
15	734	3528	0	0	0
16	719	4247	0	0	0
17	715	4962	0	0	0
18	764	5726	0	0	0
19	663	6389	1	663	27.63
20	522	6911	2	1044	43.50
21	412	7323	3	1236	51.50
22	349	7672	4	1396	58.17
23	288	7960	5	1440	60.00
24	209	8169	6	1254	52.25
25	181	8350	7	1267	52.79
26	139	8489	8	1112	46.33
27	80	8569	9	720	30.00
28	86	8655	10	860	35.83
29	46	8701	11	506	21.08
30	27	8728	12	324	13.50
31	16	8744	13	208	8.67
32	9	8753	14	126	5.25
33	6	8759	15	90	3.75
34	1	8760	16	16	0.67
35	0	8760	17	0	0.00
Total =	**8760**			**3034.00**	**510.92**

Appendix C: Simulation Input Data

External Walls

External wall constructions were modelled with 3 material layers: a concrete block layer, of 290 mm thickness, with two cement plaster layers, of 13mm thickness, on each surface. The layers' thermal properties are shown in Table 9-5

Table 9-5: Material properties of external wall constructions

Thermal Property	Concrete Block	Plaster Layers
Conductivity [W / mK]	0.62	0.22
Density [kg / m^3]	1 040	1 680
Heat capacity [J / kgK]	840	1 085
Thickness [mm]	290	13

Under steady-state conditions, the combined thermal resistance (R-value) of the construction can be determined as shown in equation 2-6 above:

$$R_{total} = \sum_i R_i = \frac{d_1}{k_1} + \frac{d_2}{k_2} + \cdots$$

Where: R_{total} is overall R-value [m²K / W]; R_i is the R-value of construction element i; d is thickness of the element [m] and k is the material's thermal conductivity. Therefore:

$$R_{total} = \frac{0.013}{0.22} + \frac{0.290}{0.62} + \frac{0.013}{0.22} = 0.586\ m^2K/W$$

$$\therefore U = \frac{1}{R_{total}} = \frac{1}{0.586} = 1.707\ \ W/m^2K$$

Occupancy

Table 9-6 shows the typical maximum occupant density of each thermal zone of the ERC simulation model. Office zone occupant numbers were determined based on the maximum number of occupants of each office in the ERC, while seminar zone occupancy was estimated based on typical sizes of classes and meetings using the seminar rooms. Other zones (kitchen, staff bathroom and corridor) were assessed assuming 1 or less occupants, in order to correct the short periods over which people use these spaces.

Table 9-6: Model input occupancy density summarised

ERC Thermal Zone	Area [m²]	Typical Maximum Occupancy [people]	Maximum Occupant Density [People / m²]
North	173.05	12	0.0693
East	95.24	10	0.1050
South	65.45	6	0.0917
West	104.83	10	0.0954
Seminar	100.23	14	0.1397
Corridor	129.57	0.5	0.0039
Kitchen	12.10	1	0.0826
Staff WC	13.51	0.5	0.0370
Total =	**693.98**	**54**	**0.0778**

Occupancy schedules for each type of zone are shown in Table 9-7, and were assumed from observations of common behaviour of ERC occupants. Their actual behaviour may deviate considerably from these assumptions, and it should be noted that statistical sampling and surveying could improve the quality of this input data.

Table 9-7: Occupancy schedules assumed for typical working days at the ERC (excluding weekends and holidays)

Hour	Office zones	Seminar zone	Corridor and Staff WC	Kitchen
00:00	0%	0%	0%	0%
01:00	0%	0%	0%	0%
02:00	0%	0%	0%	0%
03:00	0%	0%	0%	0%
04:00	0%	0%	0%	0%
05:00	0%	0%	0%	0%
06:00	0%	0%	0%	0%
07:00	15%	0%	100%	20%
08:00	60%	6.7%	100%	60%
09:00	100%	100%	100%	20%
10:00	100%	100%	100%	20%
11:00	100%	100%	100%	20%
12:00	100%	6.7%	100%	100%
13:00	100%	6.7%	100%	100%
14:00	100%	50%	100%	20%
15:00	100%	50%	100%	20%
16:00	100%	0%	100%	10%
17:00	50%	0%	100%	10%
18:00	15%	0%	100%	0%
19:00	0%	0%	0%	0%
20:00	0%	0%	0%	0%
21:00	0%	0%	0%	0%
22:00	0%	0%	0%	0%
23:00	0%	0%	0%	0%

Lighting

Table 9-8 shows input lighting power density for each thermal zone, as detailed in § 3.1.6, calculated initially assuming 140 W power consumption of each fluorescent lamp with magnetic ballast fitting.

Table 9-8: Lighting power density assumptions for each thermal zone

Thermal Zone	Area [m^2]	No. light fittings	Lighting Power Rating [W]	Lighting Power Density [W / m^2]
North	173.05	14	1 960	11.3262
East	95.24	10	1 400	14.6997
South	65.45	6	840	12.8342
West	104.83	11	1 540	14.6905
Seminar	100.23	9	1 260	12.5711
Corridor	129.57	8	1 120	8.6440
Kitchen	12.10	1	140	11.5702
Staff WC	13.51	1	140	10.3627
Total	**693.98**	**60**	**8 400**	**12.1041**

Appendix D: ERC Current Simulation Output Data

Comfort and Environmental Conditions

Table 9-9 shows monthly operative temperature data calculated by the ERC *Current* simulation, as described in § 3.3.1. The 'Ave.' column shows ERC average operative temperature, calculated as the weighted average of the individual thermal zones, according to their respective floor areas described in Appendix C. Table 9-10 shows monthly relative humidity data, with average ERC humidity determined according to the same methodology (weighted by floor area).

Table 9-9: Monthly average operative temperatures and outdoor DB temperatures for Current simulation [°C]

Month	North	East	South	West	Seminar	Corridor	Kitchen	Staff WC	Ave.	Out DB
January	24.3	24.7	24.2	24.5	24.0	24.3	24.8	24.3	24.3	20.8
February	24.9	25.4	24.8	25.3	24.7	24.9	25.4	24.9	25.0	20.9
March	23.5	23.9	23.4	23.8	23.3	23.7	24.3	23.6	23.6	19.1
April	22.2	22.2	21.8	22.3	21.6	22.3	23.1	21.9	22.1	16.5
May	21.1	21.0	20.7	20.7	20.1	21.1	22.1	20.6	20.8	14.8
June	18.4	18.4	18.6	18.2	17.7	18.8	19.8	18.2	18.4	12.8
July	18.7	18.6	18.7	18.5	17.4	18.9	19.9	18.3	18.5	12.3
August	17.5	17.5	17.3	17.5	17.0	17.4	18.1	17.1	17.4	12.9
September	19.8	20.2	20.0	20.1	19.5	20.4	21.3	19.9	20.0	14.3
October	21.9	22.3	21.9	22.2	21.6	22.3	23.0	22.0	22.1	16.0
November	22.7	23.0	22.3	23.1	22.0	23.0	23.4	22.6	22.7	18.3
December	24.5	25.0	24.4	24.7	24.1	24.6	25.1	24.6	24.6	19.8

Table 9-10: Monthly average relative humidity [%] from ERC Current simulation

Month	North	East	South	West	Seminar	Corridor	Kitchen	Staff WC	Ave.
January	54.8	53.6	55.9	54.6	56.6	53.1	49.6	53.7	54.5%
February	53.7	52.1	54.6	52.7	55.0	51.7	48.0	52.1	53.1%
March	58.8	57.3	59.6	58.0	60.4	56.7	52.4	57.4	58.2%
April	57.0	56.7	57.9	56.7	59.1	55.7	51.4	57.1	57.0%
May	55.5	55.9	56.9	57.0	58.7	54.5	50.1	56.4	56.1%
June	56.5	56.0	54.9	56.9	58.2	53.8	49.6	55.9	55.9%
July	55.2	55.2	54.7	55.9	58.5	53.7	49.0	55.8	55.3%
August	60.3	60.3	60.7	60.2	62.6	59.6	55.3	61.1	60.5%
September	56.2	55.1	55.7	55.7	58.0	53.5	49.6	55.1	55.5%
October	50.6	49.5	50.5	50.3	52.3	48.6	45.8	49.5	50.2%
November	54.2	53.4	56.0	53.2	56.5	52.0	49.4	53.4	53.9%
December	52.5	50.6	53.1	52.3	53.7	50.7	47.5	50.5	52.0%

Table 9-11 shows monthly discomfort hours as predicted by the ERC *Current* simulation (Run 1-1), as referred to in § 3.3.1, and calculated according to the ASHRAE-55 (2004) thermal comfort zone. Analysis in the dissertation text focuses on the office thermal zones (North, East, South and West), since these are of greatest interest to the majority of ERC occupants.

Table 9-11: Monthly simulated discomfort hours for each thermal zone

Month	North	East	South	West	Seminar	Corridor	Kitchen	Staff WC	Proportion
January	98.0	108.0	98.0	110.0	41.0	71.0	72.5	75.5	8.6%
February	129.5	151.5	142.5	152.0	96.5	102.0	97.5	102.5	12.5%
March	79.0	98.5	85.5	105.5	64.5	54.0	52.5	50.0	7.5%
April	42.5	45.0	45.5	49.0	42.5	36.0	33.5	34.5	4.2%
May	52.5	35.5	42.5	77.5	44.0	36.0	18.5	50.5	4.6%
June	121.0	85.5	89.5	128.5	84.5	98.5	52.0	125.5	10.0%
July	122.5	118.5	114.5	129.0	83.0	116.5	77.0	160.5	11.8%
August	173.5	161.0	176.0	176.0	97.5	193.0	153.5	204.5	17.1%
September	65.5	56.5	69.5	65.5	59.0	58.0	39.5	71.0	6.2%
October	44.5	54.0	54.5	57.5	46.0	42.5	43.0	39.5	4.9%
November	38.5	63.0	43.0	48.5	13.5	21.0	34.5	20.0	3.6%
December	93.5	121.0	93.5	108.5	29.0	84.0	90.0	82.5	9.0%
Total	**1060.5**	**1098.0**	**1054.5**	**1207.5**	**701.0**	**912.5**	**764.0**	**1016.5**	**7814.5**

Annual and Summer Design Week Heat Gains

Table 9-12 shows annual heat gains for each ERC thermal zone, according to source. Negative values indicate heat loss from thermal zone to its surroundings. Table 9-13 shows internal heat gains and summarised fabric heat losses for each thermal zone, normalised by the zone floor area.

Table 9-12: Annual heat gains and losses per ERC thermal zone [MWh_{th}]

Heat Gain Source	Thermal Zone								
	North	**East**	**South**	**West**	**Seminar**	**Corridor**	**Kitchen**	**Staff WC**	**Total**
Lighting	5.15	3.66	2.19	4.02	1.21	3.28	0.14	0.34	19.99
Equipment	2.38	1.98	1.19	1.98	1.02		1.00	0.10	9.64
Occupancy	1.90	1.53	0.94	1.57	0.97	0.09	0.06	0.09	7.16
Solar Gains	6.34	4.21	0.81	4.53	3.96	0.34		0.46	20.65
Glazing	-2.23	-1.67	-0.85	-1.82	-1.30	-0.25		-0.23	-8.35
Walls	-3.52	-2.63	-1.26	-2.83	-2.15	-0.75		-0.36	-13.50
Floors	0.57	-0.02	0.57	0.09	1.28	0.81	-0.02	0.11	3.39
Ceilings	-3.06	-1.97	-0.99	-2.05	-1.21	-1.98	-0.25	-0.20	-11.71
Int. Nat. Vent.	-0.80	-0.96	-0.08	-0.96	0.03	-0.23	-0.64	-0.01	-3.65
Ext. Infilt.	-6.36	-3.71	-2.69	-4.26	-3.96	-1.89		-0.44	-23.32
Total	**0.37**	**0.42**	**-0.16**	**0.28**	**-0.14**	**-0.59**	**0.29**	**-0.14**	**0.32**

Table 9-13: Annual heat gains per thermal zone, normalised by zone floor area [kWh_{th}/m^2]

Heat Gain Source	Thermal Zone							
	North	**East**	**South**	**West**	**Seminar**	**Corridor**	**Kitchen**	**Staff WC**
Lighting	29.8	38.4	33.5	38.4	12.1	25.3	11.3	25.3
Equipment	13.7	20.8	18.2	18.9	10.2	0.0	82.4	7.2
Occupancy	11.0	16.1	14.4	15.0	9.7	0.7	5.1	6.6
Solar Gains	36.6	44.2	12.4	43.2	39.5	2.6	0.0	34.0
Fabric	-47.6	-66.0	-38.6	-63.0	-33.7	-16.8	-22.5	-49.7

Table 9-14 to Table 9-17 shows heat gain profiles for North, East, South and West facing zones, respectively, for 18 January of the Summer Design Week simulation period, from current simulation Run 1-3, for illustrative purposes (data from other days are not shown here due to space limitations). Data from Run 1-3 was used to develop Figure 3-10 through Figure 3-13 in § 0 above.

Table 9-14: Current North zone heat balance profile for 18 January [kW_{th}]

Time	Lighting	Solar Gains	Other Internal	Ceiling	Floor	Other Fabric
00:00	0.00	0.00	0.00	-0.89	3.42	0.27
01:00	0.00	0.00	0.00	-0.93	3.38	0.00
02:00	0.00	0.00	0.00	-0.96	3.23	-0.11
03:00	0.00	0.00	0.00	-0.96	3.01	-0.09
04:00	0.00	0.00	0.00	-0.87	2.80	-0.05
05:00	0.00	0.00	0.00	-0.87	2.92	-0.31
06:00	0.00	0.09	0.00	-0.89	3.24	-0.08
07:00	0.00	0.60	0.00	-0.79	2.27	-0.13
08:00	0.80	1.92	0.73	-0.64	0.18	-0.51
09:00	1.79	2.24	1.28	-0.31	-1.26	-0.85
10:00	1.99	1.68	1.80	0.07	-1.47	-0.97
11:00	1.99	1.46	1.77	0.41	-1.62	-1.00
12:00	1.99	1.45	1.74	0.65	-1.90	-1.08
13:00	1.99	1.46	1.74	0.71	-1.87	-1.05
14:00	1.99	1.46	1.73	0.68	-1.82	-1.04
15:00	1.99	1.41	1.74	0.61	-1.64	-0.96
16:00	1.99	1.35	1.73	0.49	-1.54	-0.91
17:00	1.99	1.13	1.75	0.24	-1.03	-0.85
18:00	1.59	0.81	1.16	-0.03	0.02	-0.51
19:00	1.19	0.39	0.72	-0.24	0.60	-0.49
20:00	0.00	0.04	0.00	-0.46	2.09	-0.13
21:00	0.00	0.00	0.00	-0.64	2.36	-0.08
22:00	0.00	0.00	0.00	-0.69	2.55	-0.08
23:00	0.00	0.00	0.00	-0.72	2.64	-0.06

Table 9-15: Current East zone heat balance profile for 18 January [kW_{th}]

Time	Lighting	Solar Gains	Other Internal	Ceiling	Floor	Other Fabric
00:00	0.00	0.00	0.00	-0.55	2.30	0.31
01:00	0.00	0.00	0.00	-0.56	2.23	0.11
02:00	0.00	0.00	0.00	-0.58	2.08	0.01
03:00	0.00	0.00	0.00	-0.55	2.11	0.09
04:00	0.00	0.00	0.00	-0.50	1.93	0.09
05:00	0.00	0.00	0.00	-0.51	1.92	-0.11
06:00	0.00	0.15	0.00	-0.52	2.07	0.04
07:00	0.00	1.02	0.00	-0.48	1.16	-0.01
08:00	0.57	3.36	0.61	-0.48	-1.14	-0.35
09:00	1.27	3.48	1.06	-0.31	-2.02	-0.65
10:00	1.41	1.72	1.48	-0.05	-1.27	-0.74
11:00	1.41	0.98	1.45	0.17	-1.02	-0.75
12:00	1.41	0.97	1.42	0.31	-1.22	-0.78
13:00	1.41	0.98	1.42	0.34	-1.20	-0.76
14:00	1.41	0.98	1.42	0.33	-1.15	-0.74
15:00	1.41	0.95	1.42	0.28	-1.05	-0.68
16:00	1.41	0.91	1.42	0.21	-1.00	-0.65
17:00	1.41	0.77	1.43	0.07	-0.68	-0.62
18:00	1.13	0.55	0.96	-0.08	0.00	-0.37
19:00	0.85	0.27	0.60	-0.20	0.38	-0.35
20:00	0.00	0.03	0.00	-0.31	1.40	-0.06
21:00	0.00	0.00	0.00	-0.40	1.62	0.00
22:00	0.00	0.00	0.00	-0.41	1.83	0.05
23:00	0.00	0.00	0.00	-0.41	1.95	0.09

Table 9-16: Current South zone heat balance profile for 18 January [kW_{th}]

Time	Lighting	Solar Gains	Other Internal	Ceiling	Floor	Other Fabric
00:00	0.00	0.00	0.00	-0.32	1.50	0.11
01:00	0.00	0.00	0.00	-0.33	1.48	0.04
02:00	0.00	0.00	0.00	-0.34	1.40	0.00
03:00	0.00	0.00	0.00	-0.34	1.26	-0.01
04:00	0.00	0.00	0.00	-0.31	1.18	0.00
05:00	0.00	0.00	0.00	-0.31	1.24	-0.06
06:00	0.00	0.01	0.00	-0.31	1.37	0.00
07:00	0.00	0.05	0.00	-0.26	1.04	-0.02
08:00	0.34	0.14	0.37	-0.17	0.46	-0.13
09:00	0.76	0.22	0.65	-0.05	-0.19	-0.24
10:00	0.85	0.29	0.90	0.08	-0.55	-0.29
11:00	0.85	0.34	0.88	0.19	-0.73	-0.31
12:00	0.85	0.37	0.87	0.28	-0.86	-0.34
13:00	0.85	0.39	0.86	0.30	-0.86	-0.34
14:00	0.85	0.38	0.86	0.28	-0.84	-0.34
15:00	0.85	0.35	0.86	0.25	-0.76	-0.32
16:00	0.85	0.31	0.85	0.20	-0.69	-0.31
17:00	0.85	0.24	0.86	0.11	-0.48	-0.30
18:00	0.68	0.16	0.58	0.00	-0.04	-0.18
19:00	0.51	0.07	0.36	-0.09	0.19	-0.18
20:00	0.00	0.01	0.00	-0.17	0.84	-0.05
21:00	0.00	0.00	0.00	-0.23	0.98	-0.02
22:00	0.00	0.00	0.00	-0.25	1.04	-0.02
23:00	0.00	0.00	0.00	-0.27	1.07	-0.02

Table 9-17: Current West zone heat balance profile for 18 January [kW_{th}]

Time	Lighting	Solar Gains	Other Internal	Ceiling	Floor	Other Fabric
00:00	0.00	0.00	0.00	-0.66	2.13	0.10
01:00	0.00	0.00	0.00	-0.68	2.13	-0.10
02:00	0.00	0.00	0.00	-0.70	2.01	-0.18
03:00	0.00	0.00	0.00	-0.69	1.90	-0.13
04:00	0.00	0.00	0.00	-0.63	1.76	-0.08
05:00	0.00	0.00	0.00	-0.64	1.81	-0.32
06:00	0.00	0.02	0.00	-0.64	2.05	-0.12
07:00	0.00	0.13	0.00	-0.55	1.63	-0.11
08:00	0.62	0.35	0.61	-0.40	0.67	-0.36
09:00	1.40	0.55	1.06	-0.18	-0.28	-0.59
10:00	1.55	0.70	1.49	0.04	-0.76	-0.68
11:00	1.55	0.82	1.47	0.25	-1.01	-0.71
12:00	1.55	0.91	1.45	0.40	-1.21	-0.77
13:00	1.55	0.95	1.45	0.44	-1.19	-0.75
14:00	1.55	0.93	1.45	0.42	-1.15	-0.75
15:00	1.55	0.86	1.45	0.37	-1.01	-0.69
16:00	1.55	1.21	1.45	0.29	-1.21	-0.64
17:00	1.55	3.09	1.45	0.01	-2.26	-0.62
18:00	1.24	3.71	0.96	-0.25	-2.08	-0.37
19:00	0.93	1.75	0.59	-0.33	-0.45	-0.41
20:00	0.00	0.02	0.00	-0.39	1.51	-0.13
21:00	0.00	0.00	0.00	-0.50	1.63	-0.07
22:00	0.00	0.00	0.00	-0.52	1.74	-0.04
23:00	0.00	0.00	0.00	-0.54	1.77	-0.03

Validation Data

Table 9-18 shows the sample of air temperature data collected from the four ERC office thermal zones, compared with simulation results for corresponding time periods of the whole year *Current* simulation. The data is summarised into correlation coefficients which range between 0.50 and 0.75, as shown and discussed in § 3.3.3 above.

Table 9-18: Measured and simulated air temperature [°C] data for Current simulation

Air Temperature Comparison											
Date	**Time**	**Outdoor**		**North**		**East**		**West**		**South**	
		Actual	**Sim**	**Actual**	**Sim**	**Actual**	**Sim**	**Actual**	**Sim**	**Actual**	**Sim**
2015/03/31	09:00	22.4	18.7	26.8	24.7	26.5	24.1	26.5	23.4	26.1	23.1
2015/03/31	10:00	24.4	21.7	28.8	26.2	28.1	25.0	27.8	24.7	27.2	24.3
2015/03/31	11:00	25.4	24.3	28.6	27.5	28.4	25.7	27.9	25.3	28	25.2
2015/03/31	12:00	24.8	25.3	28.4	28.4	28.3	26.4	28.3	25.9	28.1	26.0
2015/03/31	13:00	24.9	26.4	29.4	28.4	28.7	27.1	29.6	26.6	28.6	27.0
2015/03/31	14:00	26.8	26.9	31	28.6	29.3	27.4	30.1	27.5	29.7	27.6
2015/03/31	15:00	27.6	25.8	30.9	28.5	29.8	27.1	30.5	27.5	30.1	27.4
2015/03/31	16:00	27.2	24.8	30.3	28.1	29.4	26.6	30.6	27.5	30	26.8
2015/04/01	09:00	19.8	19.9	23.2	24.7	22.5	25.6	22.6	24.9	21.7	24.6
2015/04/01	10:00	21.3	22.3	25.7	26.2	24.2	26.4	24.4	26.0	22.3	25.7
2015/04/01	11:00	23.1	24.2	26.4	27.5	25.2	26.7	25.8	26.9	24.8	26.5
2015/04/01	12:00	24.0	24.7	26.7	28.4	26	26.8	26.1	27.1	25.5	26.9
2015/04/01	13:00	24.8	25.1	27.5	28.4	26.6	26.7	26.2	27.2	26.1	27.1
2015/04/01	14:00	24.4	25.2	28.6	28.6	26.7	26.5	26.9	27.1	26.6	26.9
2015/04/01	15:00	23.9	24.0	27.9	28.5	26.5	26.1	27.2	26.9	26.2	26.5
2015/04/01	16:00	22.3	22.9	27	28.1	26.4	25.9	27	26.9	25.9	26.0
2015/04/02	09:00	21.4	19.9	24.9	24.7	26.6	25.2	25.2	24.5	25.7	24.3
2015/04/02	10:00	24.4	22.3	26.6	26.2	27.4	26.4	26.8	26.1	26.5	25.8
2015/04/02	11:00	28.1	24.2	28.3	27.5	28.3	27.6	27.2	27.4	28.1	27.1
2015/04/02	12:00	30.4	24.7	30	28.4	28.6	28.3	28.8	28.2	28.9	28.0
2015/04/02	13:00	31.2	25.1	30.3	28.4	29.9	28.6	28.9	28.3	29.8	28.1
2015/04/02	14:00	30.9	25.2	31.3	28.6	30.2	28.8	29.6	28.3	30.2	28.8
2015/04/02	15:00	30.5	24.0	30.9	28.5	30.1	28.7	29.8	28.4	30.4	28.6
2015/04/02	16:00	29.8	22.9	30.6	28.1	29.8	28.3	31	28.5	30.2	28.3

Appendix E: ERC Base Case Simulation Output Data

Comfort and Environmental Conditions

Table 9-19 shows monthly operative temperature data calculated by the ERC base cooling simulation, as described in § 3.4.1. The 'Ave.' column shows ERC average operative temperature, calculated as the weighted average of the individual thermal zones, according to their respective floor areas described in Appendix C. Table 9-20 shows monthly relative humidity data, with average ERC humidity determined according to the same methodology (weighted by floor area).

Table 9-19: Monthly average operative and outdoor DB temperatures for Base Case [°C]

Month	North	East	South	West	Seminar	Corridor	Kitchen	Staff WC	Ave.	Out DB
January	23.3	23.5	23.2	23.5	23.5	23.5	24.0	23.5	23.4	20.8
February	23.5	23.7	23.4	23.7	23.7	23.7	24.3	23.8	23.7	20.9
March	22.7	22.9	22.6	22.8	22.7	23.0	23.6	22.9	22.8	19.1
April	21.7	21.7	21.4	21.8	21.4	21.9	22.6	21.5	21.7	16.5
May	20.8	20.7	20.6	20.5	20.0	21.0	21.9	20.5	20.6	14.8
June	18.4	18.4	18.6	18.2	17.6	18.8	19.8	18.2	18.4	12.8
July	18.6	18.6	18.7	18.4	17.4	18.9	19.9	18.2	18.5	12.3
August	17.5	17.4	17.3	17.5	17.0	17.4	18.1	17.1	17.4	12.9
September	19.8	20.1	19.9	20.0	19.4	20.3	21.2	19.9	19.9	14.3
October	21.4	21.7	21.4	21.6	21.2	21.8	22.4	21.6	21.6	16.0
November	22.1	22.2	21.8	22.4	21.8	22.5	22.9	22.2	22.2	18.3
December	23.4	23.7	23.3	23.6	23.7	23.7	24.2	23.7	23.6	19.8

Table 9-20: Monthly average relative humidity [%] for Base Case

Month	North	East	South	West	Seminar	Corridor	Kitchen	Staff WC	Ave.
January	56.5	55.9	57.6	56.5	57.2	54.6	50.8	55.1	56.1%
February	56.3	55.3	56.9	55.6	56.8	54.4	50.2	54.4	55.7%
March	59.7	58.7	60.4	59.2	60.8	57.8	53.0	58.2	59.2%
April	57.4	57.3	58.1	57.2	58.8	56.2	51.3	57.1	57.3%
May	55.6	56.0	56.8	56.9	58.4	54.6	50.3	56.2	56.1%
June	56.2	55.8	54.7	56.5	57.8	53.6	49.1	55.6	55.7%
July	54.8	55.0	54.5	55.5	58.2	53.3	48.6	55.3	55.0%
August	60.0	60.1	60.4	60.0	62.4	59.3	54.4	60.7	60.2%
September	56.1	55.1	55.7	55.6	57.7	53.5	49.7	55.1	55.5%
October	51.4	50.7	51.3	51.3	52.6	49.6	46.9	50.2	51.0%
November	55.3	54.9	56.8	54.6	57.0	53.1	50.4	54.3	55.0%
December	54.5	53.0	55.0	54.5	54.5	52.7	49.2	52.3	53.9%

Table 9-21 shows monthly discomfort hours as predicted by the ERC base cooling simulation (Run 2-1), as referred to in § 3.4.1, and calculated according to the ASHRAE-55 (2004) thermal comfort zone. Analysis in the dissertation text focuses on the office thermal zones (North, East, South and West), since these are of greatest interest to the majority of ERC occupants.

Table 9-21: Monthly simulated discomfort hours for each thermal zone, for Base Case simulation

Month	North	East	South	West	Seminar	Corridor	Kitchen	Staff WC	Proportion
January	0.0	0.0	0.0	0.0	0.0	0.0	0.0	0.0	0.0%
February	0.0	0.0	0.0	0.0	0.0	0.0	0.0	0.0	0.0%
March	0.0	0.0	0.0	0.0	0.5	0.0	0.0	0.0	0.0%
April	9.0	7.5	13.0	8.5	15.5	8.5	3.5	14.5	2.0%
May	44.0	31.5	36.5	64.5	41.0	33.0	10.5	51.0	7.6%
June	121.5	87.5	89.5	129.5	83.0	100.0	52.0	126.0	19.3%
July	124.0	114.0	108.5	128.0	82.0	115.0	76.0	158.5	22.2%
August	174.0	165.0	179.5	176.0	97.5	193.5	154.5	205.0	32.9%
September	67.5	57.5	69.0	66.0	53.5	60.0	38.5	71.5	11.8%
October	17.0	14.5	26.0	17.0	13.5	18.5	7.5	23.0	3.4%
November	4.0	3.0	8.5	2.0	5.5	1.5	1.0	3.5	0.7%
December	0.0	0.0	1.0	0.0	0.0	0.0	0.0	0.0	0.0%
Total	**561.0**	**480.5**	**531.5**	**591.5**	**392.0**	**530.0**	**343.5**	**653.0**	**4083.0**

Annual and Summer Design Week Heat Gains

Table 9-22 shows disaggregated annual heat gains and losses by source for each ERC thermal zone, with Ideal Loads cooling applied to the simulation (Run 2-2). Table 9-23 shows internal heat gains, summarised fabric heat losses and cooling requirements for each thermal zone, normalised by the zone floor area. Data from these tables informed Figure 3-16 and Figure 3-17 in § 3.4.2.

Table 9-22: Annual heat gains and losses per ERC thermal zone [MWh_{th}], under the Base Case

Heat Source	Thermal Zone								
	North	East	South	West	Seminar	Corridor	Kitchen	Staff WC	Total
Lighting	5.15	3.66	2.19	4.02	1.21	3.28	0.14	0.34	19.99
Equipment	2.38	1.98	1.19	1.98	1.02		1.00	0.10	9.64
Occupancy	2.14	1.77	1.06	1.79	1.05	0.10	0.07	0.10	8.08
Solar Gains	6.34	4.21	0.81	4.53	3.96	0.34		0.46	20.65
Glazing	-1.86	-1.37	-0.74	-1.50	-1.16	-0.23		-0.20	-7.06
Walls	-3.16	-2.33	-1.15	-2.53	-2.01	-0.69		-0.33	-12.20
Floors	1.66	0.74	0.97	0.88	1.63	1.52	0.05	0.18	7.62
Ceilings	-2.49	-1.57	-0.78	-1.64	-1.07	-1.60	-0.22	-0.17	-9.53
Int. Nat. Vent.	0.39	0.18	0.27	0.04	0.11	1.79	-0.50	0.06	2.34
Ext. Infil.	-5.31	-3.01	-2.15	-3.36	-3.48	-1.59		-0.39	-19.29
Sensible Cooling	-4.91	-4.00	-1.83	-4.11	-1.31	-3.30	-0.25	-0.32	-20.03
Total Cooling	**-6.69**	**-5.19**	**-2.55**	**-5.59**	**-1.98**	**-4.83**	**-0.38**	**-0.42**	**-27.64**

Table 9-23: Annual heat gains and cooling energy per thermal zone, normalised by zone floor area [kWh_{th}/m^2]

Internal Gain	North	East	South	West	Seminar	Corridor	Kitchen	Staff WC
Lighting	29.8	38.4	33.5	38.4	12.1	25.3	11.3	25.3
Equipment	13.7	20.8	18.2	18.9	10.2	0.0	82.4	7.2
Occupancy	12.4	18.6	16.2	17.1	10.5	0.7	5.9	7.1
Solar Gains	36.6	44.2	12.4	43.2	39.5	2.6	0.0	34.0
Fabric	-33.9	-47.6	-26.2	-45.6	-26.0	-7.7	-13.8	-37.8
Total Cooling	-38.7	-54.4	-39.0	-53.3	-19.8	-37.3	0.0	-31.3

Cooling Requirements

EnergyPlus simulations determine sensible cooling requirements, which respond to heat transfer acting upon the building and regulate air temperature, as well as latent cooling requirements. The latter was assessed in the simulation of the ERC with an ideal 'humidistat', which maintained relative humidity in thermal zones between 30% and 60%. Table 9-24 and Table 9-25 show simulated base case sensible and latent cooling for ERC thermal zones, disaggregated by month.

Table 9-24: Monthly Base Case sensible cooling requirements [MWh_{th}] for ERC thermal zones

Month	North	East	South	West	Seminar	Corridor	Kitchen	Staff WC
Jan	0.90	0.74	0.36	0.74	0.20	0.55	0.03	0.06
Feb	1.05	0.85	0.41	0.87	0.44	0.75	0.04	0.08
Mar	0.61	0.52	0.24	0.55	0.22	0.41	0.03	0.04
Apr	0.35	0.27	0.12	0.28	0.05	0.21	0.02	0.02
May	0.22	0.10	0.04	0.14	0.02	0.08	0.02	0.00
Jun	0.01	0.00	0.00	0.01	0.00	0.00	0.00	0.00
Jul	0.03	0.01	0.00	0.02	0.00	0.00	0.00	0.00
Aug	0.01	0.00	0.00	0.01	0.00	0.00	0.00	0.00
Sep	0.03	0.04	0.01	0.04	0.01	0.01	0.01	0.00
Oct	0.34	0.32	0.13	0.33	0.17	0.27	0.03	0.02
Nov	0.51	0.46	0.19	0.46	0.08	0.33	0.03	0.03
Dec	0.85	0.68	0.33	0.66	0.11	0.68	0.03	0.06

Table 9-25: Monthly Base Case latent cooling requirements [MWh_{th}] for ERC thermal zones

Month	North	East	South	West	Seminar	Corridor	Kitchen	Staff WC
Jan	0.30	0.21	0.13	0.24	0.09	0.23	0.01	0.02
Feb	0.32	0.23	0.15	0.26	0.15	0.28	0.01	0.02
Mar	0.30	0.21	0.13	0.25	0.13	0.23	0.02	0.02
Apr	0.12	0.09	0.05	0.10	0.03	0.11	0.01	0.01
May	0.11	0.05	0.03	0.11	0.05	0.09	0.01	0.01
Jun	0.10	0.02	0.01	0.07	0.05	0.05	0.02	0.00
Jul	0.05	0.02	0.01	0.04	0.02	0.04	0.02	0.00
Aug	0.06	0.02	0.02	0.04	0.01	0.06	0.01	0.01
Sep	0.03	0.02	0.01	0.03	0.02	0.02	0.00	0.00
Oct	0.07	0.06	0.03	0.07	0.05	0.08	0.00	0.00
Nov	0.16	0.13	0.09	0.15	0.03	0.13	0.01	0.01
Dec	0.18	0.13	0.08	0.15	0.03	0.22	0.01	0.01

Table 9-26: Total monthly ERC Base Case cooling (sensible + latent) normalised by floor area [kWh_{th}/m^2]

Month	North	East	South	West	Seminar	Corridor	Kitchen	Staff WC
Jan	6.92	9.96	7.63	9.35	2.85	6.01	3.58	5.84
Feb	7.90	11.34	8.46	10.77	5.94	7.95	4.01	7.10
Mar	5.27	7.64	5.63	7.64	3.53	4.91	3.95	4.26
Apr	2.68	3.79	2.56	3.60	0.88	2.47	3.07	1.67
May	1.94	1.56	1.04	2.31	0.72	1.29	1.89	0.76
Jun	0.63	0.28	0.18	0.69	0.46	0.40	1.77	0.32
Jul	0.48	0.29	0.21	0.54	0.20	0.33	1.75	0.27
Aug	0.39	0.26	0.23	0.45	0.16	0.46	1.19	0.38
Sep	0.34	0.62	0.26	0.62	0.30	0.24	1.36	0.11
Oct	2.34	3.99	2.45	3.81	2.16	2.74	2.58	1.86
Nov	3.83	6.18	4.19	5.79	1.17	3.52	3.03	3.27
Dec	5.96	8.54	6.19	7.71	1.42	6.96	3.30	5.52

Table 9-27 shows the heat balance profile simulated for 15 January during the Summer Design Week, as included in Figure 3-19 in § 3.4.2 (other days during the week are not shown due to space constraints).

Table 9-27: Base Case heat balance profile [kW_{th}] for 15 Jan during Summer Design Week

Hour	Ceilings	Glazing	Walls	Floors	Lighting	Equip.	Occup.	Solar Gains	Total Cooling
00:00	-2.8	-1.2	1.2	5.6	0.0	0.1	0.0	0.0	0.0
01:00	-3.1	-1.2	1.3	6.2	0.0	0.1	0.0	0.0	0.0
02:00	-3.3	-1.1	1.2	6.1	0.0	0.1	0.0	0.0	0.0
03:00	-3.2	-0.9	1.0	5.7	0.0	0.1	0.0	0.0	0.0
04:00	-3.2	-0.8	0.7	5.0	0.0	0.1	0.0	0.0	0.0
05:00	-3.4	-1.0	0.5	4.8	0.0	0.1	0.0	0.0	0.0
06:00	-3.6	-0.9	0.4	4.8	0.0	0.1	0.0	0.4	0.0
07:00	-3.5	0.0	0.0	2.8	0.0	0.1	0.0	2.2	0.0
08:00	-2.0	1.2	-1.6	-4.3	3.5	2.0	0.5	6.6	-6.1
09:00	2.4	2.1	-2.8	-8.5	6.5	2.6	1.8	7.5	-18.8
10:00	8.4	2.3	-3.0	-8.3	7.1	3.0	3.0	5.5	-41.4
11:00	14.8	2.8	-3.1	-8.6	7.1	3.0	3.1	4.9	-55.6
12:00	18.1	2.6	-2.9	-8.4	7.1	3.0	3.2	5.3	-49.3
13:00	17.3	2.9	-2.5	-7.3	7.2	3.4	3.3	5.1	-50.8
14:00	19.0	3.2	-2.3	-7.3	7.2	3.4	3.3	5.1	-63.4
15:00	20.3	3.5	-1.9	-6.6	7.1	3.0	3.3	4.7	-60.4
16:00	18.4	3.4	-1.4	-6.1	7.1	3.0	3.3	4.9	-66.9
17:00	16.3	3.5	-1.0	-6.4	7.1	3.0	3.3	7.0	-59.9
18:00	11.4	2.6	-0.2	-5.0	5.9	2.4	1.6	7.2	-34.2
19:00	6.1	1.4	0.7	-1.6	4.7	2.0	0.5	3.7	-25.5
20:00	2.3	0.0	1.1	1.1	0.0	0.1	0.0	0.1	0.0
21:00	-0.5	-0.8	1.0	0.0	0.0	0.1	0.0	0.0	0.0
22:00	-2.3	-1.1	1.5	1.4	0.0	0.1	0.0	0.0	0.0
23:00	-3.4	-0.8	1.8	2.6	0.0	0.1	0.0	0.0	0.0

Electricity Consumption

Table 9-28 shows predicted electricity consumption according to end uses that impact on the thermal environment of the ERC thermal zones, based on ideal loads assumptions and calculated from equation 3-3, as described in § 3.4.2.

Table 9-28: Estimated annual electricity consumption [MWh] for Base Case simulation

Thermal Zone	Equipment	Lights	Cooling
North	2.38	5.15	2.23
East	1.98	3.66	1.73
South	1.19	2.19	0.85
West	1.98	4.03	1.86
Seminar	1.02	1.21	0.66
Corridor	0.00	3.28	1.61
Kitchen	1.00	0.14	0.13
Staff WC	0.10	0.34	0.14
Total	**9.64**	**19.99**	**9.21**

Appendix F: ERC Cooling-Insulation Simulation Output Data

Operative Temperature Profiles

Table 9-29 through Table 9-33 show average daily temperature profiles, calculated from Summer Design Week simulations of varying insulation thicknesses (simulations Run 3-1 through 3-4).

Table 9-29: Average operative temperature profile [°C] during Summer Design Week per thermal zone, with no insulation

Hour	North	East	South	West	Seminar	Corridor	Kitchen	Staff WC
00:00	23.18	23.52	22.79	22.91	22.99	23.23	23.87	23.34
01:00	23.13	23.49	22.70	22.85	22.94	23.18	23.85	23.32
02:00	23.00	23.35	22.56	22.71	22.80	23.10	23.79	23.21
03:00	22.77	23.07	22.30	22.55	22.56	23.00	23.72	22.99
04:00	22.61	22.90	22.11	22.37	22.36	22.90	23.62	22.85
05:00	22.58	22.89	22.07	22.20	22.25	22.80	23.55	22.83
06:00	22.54	22.90	22.00	22.09	22.16	22.74	23.50	22.79
07:00	22.78	23.34	22.24	22.27	22.39	22.78	23.52	23.07
08:00	24.16	25.45	23.58	23.67	23.06	23.81	24.11	24.58
09:00	25.71	27.13	25.15	25.22	24.06	25.08	25.92	25.93
10:00	26.81	27.84	26.43	26.45	25.04	26.17	26.56	26.73
11:00	27.71	28.46	27.48	27.46	26.44	27.15	27.42	27.42
12:00	28.57	29.21	28.45	28.26	27.43	28.07	28.23	28.18
13:00	28.60	29.21	28.74	28.25	27.39	28.10	29.46	28.22
14:00	27.87	28.60	28.17	27.53	26.78	27.26	28.89	27.63
15:00	27.51	28.22	27.92	27.12	26.82	26.71	27.27	27.14
16:00	27.26	28.05	27.70	26.92	26.69	26.31	26.55	26.87
17:00	27.29	28.03	27.77	27.43	26.54	26.33	26.37	26.78
18:00	27.01	27.67	27.37	27.66	26.54	26.40	26.34	26.48
19:00	26.21	26.84	26.36	26.89	25.87	25.89	25.89	25.92
20:00	25.23	25.77	25.21	25.61	25.01	25.28	25.48	25.22
21:00	24.89	25.38	24.84	25.22	24.73	24.91	25.24	24.89
22:00	24.77	25.22	24.73	25.08	24.64	24.74	25.15	24.76
23:00	24.50	24.93	24.40	24.67	24.29	24.49	24.94	24.52

Table 9-30: Average zonal operative temperature profile [°C] during Summer Design Week, with 40 mm PF insulation

Hour	North	East	South	West	Seminar	Corridor	Kitchen	Staff WC
00:00	23.23	23.58	22.79	22.94	23.02	23.27	23.91	23.38
01:00	23.20	23.58	22.73	22.90	23.00	23.25	23.93	23.38
02:00	23.10	23.47	22.62	22.79	22.88	23.20	23.90	23.30
03:00	22.88	23.21	22.37	22.64	22.65	23.12	23.84	23.09
04:00	22.74	23.05	22.20	22.48	22.47	23.03	23.77	22.97
05:00	22.71	23.04	22.17	22.32	22.37	22.94	23.70	22.95
06:00	22.68	23.06	22.12	22.21	22.29	22.89	23.66	22.93
07:00	22.94	23.52	22.36	22.40	22.53	22.94	23.69	23.22
08:00	24.31	25.65	23.69	23.75	23.16	23.93	24.25	24.73
09:00	25.66	27.19	25.05	25.13	23.94	25.03	25.90	25.93
10:00	26.50	27.65	26.10	26.15	24.66	25.88	26.27	26.50
11:00	27.17	28.05	26.93	26.96	25.81	26.61	26.84	26.94
12:00	27.85	28.63	27.72	27.59	26.65	27.32	27.43	27.53
13:00	27.91	28.64	28.03	27.60	26.62	27.39	28.73	27.60
14:00	27.32	28.15	27.61	27.00	26.15	26.66	28.30	27.13
15:00	27.09	27.87	27.47	26.70	26.33	26.23	26.74	26.73
16:00	26.91	27.77	27.33	26.56	26.28	25.91	26.09	26.53
17:00	26.99	27.80	27.45	27.15	26.17	26.00	25.97	26.48
18:00	26.75	27.47	27.09	27.44	26.21	26.12	26.00	26.22
19:00	26.02	26.71	26.14	26.75	25.62	25.70	25.63	25.73
20:00	25.12	25.71	25.06	25.52	24.84	25.16	25.32	25.10
21:00	24.84	25.37	24.75	25.18	24.62	24.84	25.15	24.83
22:00	24.76	25.24	24.69	25.07	24.57	24.72	25.11	24.74
23:00	24.52	24.98	24.39	24.69	24.25	24.51	24.95	24.53

Table 9-31: Average zonal operative temperature profile [°C] during Summer Design Week, with 75 mm PF insulation

Hour	North	East	South	West	Seminar	Corridor	Kitchen	Staff WC
00:00	23.24	23.60	22.78	22.94	23.02	23.28	23.92	23.38
01:00	23.22	23.61	22.73	22.91	23.01	23.27	23.95	23.40
02:00	23.13	23.50	22.63	22.80	22.90	23.23	23.93	23.32
03:00	22.91	23.24	22.39	22.66	22.67	23.15	23.88	23.12
04:00	22.77	23.09	22.22	22.51	22.49	23.07	23.81	23.00
05:00	22.75	23.08	22.19	22.35	22.40	22.98	23.74	22.99
06:00	22.72	23.11	22.14	22.25	22.32	22.93	23.70	22.97
07:00	22.98	23.58	22.39	22.44	22.57	22.99	23.74	23.26
08:00	24.33	25.70	23.70	23.77	23.16	23.99	24.29	24.77
09:00	25.63	27.20	25.00	25.09	23.88	25.00	25.88	25.92
10:00	26.36	27.57	25.96	26.03	24.49	25.73	26.13	26.39
11:00	26.98	27.90	26.73	26.78	25.63	26.39	26.63	26.76
12:00	27.60	28.42	27.48	27.35	26.40	27.01	27.12	27.27
13:00	27.67	28.43	27.80	27.35	26.36	27.07	28.45	27.33
14:00	27.15	28.00	27.42	26.81	25.95	26.41	28.09	26.91
15:00	26.94	27.74	27.31	26.54	26.16	26.03	26.56	26.55
16:00	26.79	27.67	27.20	26.43	26.14	25.75	25.93	26.39
17:00	26.89	27.71	27.34	27.05	26.05	25.86	25.82	26.36
18:00	26.66	27.40	27.00	27.36	26.10	26.00	25.87	26.10
19:00	25.96	26.66	26.07	26.69	25.53	25.61	25.54	25.64
20:00	25.08	25.68	25.01	25.48	24.78	25.10	25.26	25.04
21:00	24.81	25.36	24.72	25.16	24.57	24.81	25.12	24.80
22:00	24.74	25.24	24.66	25.06	24.54	24.70	25.09	24.71
23:00	24.52	24.99	24.37	24.69	24.23	24.50	24.94	24.52

Table 9-32: Average zonal operative temperature profile [°C] during Summer Design Week, with 100 mm PF insulation

Hour	North	East	South	West	Seminar	Corridor	Kitchen	Staff WC
00:00	23.25	23.61	22.78	22.94	23.03	23.29	23.93	23.39
01:00	23.23	23.62	22.74	22.92	23.02	23.28	23.96	23.41
02:00	23.15	23.52	22.64	22.82	22.92	23.24	23.95	23.34
03:00	22.93	23.27	22.40	22.67	22.69	23.17	23.90	23.14
04:00	22.80	23.12	22.24	22.52	22.51	23.09	23.83	23.02
05:00	22.77	23.11	22.21	22.37	22.42	23.01	23.76	23.01
06:00	22.75	23.13	22.16	22.27	22.34	22.95	23.73	22.99
07:00	23.01	23.60	22.41	22.46	22.59	23.02	23.77	23.29
08:00	24.35	25.72	23.71	23.78	23.17	24.01	24.31	24.79
09:00	25.61	27.21	24.98	25.07	23.86	24.99	25.87	25.92
10:00	26.32	27.55	25.91	25.98	24.45	25.69	26.11	26.36
11:00	26.88	27.83	26.64	26.69	25.49	26.29	26.53	26.68
12:00	27.48	28.32	27.35	27.24	26.27	26.89	27.01	27.17
13:00	27.56	28.34	27.69	27.25	26.25	26.95	28.33	27.23
14:00	27.06	27.93	27.34	26.73	25.86	26.31	27.99	26.83
15:00	26.87	27.69	27.24	26.48	26.08	25.96	26.48	26.49
16:00	26.73	27.63	27.14	26.38	26.08	25.68	25.86	26.33
17:00	26.84	27.68	27.29	27.00	25.99	25.81	25.76	26.31
18:00	26.62	27.37	26.95	27.32	26.05	25.96	25.82	26.06
19:00	25.93	26.64	26.03	26.67	25.49	25.58	25.49	25.61
20:00	25.06	25.67	24.99	25.47	24.75	25.08	25.23	25.03
21:00	24.81	25.36	24.70	25.15	24.56	24.80	25.10	24.79
22:00	24.74	25.25	24.65	25.06	24.52	24.70	25.08	24.71
23:00	24.52	25.00	24.37	24.69	24.23	24.50	24.94	24.52

Table 9-33: Average zonal operative temperature profile [°C] during Summer Design Week, with 135 mm PF insulation

Hour	North	East	South	West	Seminar	Corridor	Kitchen	Staff WC
00:00	23.25	23.62	22.78	22.95	23.03	23.30	23.94	23.40
01:00	23.24	23.64	22.75	22.93	23.03	23.30	23.98	23.42
02:00	23.16	23.54	22.65	22.83	22.93	23.26	23.97	23.35
03:00	22.95	23.29	22.41	22.69	22.71	23.19	23.92	23.15
04:00	22.82	23.14	22.26	22.54	22.53	23.11	23.85	23.04
05:00	22.79	23.13	22.23	22.39	22.44	23.03	23.79	23.03
06:00	22.77	23.16	22.18	22.29	22.36	22.98	23.75	23.01
07:00	23.04	23.63	22.43	22.48	22.62	23.04	23.80	23.31
08:00	24.36	25.74	23.72	23.79	23.18	24.03	24.33	24.81
09:00	25.60	27.20	24.96	25.05	23.84	24.98	25.86	25.91
10:00	26.27	27.51	25.85	25.93	24.39	25.64	26.06	26.32
11:00	26.79	27.76	26.54	26.61	25.41	26.21	26.43	26.60
12:00	27.36	28.23	27.23	27.14	26.15	26.77	26.87	27.07
13:00	27.44	28.24	27.58	27.15	26.12	26.85	28.21	27.13
14:00	26.97	27.86	27.25	26.65	25.77	26.22	27.90	26.75
15:00	26.81	27.64	27.18	26.42	26.01	25.89	26.40	26.43
16:00	26.68	27.59	27.08	26.33	26.02	25.63	25.79	26.28
17:00	26.80	27.64	27.25	26.96	25.94	25.76	25.71	26.27
18:00	26.58	27.34	26.91	27.29	26.01	25.92	25.77	26.02
19:00	25.90	26.62	26.00	26.65	25.46	25.55	25.46	25.58
20:00	25.05	25.67	24.97	25.46	24.73	25.07	25.21	25.01
21:00	24.80	25.36	24.69	25.15	24.54	24.79	25.09	24.78
22:00	24.74	25.25	24.65	25.06	24.51	24.70	25.08	24.71
23:00	24.53	25.01	24.37	24.70	24.22	24.51	24.94	24.52

Heat Gain and Cooling Profiles

Annual heat gains for the *75 mm-Insulation* simulation run (ERC Cooling with 75 mm PF ceiling insulation for all thermal zones) are shown in Table 9-34.

Table 9-34: Annual heat gains and losses per ERC thermal zone [MWh_{th}], with 75 mm PF ceiling insulation

Heat Source	Thermal Zone								
	North	East	South	West	Seminar	Corridor	Kitchen	Staff WC	Total
Lighting	5.15	3.66	2.19	4.02	1.21	3.28	0.14	0.34	19.99
Equipment	2.38	1.98	1.19	1.98	1.02		1.00	0.10	9.64
Occupancy	2.14	1.77	1.06	1.79	1.05	0.10	0.07	0.10	8.08
Solar Gains	6.34	4.21	0.81	4.53	3.96	0.34		0.46	20.65
Glazing	-1.86	-1.37	-0.74	-1.50	-1.16	-0.23		-0.20	-7.06
Walls	-3.16	-2.33	-1.15	-2.53	-2.01	-0.69		-0.33	-12.20
Floors	1.66	0.74	0.97	0.88	1.63	1.52	0.05	0.18	7.62
Ceilings	-2.49	-1.57	-0.78	-1.64	-1.07	-1.60	-0.22	-0.17	-9.53
Int. Nat. Vent.	0.39	0.18	0.27	0.04	0.11	1.79	-0.50	0.06	2.34
Ext. Infil.	-5.31	-3.01	-2.15	-3.36	-3.48	-1.59		-0.39	-19.29
Sensible Cooling	-4.91	-4.00	-1.83	-4.11	-1.31	-3.30	-0.25	-0.32	-20.03
Total Cooling	**-6.69**	**-5.19**	**-2.55**	**-5.59**	**-1.98**	**-4.83**	**-0.38**	**-0.42**	**-27.64**

Heat balance profiles, showing ceiling heat gains and cooling loads for the warmest day of the Summer Design Week, as determined by simulation runs 3-9 through 3-12 with varying polyester fibre insulation thickness, are shown in Table 9-35 through Table 9-38.

Table 9-35: Aggregate heat balance profile [kW_{th}] for 15 Jan with cooling and 40 mm PF insulation

Hour	Ceilings	Glazing	Walls	Floors	Lighting	Equip.	Occup.	Solar Gains	Total Cooling
00:00	-1.5	-1.2	1.0	4.8	0.0	0.1	0.0	0.0	0.0
01:00	-1.7	-1.2	1.1	5.3	0.0	0.1	0.0	0.0	0.0
02:00	-1.8	-1.1	1.0	5.2	0.0	0.1	0.0	0.0	0.0
03:00	-1.8	-0.9	0.8	4.8	0.0	0.1	0.0	0.0	0.0
04:00	-1.8	-0.9	0.5	4.1	0.0	0.1	0.0	0.0	0.0
05:00	-1.9	-1.1	0.3	3.8	0.0	0.1	0.0	0.0	0.0
06:00	-2.1	-1.0	0.2	3.8	0.0	0.1	0.0	0.4	0.0
07:00	-2.1	-0.1	-0.3	1.8	0.0	0.1	0.0	2.2	0.0
08:00	-1.4	1.1	-1.7	-4.7	3.5	2.0	0.5	6.6	-7.0
09:00	1.0	2.1	-2.5	-7.6	6.5	2.6	1.8	7.5	-18.6
10:00	4.3	2.3	-2.6	-6.7	7.1	3.0	3.0	5.5	-37.6
11:00	7.8	2.8	-2.6	-6.5	7.1	3.0	3.1	4.9	-48.7
12:00	9.6	2.6	-2.5	-6.4	7.1	3.0	3.1	5.3	-40.8
13:00	9.2	2.9	-2.1	-5.6	7.2	3.4	3.2	5.1	-43.2
14:00	10.0	3.1	-1.9	-5.5	7.2	3.4	3.2	5.1	-53.6
15:00	10.9	3.5	-1.5	-5.0	7.1	3.0	3.2	4.7	-50.4
16:00	9.9	3.4	-1.1	-4.7	7.1	3.0	3.2	4.9	-57.6
17:00	9.0	3.4	-0.8	-5.5	7.1	3.0	3.2	7.0	-51.6
18:00	6.5	2.6	-0.2	-4.5	5.9	2.4	1.6	7.2	-30.3
19:00	3.7	1.4	0.7	-1.5	4.7	2.0	0.5	3.7	-23.1
20:00	1.6	0.1	1.2	1.1	0.0	0.1	0.0	0.1	0.0
21:00	-0.1	-0.7	0.9	-0.3	0.0	0.1	0.0	0.0	0.0
22:00	-1.2	-1.1	1.3	0.7	0.0	0.1	0.0	0.0	0.0
23:00	-1.8	-0.8	1.6	1.5	0.0	0.1	0.0	0.0	0.0

Table 9-36: Aggregate heat balance profile [kW_{th}] for 15 Jan with cooling and 75 mm PF insulation

Hour	Ceilings	Glazing	Walls	Floors	Lighting	Equip.	Occup.	Solar Gains	Total Cooling
00:00	-1.0	-1.2	1.0	4.5	0.0	0.1	0.0	0.0	0.0
01:00	-1.2	-1.2	1.0	5.0	0.0	0.1	0.0	0.0	0.0
02:00	-1.3	-1.2	0.9	4.8	0.0	0.1	0.0	0.0	0.0
03:00	-1.3	-1.0	0.7	4.5	0.0	0.1	0.0	0.0	0.0
04:00	-1.3	-0.9	0.4	3.8	0.0	0.1	0.0	0.0	0.0
05:00	-1.4	-1.1	0.2	3.5	0.0	0.1	0.0	0.0	0.0
06:00	-1.5	-1.0	0.1	3.4	0.0	0.1	0.0	0.4	0.0
07:00	-1.6	-0.1	-0.3	1.5	0.0	0.1	0.0	2.2	0.0
08:00	-1.1	1.1	-1.7	-4.8	3.5	2.0	0.5	6.6	-7.5
09:00	0.5	2.1	-2.4	-7.3	6.5	2.6	1.8	7.5	-18.5
10:00	2.8	2.3	-2.4	-6.1	7.1	3.0	3.0	5.5	-36.5
11:00	5.3	2.8	-2.4	-5.7	7.1	3.0	3.0	4.9	-46.2
12:00	6.7	2.6	-2.3	-5.7	7.1	3.0	3.1	5.3	-37.8
13:00	6.5	2.9	-2.0	-5.0	7.2	3.4	3.2	5.1	-40.6
14:00	7.0	3.1	-1.7	-4.8	7.2	3.4	3.2	5.1	-50.4
15:00	7.7	3.4	-1.4	-4.4	7.1	3.0	3.1	4.7	-47.0
16:00	7.1	3.4	-1.0	-4.2	7.1	3.0	3.1	4.9	-54.5
17:00	6.5	3.4	-0.7	-5.1	7.1	3.0	3.1	7.0	-48.8
18:00	4.8	2.6	-0.1	-4.3	5.9	2.4	1.6	7.2	-28.9
19:00	2.8	1.4	0.7	-1.5	4.7	2.0	0.5	3.7	-22.4
20:00	1.3	0.1	1.2	1.1	0.0	0.1	0.0	0.1	0.0
21:00	0.0	-0.7	0.9	-0.4	0.0	0.1	0.0	0.0	0.0
22:00	-0.8	-1.1	1.3	0.4	0.0	0.1	0.0	0.0	0.0
23:00	-1.3	-0.8	1.5	1.2	0.0	0.1	0.0	0.0	0.0

Table 9-37: Aggregate heat balance profile [kW_{th}] for 15 Jan with cooling and 100 mm PF insulation

Hour	Ceilings	Glazing	Walls	Floors	Lighting	Equip.	Occup.	Solar Gains	Total Cooling
00:00	-0.8	-1.2	1.0	4.4	0.0	0.1	0.0	0.0	0.0
01:00	-1.0	-1.2	1.0	4.9	0.0	0.1	0.0	0.0	0.0
02:00	-1.1	-1.2	0.9	4.7	0.0	0.1	0.0	0.0	0.0
03:00	-1.1	-1.0	0.7	4.3	0.0	0.1	0.0	0.0	0.0
04:00	-1.1	-0.9	0.4	3.7	0.0	0.1	0.0	0.0	0.0
05:00	-1.2	-1.1	0.2	3.3	0.0	0.1	0.0	0.0	0.0
06:00	-1.2	-1.0	0.1	3.3	0.0	0.1	0.0	0.4	0.0
07:00	-1.3	-0.1	-0.4	1.3	0.0	0.1	0.0	2.2	0.0
08:00	-1.1	1.1	-1.7	-4.8	3.5	2.0	0.5	6.6	-7.6
09:00	0.2	2.1	-2.4	-7.1	6.5	2.6	1.8	7.5	-18.4
10:00	2.2	2.3	-2.4	-5.8	7.1	3.0	3.0	5.5	-35.9
11:00	4.2	2.8	-2.4	-5.4	7.1	3.0	3.0	4.9	-45.2
12:00	5.5	2.6	-2.2	-5.4	7.1	3.0	3.1	5.3	-36.6
13:00	5.4	2.9	-1.9	-4.8	7.2	3.4	3.1	5.1	-39.5
14:00	5.7	3.1	-1.6	-4.5	7.2	3.4	3.2	5.1	-49.0
15:00	6.4	3.4	-1.3	-4.2	7.1	3.0	3.1	4.7	-45.6
16:00	5.9	3.4	-1.0	-4.0	7.1	3.0	3.1	4.9	-53.2
17:00	5.5	3.4	-0.7	-5.0	7.1	3.0	3.1	7.0	-47.6
18:00	4.2	2.6	-0.1	-4.2	5.9	2.4	1.6	7.2	-28.4
19:00	2.5	1.4	0.7	-1.4	4.7	2.0	0.5	3.7	-22.0
20:00	1.2	0.1	1.2	1.1	0.0	0.1	0.0	0.1	0.0
21:00	0.1	-0.7	0.9	-0.5	0.0	0.1	0.0	0.0	0.0
22:00	-0.6	-1.1	1.2	0.3	0.0	0.1	0.0	0.0	0.0
23:00	-1.0	-0.8	1.5	1.0	0.0	0.1	0.0	0.0	0.0

Table 9-38: Aggregate heat balance profile [kW_{th}] for 15 Jan with cooling and 135 mm PF insulation

Hour	Ceilings	Glazing	Walls	Floors	Lighting	Equip.	Occup.	Solar Gains	Total Cooling
00:00	-0.6	-1.2	0.9	4.2	0.0	0.1	0.0	0.0	0.0
01:00	-0.8	-1.2	1.0	4.7	0.0	0.1	0.0	0.0	0.0
02:00	-0.9	-1.2	0.8	4.5	0.0	0.1	0.0	0.0	0.0
03:00	-0.9	-1.0	0.6	4.2	0.0	0.1	0.0	0.0	0.0
04:00	-0.9	-0.9	0.4	3.6	0.0	0.1	0.0	0.0	0.0
05:00	-0.9	-1.1	0.2	3.2	0.0	0.1	0.0	0.0	0.0
06:00	-1.0	-1.0	0.1	3.1	0.0	0.1	0.0	0.4	0.0
07:00	-1.1	-0.1	-0.4	1.2	0.0	0.1	0.0	2.2	0.0
08:00	-1.0	1.1	-1.7	-4.8	3.5	2.0	0.5	6.6	-7.8
09:00	0.0	2.1	-2.3	-7.0	6.5	2.6	1.8	7.5	-18.3
10:00	1.5	2.3	-2.3	-5.6	7.1	3.0	3.0	5.5	-35.4
11:00	3.2	2.8	-2.3	-5.1	7.1	3.0	3.0	4.9	-44.3
12:00	4.4	2.6	-2.2	-5.1	7.1	3.0	3.0	5.3	-35.6
13:00	4.4	2.9	-1.9	-4.6	7.2	3.4	3.1	5.1	-38.6
14:00	4.6	3.1	-1.6	-4.2	7.2	3.4	3.1	5.1	-47.7
15:00	5.1	3.4	-1.3	-3.9	7.1	3.0	3.1	4.7	-44.3
16:00	4.8	3.4	-0.9	-3.8	7.1	3.0	3.1	4.9	-52.0
17:00	4.5	3.4	-0.7	-4.8	7.1	3.0	3.1	7.0	-46.4
18:00	3.5	2.6	-0.1	-4.1	5.9	2.4	1.6	7.2	-28.0
19:00	2.2	1.4	0.7	-1.4	4.7	2.0	0.5	3.7	-21.8
20:00	1.2	0.1	1.2	1.1	0.0	0.1	0.0	0.1	0.0
21:00	0.2	-0.7	0.8	-0.5	0.0	0.1	0.0	0.0	0.0
22:00	-0.4	-1.1	1.2	0.1	0.0	0.1	0.0	0.0	0.0
23:00	-0.8	-0.8	1.5	0.8	0.0	0.1	0.0	0.0	0.0

Appendix G: ERC Cooling + Lighting Upgrade Output Data

Basic Lighting Control (Run 4-1)

Annual heat gain results for the *Basic Lighting Control* simulation (including *75 mm-Insulation*) are shown in Table 9-39 below; total values were used as aggregate ERC data for Figure 4-5 in § 4.2.1.

Table 9-39: Annual heat gains per thermal zone [MWh_{th}] for Basic Lighting Control simulation

Heat Source	Thermal Zone								
	North	East	South	West	Seminar	Corridor	Kitchen	Staff WC	Total
Lighting	1.13	1.18	1.89	1.85	0.26	3.24	0.14	0.22	9.90
Equipment	2.38	1.98	1.19	1.98	1.02		1.00	0.10	9.64
Occupancy	2.12	1.75	1.05	1.77	1.05	0.09	0.07	0.10	8.00
Solar Gains	6.39	4.16	0.86	3.96	3.93	0.34		0.42	20.05
Glazing	-1.92	-1.42	-0.79	-1.61	-1.20	-0.24		-0.22	-7.40
Walls	-3.03	-2.28	-1.21	-2.47	-2.00	-0.72		-0.33	-12.04
Floors	1.76	0.78	0.72	1.00	1.54	1.14	0.00	0.17	7.11
Ceilings	-1.01	-0.63	-0.39	-0.65	-0.48	-0.78	-0.10	-0.08	-4.11
Int. Nat. Vent.	0.21	0.07	0.15	-0.07	0.11	1.21	-0.57	0.05	1.17
Ext. Infil.	-5.42	-3.08	-2.23	-3.45	-3.52	-1.63		-0.39	-19.73
Sensible Cooling	-2.58	-2.50	-1.40	-2.47	-0.79	-2.29	-0.23	-0.21	-12.46
Total Cooling	**-4.00**	**-3.48**	**-2.04**	**-3.70**	**-1.36**	**-3.52**	**-0.35**	**-0.30**	**-18.75**

Table 9-40 below shows the *DesignBuilder* lighting summary report generated as part of the *Basic Lighting Control* simulation, used to determine simulated lighting energy consumption with automatic daylighting control.

Table 9-40: DesignBuilder Lighting Summary Report for Basic Lighting Control Simulation

Report: Lighting Summary
For: Entire Facility
Timestamp: 2017-01-10 09:55:02
Interior Lighting

Zone	Lighting Power Density [W/m2]	Zone Area [m2]	Total Power [W]	Schedule Name	Scheduled Hours/Week [hr]	Full Load Hours/ Week [hr]	Return Air Fraction	Conditioned (Y/N)	Consumption [GJ]
MENZIES LEVEL5:ZONELEVEL5	9.9	1757.83	17402.52	D1_EDU_HIGHDENSIT_LIGHT	40.72	40.5	0	Y	132.31
MENZIES LEVEL6: NONERC	10	897.56	8975.65	OFFICE_OPENOFF_LIGHT	60.07	60.07	0	N	101.2
MENZIES LEVEL6:ERC005SEMINAR	12.5711	100.44	1262.64	ERC SEMINAR ROOM PROFILES	18.68	3.91	0	Y	0.93

Zone	Lighting Power Density [W/m2]	Zone Area [m2]	Total Power [W]	Schedule Name	Scheduled Hours/Week [hr]	Full Load Hours/ Week [hr]	Return Air Fraction	Conditioned (Y/N)	Consumption [GJ]
MENZIES LEVEL6:ERC006CORRIDOR	8.6440	129.63	1120.52	CORRIDOR LIGHTING	55.92	54.97	0	Y	11.65
MENZIES LEVEL6:ERC001NORTH	11.3262	173.36	1963.51	ECMP LIGHTING PROFILES 2	49.86	10.87	0	Y	4.06
MENZIES LEVEL6:ERC008STAFFWC	10.3627	13.54	140.31	ECMP CORRIDOR AND BATHROOM PROFILES	46.6	30.12	0	Y	0.8
MENZIES LEVEL6:ERC007KITCHEN	11.5702	12.1	140.00	MODIFIED ECMP KITCHEN PROFILES	18.64	18.56	0	Y	0.49
MENZIES LEVEL6:ERC003SOUTH	12.8342	65.55	841.28	ECMP LIGHTING PROFILES 2	49.86	42.76	0	Y	6.8
MENZIES LEVEL6:ERC002EAST	14.6997	95.45	1403.09	ECMP LIGHTING PROFILES 2	49.86	16.07	0	Y	4.26
MENZIES LEVEL6:ERC004WEST	14.6905	105.06	1543.38	ECMP LIGHTING PROFILES 2	49.86	22.81	0	Y	6.66
Total	10.3843	3350.52	34792.91						269.16

Delamping Simulation

Annual heat gain results for the *Delamping* simulation (Run 4-2, including *75 mm-Insulation*) are shown in Table 9-41 below.

Table 9-41: Annual heat gains per thermal zone [MWh_{th}] as for the Delamping simulation

Heat Source	Thermal Zone								
	North	East	South	West	Seminar	Corridor	Kitchen	Staff WC	Total
Lighting	2.91	2.08	2.19	2.28	0.69	3.28	0.14	0.19	13.75
Equipment	2.38	1.98	1.19	1.98	1.02		1.00	0.10	9.64
Occupancy	2.12	1.75	1.04	1.77	1.04	0.09	0.07	0.10	7.99
Solar Gains	6.34	4.21	0.81	4.53	3.96	0.34		0.46	20.65
Glazing	-1.99	-1.44	-0.80	-1.58	-1.23	-0.24		-0.21	-7.49
Walls	-3.25	-2.39	-1.23	-2.57	-2.09	-0.73		-0.34	-12.60
Floors	1.37	0.60	0.67	0.76	1.41	1.06	0.00	0.16	6.03
Ceilings	-1.11	-0.67	-0.40	-0.70	-0.52	-0.80	-0.10	-0.08	-4.37
Int. Nat. Vent.	0.18	0.06	0.14	-0.11	0.09	1.14	-0.57	0.05	0.97
Ext. Infil.	-5.50	-3.11	-2.24	-3.48	-3.57	-1.65		-0.39	-19.93
Sensible Cooling	-3.27	-2.97	-1.52	-2.93	-0.88	-2.38	-0.23	-0.21	-14.41
Total Cooling	**-4.81**	**-4.02**	**-2.19**	**-4.25**	**-1.47**	**-3.62**	**-0.36**	**-0.30**	**-21.02**

Table 9-42: Comparison of annual lighting energy between 75 mm-Insulation and Delamping simulation results [MWh]

Simulation	North	East	South	West	Seminar	Corridor	Kitchen	Staff WC	Total
75-Insul.	5.15	3.66	2.19	4.02	1.21	3.28	0.14	0.34	19.99
Delamping	2.91	2.08	2.19	2.28	0.69	3.28	0.14	0.19	13.75
% Change	-44%	-43%	0%	-43%	-43%	0%	0%	-43%	-31%

Relamping Simulation

Annual heat gain results for the *Relamping* simulation (Run 4-3, including *75 mm-Insulation*) are shown in Table 9-41 below.

Table 9-43: Annual heat gains per thermal zone [MWh_{th}] for Delamping simulation

Heat Source	Thermal Zone								
	North	East	South	West	Seminar	Corridor	Kitchen	Staff WC	Total
Lighting	2.91	2.08	2.19	2.28	0.69	3.28	0.14	0.19	13.75
Equipment	2.38	1.98	1.19	1.98	1.02		1.00	0.10	9.64
Occupancy	2.12	1.75	1.04	1.77	1.04	0.09	0.07	0.10	7.99
Solar Gains	6.34	4.21	0.81	4.53	3.96	0.34		0.46	20.65
Glazing	-1.99	-1.44	-0.80	-1.58	-1.23	-0.24		-0.21	-7.49
Walls	-3.25	-2.39	-1.23	-2.57	-2.09	-0.73		-0.34	-12.60
Floors	1.37	0.60	0.67	0.76	1.41	1.06	0.00	0.16	6.03
Ceilings	-1.11	-0.67	-0.40	-0.70	-0.52	-0.80	-0.10	-0.08	-4.37
Int. Nat. Vent.	0.18	0.06	0.14	-0.11	0.09	1.14	-0.57	0.05	0.97
Ext. Infil.	-5.50	-3.11	-2.24	-3.48	-3.57	-1.65		-0.39	-19.93
Sensible Cooling	-3.27	-2.97	-1.52	-2.93	-0.88	-2.38	-0.23	-0.21	-14.41
Total Cooling	**-4.81**	**-4.02**	**-2.19**	**-4.25**	**-1.47**	**-3.62**	**-0.36**	**-0.30**	**-21.02**

Table 9-44: Aggregate ERC heat balance profile [kW_{th}] on 15 Jan for Delamping simulation

Hour	Ceilings	Glazing	Walls	Floors	Lighting	Equip.	Occup.	Solar Gains	Total Cooling
00:00	-1.0	-1.2	1.0	4.4	0.0	0.1	0.0	0.0	0.0
01:00	-1.2	-1.2	1.0	4.9	0.0	0.1	0.0	0.0	0.0
02:00	-1.3	-1.1	0.9	4.8	0.0	0.1	0.0	0.0	0.0
03:00	-1.3	-0.9	0.7	4.4	0.0	0.1	0.0	0.0	0.0
04:00	-1.3	-0.9	0.4	3.8	0.0	0.1	0.0	0.0	0.0
05:00	-1.4	-1.1	0.2	3.4	0.0	0.1	0.0	0.0	0.0
06:00	-1.5	-1.0	0.1	3.4	0.0	0.1	0.0	0.4	0.0
07:00	-1.5	-0.1	-0.3	1.4	0.0	0.1	0.0	2.2	0.0
08:00	-1.1	1.1	-1.6	-4.5	2.7	2.0	0.5	6.6	-6.7
09:00	0.6	2.1	-2.2	-6.7	4.5	2.6	1.8	7.5	-16.8
10:00	2.9	2.3	-2.3	-5.6	4.9	3.0	3.0	5.5	-34.4
11:00	5.3	2.8	-2.3	-5.3	4.9	3.0	3.0	4.9	-43.9
12:00	6.8	2.6	-2.2	-5.3	4.9	3.0	3.0	5.3	-35.6
13:00	6.6	2.8	-1.9	-4.7	5.0	3.4	3.1	5.1	-38.5
14:00	7.1	3.1	-1.6	-4.5	5.0	3.4	3.1	5.1	-47.9
15:00	7.8	3.4	-1.3	-4.1	4.9	3.0	3.1	4.7	-44.7
16:00	7.2	3.4	-0.9	-3.9	4.9	3.0	3.1	4.9	-51.9
17:00	6.6	3.4	-0.7	-4.9	4.9	3.0	3.1	7.0	-46.2
18:00	4.9	2.6	-0.1	-4.2	4.1	2.4	1.6	7.2	-27.1
19:00	2.9	1.4	0.7	-1.4	3.4	2.0	0.5	3.7	-20.8
20:00	1.3	0.1	1.1	0.9	0.0	0.1	0.0	0.1	0.0
21:00	0.1	-0.7	0.9	-0.5	0.0	0.1	0.0	0.0	0.0
22:00	-0.8	-1.1	1.3	0.3	0.0	0.1	0.0	0.0	0.0
23:00	-1.3	-0.7	1.5	1.1	0.0	0.1	0.0	0.0	0.0

Table 9-45: Aggregate ERC heat balance profile [kW_{th}] on 15 Jan for Relamping simulation

Hour	Ceilings	Glazing	Walls	Floors	Lighting	Equip.	Occup.	Solar Gains	Total Cooling
00:00	-1.0	-1.2	1.0	4.4	0.0	0.1	0.0	0.0	0.0
01:00	-1.2	-1.2	1.0	4.9	0.0	0.1	0.0	0.0	0.0
02:00	-1.3	-1.1	0.9	4.7	0.0	0.1	0.0	0.0	0.0
03:00	-1.3	-0.9	0.7	4.4	0.0	0.1	0.0	0.0	0.0
04:00	-1.3	-0.9	0.4	3.7	0.0	0.1	0.0	0.0	0.0
05:00	-1.4	-1.1	0.2	3.4	0.0	0.1	0.0	0.0	0.0
06:00	-1.5	-1.0	0.1	3.4	0.0	0.1	0.0	0.4	0.0
07:00	-1.5	-0.1	-0.4	1.4	0.0	0.1	0.0	2.2	0.0
08:00	-1.1	1.1	-1.6	-4.3	2.1	2.0	0.5	6.6	-6.4
09:00	0.6	2.1	-2.1	-6.4	3.6	2.6	1.7	7.5	-16.0
10:00	2.9	2.3	-2.2	-5.3	3.9	3.0	2.9	5.5	-33.3
11:00	5.4	2.8	-2.3	-5.1	3.9	3.0	3.0	4.9	-42.8
12:00	6.8	2.6	-2.2	-5.2	3.9	3.0	3.0	5.3	-34.6
13:00	6.6	2.8	-1.8	-4.5	4.0	3.4	3.1	5.1	-37.5
14:00	7.1	3.1	-1.6	-4.3	4.0	3.4	3.1	5.1	-46.7
15:00	7.8	3.4	-1.3	-4.0	3.9	3.0	3.1	4.7	-43.6
16:00	7.2	3.4	-0.9	-3.8	3.9	3.0	3.1	4.9	-50.7
17:00	6.6	3.4	-0.6	-4.8	3.9	3.0	3.1	7.0	-44.9
18:00	4.9	2.6	-0.1	-4.1	3.3	2.4	1.5	7.2	-26.3
19:00	2.9	1.4	0.7	-1.4	2.7	2.0	0.5	3.7	-20.2
20:00	1.3	0.1	1.0	0.8	0.0	0.1	0.0	0.1	0.0
21:00	0.1	-0.7	0.9	-0.5	0.0	0.1	0.0	0.0	0.0
22:00	-0.7	-1.1	1.2	0.3	0.0	0.1	0.0	0.0	0.0
23:00	-1.2	-0.7	1.5	1.1	0.0	0.1	0.0	0.0	0.0

Shading Retrofit

Table 9-46: Annual heat gains per thermal zone [MWh_{th}] as under Shading simulation

Heat Source	Thermal Zone								
	North	East	South	West	Seminar	Corridor	Kitchen	Staff WC	Total
Lighting	2.18	1.56	1.87	1.71	0.52	2.79	0.12	0.15	10.88
Equipment	2.38	1.98	1.19	1.98	1.02		1.00	0.10	9.64
Occupancy	2.14	1.76	1.05	1.78	1.05	0.10	0.07	0.10	8.04
Solar Gains	5.81	4.10	1.16	4.27	4.57	0.34		0.50	20.74
Glazing	-3.79	-2.78	-1.43	-2.83	-2.61	-0.23		-0.39	-14.06
Walls	-2.93	-2.20	-1.17	-2.37	-1.95	-0.70		-0.32	-11.64
Floors	2.47	1.17	0.87	1.42	1.79	1.36	0.02	0.21	9.32
Ceilings	-0.87	-0.55	-0.35	-0.56	-0.42	-0.72	-0.09	-0.07	-3.63
Int. Nat. Vent.	0.37	0.14	0.21	0.02	0.16	1.42	-0.55	0.07	1.84
Ext. Infil.	-5.27	-3.02	-2.17	-3.35	-3.43	-1.60		-0.38	-19.22
Sensible Cooling	-2.49	-2.21	-1.37	-2.34	-0.75	-2.15	-0.21	-0.18	-11.70
Total Cooling	**-3.94**	**-3.15**	**-2.02**	**-3.57**	**-1.33**	**-3.38**	**-0.34**	**-0.27**	**-18.00**

Table 9-47: Aggregate ERC heat balance profile [kW_{th}] on 15 Jan for Shading simulation

Hour	Ceilings	Glazing	Walls	Floors	Lighting	Equip.	Occup.	Solar Gains	Total Cooling
00:00	-1.0	-2.0	1.1	4.8	0.0	0.1	0.0	0.0	0.0
01:00	-1.2	-2.0	1.1	5.4	0.0	0.1	0.0	0.0	0.0
02:00	-1.3	-1.9	1.0	5.2	0.0	0.1	0.0	0.0	0.0
03:00	-1.3	-1.6	0.8	4.7	0.0	0.1	0.0	0.0	0.0
04:00	-1.3	-1.5	0.5	4.1	0.0	0.1	0.0	0.0	0.0
05:00	-1.3	-1.8	0.3	3.8	0.0	0.1	0.0	0.0	0.0
06:00	-1.4	-1.8	0.2	3.7	0.0	0.1	0.0	0.5	0.0
07:00	-1.5	-1.1	-0.3	1.3	0.0	0.1	0.0	3.1	0.0
08:00	-1.0	1.1	-1.4	-2.2	2.1	2.0	0.5	3.6	-4.7
09:00	0.6	1.9	-2.1	-5.2	3.6	2.6	1.7	4.8	-13.6
10:00	2.9	1.8	-2.2	-5.5	3.9	3.0	2.9	4.5	-30.9
11:00	5.4	2.2	-2.3	-5.9	3.9	3.0	3.0	5.0	-41.0
12:00	6.8	2.1	-2.2	-5.9	3.9	3.0	3.0	5.6	-33.0
13:00	6.6	2.4	-1.9	-5.3	4.0	3.4	3.1	5.5	-36.4
14:00	7.1	2.5	-1.7	-5.0	4.0	3.4	3.1	5.4	-45.5
15:00	7.8	3.0	-1.3	-4.7	3.9	3.0	3.1	5.0	-42.4
16:00	7.2	2.8	-0.9	-4.0	3.9	3.0	3.1	4.6	-49.3
17:00	6.6	3.0	-0.7	-4.7	3.9	3.0	3.1	6.6	-44.1
18:00	4.9	2.3	-0.1	-3.6	3.3	2.4	1.5	6.0	-25.1
19:00	2.9	1.1	0.6	-1.8	2.7	2.0	0.5	3.7	-19.3
20:00	1.4	-0.2	1.1	0.6	0.0	0.1	0.0	0.2	0.0
21:00	0.1	-1.3	1.0	-0.2	0.0	0.1	0.0	0.0	0.0
22:00	-0.7	-1.8	1.4	0.8	0.0	0.1	0.0	0.0	0.0
23:00	-1.2	-1.4	1.6	1.5	0.0	0.1	0.0	0.0	0.0

Appendix H: Cooling Cost Assessment

Preventative Measures Cost Data

Financial and installation cost assumptions, as well as calculations for the four preventative measures, are shown in Table 9-48, as described in § 5.2.

Table 9-48: Summary of cost assumptions for cooling preventative measures

Cost parameter assumptions	
Monetary units	2015 ZAR
Year 1 Elec Price [R/kWh]	1.20
Annual electricity price rise	9.4%
Annual Inflation rate	6.0%
Real annual energy price rise	3.21%
Nominal interest rate	7.0%
Insulation Costs	
Assumed price per sqm for 75 mm PF insulation [2015 ZAR]	60.00
Labour Cost to remove existing insulation [2015 ZAR per sqm]	20.00
Ceiling area [m2]	735
Total cost of upgrade [2015 ZAR]	**58 800.00**
Lighting Costs	
New T12 Lamp Cost (Year 1)	20.00
New T8 Lamp Cost (Year 1)	30.00
Electronic ballast unit cost	250.00
Delamping labour rate [R per lamp]	30.00
Relamping labour rate [R per fixture]	65.00
No. T12 removed	45
No. T8 replaced	75
No. Ballasts replaced	60
Total cost of upgrade	
… Delamping [2015 ZAR]	**1 350.00**
Lamp replacement cost [2015 ZAR] (Year 1)	1 500.00
… Relamping [2015 ZAR]	**22 500.00**
Lamp replace cost [2015 ZAR] (Year 1)	2 250.00
All lamps replaced every four years	
Shading costs	
Labour cost remove existing solar film per sqm [2015 ZAR]	20.00
Installation cost per m - Aluminium 25 mm Venetian blinds with 730mm drop [2015 ZAR]	350.00
Total glass area [m2]	91.25
Total length [m]	125.0
Total cost of upgrade [2015 ZAR]	**45 575.00**

Annual Cost Projections

Table 9-49 through Table 9-52 shows annual cost projections and savings, relative to the ERC *Base Case*, for each progressive Preventative Scenario (*75 mm-Insulation*, *Delamping*, *Relamping* and *Shading* retrofits).

Table 9-49: Annual cost forecasts under the 75 mm-Insulation scenario [2015 ZAR]

	Capital Costs				O&M Costs		Energy Costs		Total Costs		Savings	
Year	AC System	Insulation	Lighting Upgrade	Shading	Light Replacement	AC System	AC System	Lighting System	Total Annual Costs	Cumulative Costs	Annual Saving	Cumulative Saving
1	296 806.98	58 800.00	0.00	0.00	0.00	8 904.21	9 580.87	23 993.20	398 085.26	398 085.26	-11 915.03	-11 915.03
2	0.00	0.00	0.00	0.00	0.00	8 820.99	9 888.18	24 762.79	43 471.97	441 557.23	2 832.32	-9 082.71
3	0.00	0.00	0.00	0.00	0.00	8 656.88	10 205.35	25 557.07	44 419.30	485 976.53	2 856.77	-6 225.94
4	0.00	0.00	0.00	0.00	2 333.34	8 416.43	10 532.69	26 376.82	47 659.28	533 635.82	2 871.43	-3 354.51
5	0.00	0.00	0.00	0.00	0.00	8 106.18	10 870.54	27 222.87	46 199.59	579 835.40	2 877.35	-477.15
6	0.00	0.00	0.00	0.00	0.00	7 734.40	11 219.21	28 096.06	47 049.67	626 885.07	2 875.80	2 398.65
7	0.00	0.00	0.00	0.00	0.00	7 310.70	11 579.07	28 997.25	47 887.03	674 772.10	2 868.26	5 266.90
8	0.00	0.00	0.00	0.00	2 247.32	6 845.64	11 950.48	29 927.35	50 970.79	725 742.89	2 856.34	8 123.25
9	0.00	0.00	0.00	0.00	0.00	6 350.25	12 333.80	30 887.29	49 571.33	775 314.22	2 841.76	10 965.01
10	0.00	0.00	0.00	0.00	0.00	5 835.65	12 729.41	31 878.01	50 443.07	825 757.29	2 826.22	13 791.23

Table 9-50: Annual cost forecasts under the Delamping scenario [2015 ZAR]

	Capital Costs				O&M Costs		Energy Costs		Total Costs		Savings	
Year	AC System	Insulation	Lighting Upgrade	Shading	Light Replacement	AC System	AC System	Lighting System	Total Annual Costs	Cumulative Costs	Annual Saving	Cumulative Saving
1	285 785.09	56 000.00	1 350.00	0.00	0.00	8 573.55	8 408.58	16 505.09	376 622.31	376 622.31	9 547.92	9 547.92
2	0.00	0.00	0.00	0.00	0.00	8 493.43	8 678.29	17 034.50	34 206.22	410 828.53	12 098.07	21 645.99
3	0.00	0.00	0.00	0.00	0.00	8 335.41	8 956.65	17 580.89	34 872.95	445 701.48	12 403.12	34 049.11
4	0.00	0.00	0.00	0.00	1 458.34	8 103.89	9 243.94	18 144.81	36 950.97	482 652.45	13 579.75	47 628.86
5	0.00	0.00	0.00	0.00	0.00	7 805.16	9 540.44	18 726.81	36 072.41	518 724.86	13 004.53	60 633.38
6	0.00	0.00	0.00	0.00	0.00	7 447.18	9 846.46	19 327.48	36 621.12	555 345.99	13 304.35	73 937.73
7	0.00	0.00	0.00	0.00	0.00	7 039.22	10 162.29	19 947.42	37 148.93	592 494.92	13 606.36	87 544.09
8	0.00	0.00	0.00	0.00	1 404.58	6 591.42	10 488.25	20 587.24	39 071.49	631 566.41	14 755.64	102 299.74
9	0.00	0.00	0.00	0.00	0.00	6 114.43	10 824.66	21 247.59	38 186.68	669 753.09	14 226.41	116 526.15
10	0.00	0.00	0.00	0.00	0.00	5 618.94	11 171.87	21 929.11	38 719.93	708 473.02	14 549.36	131 075.51

Table 9-51: Annual cost forecasts under the Relamping scenario [2015 ZAR]

	Capital Costs				O&M Costs		Energy Costs		Total Costs		Savings	
Year	AC System	Insulation	Lighting Upgrade	Shading	Light Replacement	AC System	AC System	Lighting System	Total Annual Costs	Cumulative Costs	Annual Saving	Cumulative Saving
1	282 111.12	56 000.00	22 500.00	0.00	0.00	8 463.33	7 915.49	13 058.94	390 048.88	390 048.88	-3 878.64	-3 878.64
2	0.00	0.00	0.00	0.00	0.00	8 384.24	8 169.38	13 477.81	30 031.43	420 080.30	16 272.86	12 394.22
3	0.00	0.00	0.00	0.00	0.00	8 228.25	8 431.42	13 910.12	30 569.79	450 650.09	16 706.28	29 100.50
4	0.00	0.00	0.00	0.00	2 187.50	7 999.71	8 701.86	14 356.29	33 245.36	483 895.44	17 285.36	46 385.86
5	0.00	0.00	0.00	0.00	0.00	7 704.82	8 980.97	14 816.77	31 502.57	515 398.01	17 574.37	63 960.24
6	0.00	0.00	0.00	0.00	0.00	7 351.45	9 269.04	15 292.03	31 912.52	547 310.53	18 012.95	81 973.19
7	0.00	0.00	0.00	0.00	0.00	6 948.73	9 566.35	15 782.53	32 297.61	579 608.14	18 457.68	100 430.87
8	0.00	0.00	0.00	0.00	2 106.87	6 506.69	9 873.20	16 288.76	34 775.51	614 383.65	19 051.63	119 482.50
9	0.00	0.00	0.00	0.00	0.00	6 035.82	10 189.88	16 811.23	33 036.94	647 420.59	19 376.15	138 858.65
10	0.00	0.00	0.00	0.00	0.00	5 546.71	10 516.73	17 350.46	33 413.90	680 834.48	19 855.39	158 714.04

Table 9-52: Annual cost forecasts under the Shading scenario [2015 ZAR]

	Capital Costs				O&M Costs		Energy Costs		Total Costs		Savings	
Year	AC System	Insulation	Lighting Upgrade	Shading	Light Replacement	AC System	AC System	Lighting System	Total Annual Costs	Cumulative Costs	Annual Saving	Cumulative Saving
1	278 437.15	56 000.00	22 500.00	45 575.00	0.00	8 353.11	7 200.01	13 058.94	431 124.21	431 124.21	-44 953.98	-44 953.98
2	0.00	0.00	0.00	0.00	0.00	8 275.05	7 430.95	13 477.81	29 183.81	460 308.02	17 120.48	-27 833.50
3	0.00	0.00	0.00	0.00	0.00	8 121.10	7 669.30	13 910.12	29 700.52	490 008.54	17 575.55	-10 257.95
4	0.00	0.00	0.00	0.00	2 187.50	7 895.52	7 915.30	14 356.29	32 354.62	522 363.16	18 176.10	7 918.15
5	0.00	0.00	0.00	0.00	0.00	7 604.48	8 169.19	14 816.77	30 590.44	552 953.60	18 486.50	26 404.65
6	0.00	0.00	0.00	0.00	0.00	7 255.71	8 431.22	15 292.03	30 978.95	583 932.55	18 946.52	45 351.17
7	0.00	0.00	0.00	0.00	0.00	6 858.23	8 701.65	15 782.53	31 342.42	615 274.97	19 412.87	64 764.04
8	0.00	0.00	0.00	0.00	2 106.87	6 421.95	8 980.76	16 288.76	33 798.34	649 073.31	20 028.80	84 792.84
9	0.00	0.00	0.00	0.00	0.00	5 957.22	9 268.82	16 811.23	32 037.27	681 110.58	20 375.82	105 168.65
10	0.00	0.00	0.00	0.00	0.00	5 474.47	9 566.13	17 350.46	32 391.06	713 501.64	20 878.23	126 046.88

End

EBE Faculty: Assessment of Ethics in Research Projects

Any person planning to undertake research in the Faculty of Engineering and the Built Environment at the University of Cape Town is required to complete this form before collecting or analysing data. When completed it should be submitted to the supervisor (where applicable) and from there to the Head of Department. If any of the questions below have been answered YES, and the applicant is NOT a fourth year student, the Head should forward this form for approval by the Faculty EIR committee: submit to Ms Zulpha Geyer (Zulpha.Geyer@uct.ac.za; Chem Eng Building, Ph 021 650 4791). Students must include a copy of the completed form with the thesis when it is submitted for examination.

Name of Principal Researcher/Student: Guy Cunliffe Department: Energy Research Centre

If a Student: Degree: MSc Eng (Sustainable Energy) Supervisor: Andrew Hibberd & Mascha Moorlach

If a Research Contract indicate source of funding/sponsorship:

Research Project Title: Thermal Energy Efficiency of the Energy Research Centre

Overview of ethics issues in your research project:

Question 1: Is there a possibility that your research could cause harm to a third party (i.e. a person not involved in your project)?	YES	~~NO~~
Question 2: Is your research making use of human subjects as sources of data? If your answer is YES, please complete Addendum 2.	~~YES~~ ✓	~~NO~~
Question 3: Does your research involve the participation of or provision of services to communities? If your answer is YES, please complete Addendum 3.	YES	~~NO~~
Question 4: If your research is sponsored, is there any potential for conflicts of interest? If your answer is YES, please complete Addendum 4.	YES	~~NO~~

If you have answered YES to any of the above questions, please append a copy of your research proposal, as well as any interview schedules or questionnaires (Addendum 1) and please complete further addenda as appropriate.

I hereby undertake to carry out my research in such a way that

- there is no apparent legal objection to the nature or the method of research; and
- the research will not compromise staff or students or the other responsibilities of the University;
- the stated objective will be achieved, and the findings will have a high degree of validity;
- limitations and alternative interpretations will be considered;
- the findings could be subject to peer review and publicly available; and
- I will comply with the conventions of copyright and avoid any practice that would constitute plagiarism.

Signed by:

	Full name and signature	Date
Principal Researcher/Student:	GUY CUNLIFFE	09/02/15

This application is approved by:

Supervisor (if applicable):	ANDREW HIBBERD	09/02/15
HOD (or delegated nominee): Final authority for all assessments with NO to all questions and for all undergraduate research.	HARALD WINKLER	
Chair : Faculty EIR Committee For applicants other than undergraduate students who have answered YES to any of the above questions.	G. Sithole	13/05/2015

ADDENDUM 1:
Please append a copy of the research proposal here, as well as any interview schedules or questionnaires:

ADDENDUM 2: To be completed if you answered YES to Question 2: See Appendix A of Proposal (attached)

It is assumed that you have read the UCT Code for Research involving Human Subjects (available at http://web.uct.ac.za/depts/educate/download/uctcodeforresearchinvolvinghumansubjects.pdf) in order to be able to answer the questions in this addendum.

2.1 Does the research discriminate against participation by individuals, or differentiate between participants, on the grounds of gender, race or ethnic group, age range, religion, income, handicap, illness or any similar classification?	YES	NO
2.2 Does the research require the participation of socially or physically vulnerable people (children, aged, disabled, etc) or legally restricted groups?	YES	NO
2.3 Will you not be able to secure the informed consent of all participants in the research? (In the case of children, will you not be able to obtain the consent of their guardians or parents?)	YES	NO
2.4 Will any confidential data be collected or will identifiable records of individuals be kept?	YES	NO
2.5 In reporting on this research is there any possibility that you will not be able to keep the identities of the individuals involved anonymous?	YES	NO
2.6 Are there any foreseeable risks of physical, psychological or social harm to participants that might occur in the course of the research?	YES	NO
2.7 Does the research include making payments or giving gifts to any participants?	YES	NO

If you have answered YES to any of these questions, please describe how you plan to address these issues (append to form):

ADDENDUM 3: To be completed if you answered YES to Question 3:

3.1 Is the community expected to make decisions for, during or based on the research?	YES	NO
3.2 At the end of the research will any economic or social process be terminated or left unsupported, or equipment or facilities used in the research be recovered from the participants or community?	YES	NO
3.3 Will any service be provided at a level below the generally accepted standards?	YES	NO

If you have answered YES to any of these questions, please describe how you plan to address these issues (append to form)

ADDENDUM 4: To be completed if you answered YES to Question 4

4.1 Is there any existing or potential conflict of interest between a research sponsor, academic supervisor, other researchers or participants?	YES	NO
4.2 Will information that reveals the identity of participants be supplied to a research sponsor, other than with the permission of the individuals?	YES	NO
4.3 Does the proposed research potentially conflict with the research of any other individual or group within the University?	YES	NO

If you have answered YES to any of these questions, please describe how you plan to address these issues(append to form)

Dissertation Proposal for MSc (Eng)

Guy Cunliffe; MSc (Eng) candidate at the Energy Research Centre; February 2015

Introduction

This report outlines the research proposal for a Masters dissertation on sustainable energy engineering that focuses on an energy efficient solution to the problem of thermal comfort in an existing building. This research aims to show that passive design strategies, such as improved insulation and the use of natural ventilation principles, can achieve desired cooling effects for a building subject to heat gains in summer, particularly if employed in conjunction with an innovative mechanical thermal regulation system. Such a solution is expected to have benefits in terms of energy efficiency, and overall sustainability, over a conventional air cooling/conditioning system.

This dissertation shall fulfill the requirements of the MEC5061Z Dissertation in Sustainable Energy Engineering course, worth 120 NQF credits, and partial completion of the MSc Eng (Sustainable Energy Engineering) programme.

Dissertation Title

The Thermal Energy Efficiency of the Energy Research Centre (ERC) Building

Proposed Research Question & Problem Description

The research question for this dissertation shall be broken into two parts:

1. Describe and quantify the external and internal thermal loads and heat gains on the ERC building during a typical day in the summer months, and the effects these have on internal building conditions and the comfort levels of its occupants.
2. Discuss, design and/or specify potential conventional and innovative engineering solutions that could be practically applied to the ERC building that would alleviate the excessive heat loads, and allow for thermally comfortable environmental properties to prevail.

The problem arises out of the design and build of the ERC department, situated on the sixth floor of the Menzies building (University of Cape Town, Upper Campus) which, in its existing state, causes significant heat gains during daylight hours in summer, and at least partially inhibits the natural circulation of air. There is a general perception, amongst the ERC researchers and support staff working in the building, of discomfort during office hours resulting from these heat gains, due to the elevated ambient air temperatures, as well as increased relative humidity. While some individuals within the building have resorted to using fans, and other ad hoc cooling solutions, it is generally felt that a cooling system, designed to alleviate the heat gains throughout the building, would greatly enhance the occupants' levels of comfort, and would lead to subsequent improvements in their productivity, and overall health and well-being.

A 'simple' solution would be to install a conventional air-conditioning system, which draws electrical energy from the Menzies building transformer and uses a refrigeration cycle to absorb heat within the building envelope and transfer it to the external environment. However, this dissertation hypothesizes that the design and application of an alternative solution, encompassing various passive design features including insulation and natural ventilation, coupled with an unconventional cooling system, would achieve the same ends of thermal comfort. However, the latter would have advantages over the conventional system in terms of performance and energy efficiency that would render it more sustainable and beneficial in the long term, in spite of possible higher capital costs upfront.

Dissertation Objectives

In undertaking this project and attempting to respond to the afore-mentioned research questions, it is envisaged that the dissertation will fulfill the following objectives:

- To conduct an extensive review of the literature on human perceptions of comfort in their working environment; assessment and quantification of external and internal thermal loads on a building, and the effects of heat transfer on internal building conditions; and various means of alleviating these thermal loads, via conventional and unconventional cooling systems, as well as passive design features;
- To survey the experiences of comfort and/or discomfort amongst the ERC researchers and staff during their working hours in Cape Town's summer months (i.e. November to April);
- To apply the literature in a practical assessment of the thermal loading and heat gains within the ERC building envelope;
- To design an overarching cooling solution incorporating both passive features and an unconventional cooling system that could be practically implemented within the building;
- Compare the specifications, components and performance of the above design with a conventional air conditioning system that achieves the same cooling effects, in terms of energy efficiency, practicality and other appropriate attributes;
- And, to draw conclusions on the merit and effectiveness of green-building solutions to thermal regulation over conventional methods.

Scope Limitations

The scope of this dissertation is limited to considering the effects of thermal loading on perceptions of comfort of people within the ERC building during summer – when heat gains cause the internal building temperature to rise, causing people to feel 'too hot'. The design and construction features of the building that allow these discomforting summer conditions, such as building orientation, natural air flow and (lack of) existing insulation material, are likely to cause the opposite conditions in winter. Thermal loads in the winter months escaping the building to the surrounding atmosphere are likely to make the occupants feel too cold, which may compromise their comfort in equal or greater measures than is the case in summer. However, for the sake of limiting the scope of research in accordance with satisfying the requirements of the 120 credit ('half') dissertation, this shall not be considered or explored here.

Research Methodology

The objectives of the dissertation shall be fulfilled by means of the following methodology:

Literature Review

Academic and technical literature, as well as other veracious sources, shall be consulted and extensively reviewed, and will constitute the foundation from which this research is conducted. This is particularly important for assessing people's perceptions of comfort and well-being in their environments, and establishing and quantifying the relationships between physiology and thermodynamic properties. Thus literature will be referred to, in order to ascertain ranges of ambient air temperature, humidity, and air quality which people commonly consider to be comfortable (Çengel & Boles, 2011). The causal link between comfort levels, productivity and well-being will also be explored and discussed in some detail.

A technical review of thermodynamic principles, including the three modes of heat transfer (conduction, convection and radiation), and the governing equations that determine these, will be performed. The fundamental principle of heat transfer – that heat fluxes through a surface between a temperature differential over a given length in proportion to the conductivity of that surface – will be expanded to explain the effects of infiltration, radiation and other external heat gains on a building through a wall, window or ceiling (Burdick, 2011). The effects of building orientation and location, and physical features and phenomena such as insulation materials, shading and thermal mass, will be explored. This will enable a response to the research question of what causes the uncomfortably warm temperatures within the building, and an analysis and quantification of these thermal loads.

The literature review shall also include examining case studies, and other appropriate examples of where innovative 'green building' solutions have been applied to the problem of internal heat gains. Thus technical reviews of the principles and applications of features such as building shading, night flushing, window glazing, and natural ventilation strategies will be conducted. This will allow the identification of appropriate passive design features that could be implemented in the ERC, which would allow at least partial cooling to take place without requiring an external energy source (GBCSA, 2014). Such a scenario would naturally provide the most sustainable, energy efficient solution to the problem.

Data Collection: Surveys and Measurements

A survey shall be distributed to ERC researcher team, and staff, that will attempt to gauge their existing levels of comfort within the building during summer. It is envisaged that the respondents will have different experiences and reactions to similar environmental conditions, based on personal preference and characteristics. However, given a data sample that encompasses all or most of the building occupants, statistical analysis and regression should be able to reveal a range of temperatures which the majority of occupants will feel comfortable and/or uncomfortable. This survey will also attempt to create an inventory of the electronic equipment and lighting used within the building, and any existing 'ad hoc' means employed to mitigate the heat gains experienced throughout the day. This would include the use of desk fans, or leaving windows slightly ajar overnight, or any other means employed to reduce the heat.

Appendix A shows the questions proposed for inclusion in this survey.

Temperature measurements will be taken to accompany the survey responses that can validate or contradict the information reported by the respondents, and thus allow the quantification of their respective comfort levels. Thus it will be possible to reflect, for example, that at 30°C Person A feels strong discomfort, whereas Person B feels comfortable. A temperature logger may also be used to determine the temperatures throughout a specified period. This would indicate the time variance of the thermal loads and timing of the peaks and troughs in temperature, taking into account factors such as absorb and release periods of the concrete walls. This data could be used in conjunction with the survey responses to ascertain which periods of the day are the most uncomfortable, and what the leading sources of heat gain are at such times.

Thermal Energy Modelling

Modelling software, namely Energy Plus, shall be used to model the ERC's thermal loads in summer, allowing numerical analysis of the heat conditions. This software inputs factors such as the building's orientation, its location, and the external temperature ranges experienced throughout the day, to determine the exact heat transfer into the building. It accounts for the building materials, and any insulation within the ceilings or walls that reduces their thermal conductivity. Thus, the software will enable a complete and accurate description of the thermal loading cycles, which the cooling interventions would be required to overcome. The software would be able to add these interventions to the 'base model', and thus determine their effectiveness and mitigating the heat loads.

Interventions would collectively form the overall cooling system, and would be drawn out of findings from the literature review. This would enable the ultimate design and specification of the system, which may include component sizes and ratings. Interventions would initially be limited to passive design features, before additional means of air conditioning and heat removal would be considered and analysed. For example, a solar absorption refrigeration cycle may be considered. This would employ an air conditioning cycle that is similar to most conventional units, but would be driven by solar energy through an absorptive chiller, rather than electrical energy. Thus, such a system would be preferable in terms of energy efficiency, in that solar energy input is abundant and renewable, and does not have a cost associated with it as would electricity.

Analysis and Discussion

Comparisons would be drawn between the innovative cooling system and conventional air conditioning, as would be installed by a regular commercial utility. A basic, if not exceptionally detailed, design of such a conventional system would be developed in order to facilitate this comparison, without oversimplifying the analysis, or adding excessively to the scope of the dissertation. Key comparisons and conclusions would be drawn between the differences in performance, energy efficiency, practicality and overall system costs – including upfront and long term energy and maintenance cost estimates. Brief discussion may be provided on additional, alternative solutions to those examined in this research. These would likely not be covered in great detail in this dissertation, but would provide an indication of possible areas for future research.

Proposed Dissertation Structure

The following is a brief indication of the possible sequence of chapters that would be included in the final dissertation report.

- Introduction
- Research Outline & Methodology
- Literature Review
- ERC Comfort Perceptions Findings
- Thermal Loading Analysis
- Innovative Cooling System Design
- Convention vs Innovation Analysis
- Discussion
- Conclusions
- Recommendations
- References
- Appendices

Dissertation Timeline

This dissertation focuses on the internal ambient conditions of the ERC during the summer months. Thus it is critical that data collection, including surveying perceptions and recording temperature ranges, be concluded before the onset of winter, which typically occurs during April each year. Ideally, temperatures, and people's experiences within them, shall be recorded over a week-long, or two-week-long, period in early March. Hence, the overall dissertation milestones would be set as follows:

Date	Completed:
(2 – 13) March 2015	Data collection (surveys and temperatures)
June/July 2015	Literature review
October 2015	First draft for edit and revision
June 2016	Graduation

Conclusion

This research is expected to satisfy the requirements for the MEC5061Z Sustainable Energy Engineering requirements. In particular, the analytical investigation into the heat gains and thermal loads experienced by the ERC building, and the specifications for a potential cooling system, should ultimately fulfill the 'engineering content' requirement of the programme. The research is relevant to the Sustainable Energy programme in that it applies engineering sciences with an understanding of the principles of energy efficiency to a practical, actual problem scenario at the University of Cape Town.

References

Burdick, A. 2011. *Strategy Guidelines: Accurate Heating and Cooling Load Calculations.* Oak Ridge, TN: U.S. Department of Energy. Available: http://www.nrel.gov/docs/fy11osti/51603.pdf. [12 February 2015].

Çengel, Y.A. & Boles, M.A. 2011. *Thermodynamics: An Engineering Approach, Seventh Edition*. New York: McGraw-Hill.

Appendix A: Proposed Survey to ERC Researchers/Staff

The following is a list of questions that shall be distributed to the ERC, to ascertain their levels of comfort or discomfort in the building during summer.

1. What is your office number, and how many occupants (including yourself) use that office?

2. How many light fittings are there in your office, and what types of lights are installed?

3. Do you typically use your ceiling lights or a desk lamp during daylight hours in summer?

4. What other electronic equipment does you use in your office (e.g. laptop, PC, desk lamp etc)?

5. a. Do you ever find the temperature in your office becoming uncomfortably warm during summer?

   b. At what times of the day do your find office feel warmest? (e.g. "2-4 pm" or "late afternoon"/ "mid-morning")

   c. Do you employ any physical or mechanical means of cooling down your office (e.g. using a desk fan or leaving a window open overnight)? Please specify:

6. What would you estimate an ideal temperature range for your office to be during the day?

7. Do you ever find your office becoming exceptionally/uncomfortably humid?

8. What would you say is your overall experience of thermal comfort in the ERC during summer? (e.g. I am generally very comfortable in my office during the day, or I frequently feel uncomfortable etc.)